Relationship between Surface and Indwelling EMG Spike Shape Measures

Justin Parro, BSc. Kin

Submitted in partial fulfillment of the requirements for the degree of Master of Science in Applied Health Sciences
(Kinesiology)

Under the supervision of David A. Gabriel, PhD

Faculty of Applied Health Sciences
Brock Univeristy
St. Catharines

Abstract

Indwelling electromyography (EMG) has great diagnostic value but its invasive and often painful characteristics make it inappropriate for monitoring human movement. Spike shape analysis of the surface electromyographic signal responds to the call for non-invasive EMG measures for monitoring human movement and detecting neuromuscular disorders. The present study analyzed the relationship between surface and indwelling EMG interference patterns. Twenty four males and twenty four females performed three isometric dorsiflexion contractions at five force levels from 20% to maximal force.

The amplitude measures increased differently between electrode types, attributed to the electrode sensitivity. The frequency measures were different between traditional and spike shape measures due to different noise rejection criteria. These measures were also different between surface and indwelling EMG due to the low-pass tissue filtering effect. The spike shape measures, thought to collectively function as a means to differentiate between motor unit characteristics, changed independent of one another.

Acknowledgements

I must thank my supervisor Dr. David Gabriel, who has devoted countless time, effort, and sacrafices to my academic development and towards the completion of this project. I could not have asked for a better, more fulfilling experience with the numerous opportunities that you have provided me. First, this project alone has pushed me to grow tremendously as an academic and second, the countless opportunities to travel, network, learn, and experience life including an unforgettable trip to Australia. Thank for all of this and much more. I am proud to have been one of your students.

I also need to thank my committee members: Dr. Alan Adkin, Dr. Kim Gammage, and Dr. Anita Christie. You challenged me in a very positive manner throughout the process and contributed to the improvement of this project.

I owe a huge thank you to Greig, Lara, and Jessica. The three of you have been a great team to work with day in and day out for years in the lab. Greig, this project would not have been possible without the countless hours you have spent with me in the lab, recruiting, performing testing, being my expert, and being a great friend. Lara, without your support and friendship I certainly would not be where I am today. Our long hours in lab, whether it was for your projects or mine, were fun, productive, and memorable.

Finally, the love and support from my entire family has made me proud of my accomplishments and hungry to pursue the future. I am extremely thankful to my parents for so much support in so many ways. You are the reason for my success and accomplishments!

Table of Contents

List of Tables

List of Figures

Chapter 1: Development of the Problem

1.1. Introduction

A motor unit (MU) is a single alpha-motor neuron and all the muscle fibers that it innervates (Basmajian & De Luca, 1985). Electrical activity is generated when the nervous system activates the peripheral nerve to recruit motor units involved in skeletal muscle contraction. Electromyography (EMG) is used in both clinical and research settings as a tool to measure electrical activity associated with neural activation of skeletal muscle (Adrian & Bronk, 1928; Basmajian, 1972). There are two types of recording methods; one secures a disc electrode to the skin surface, and the other inserts a needle electrode through the skin directly into the muscle. Each method is associated with different strengths and weaknesses.

Surface EMG (sEMG) is a painless, non-invasive technique where electrodes record from a large volume of tissue representing global muscle activity. Thus, there are challenges associated with identifying the relationship between sEMG and MU behaviour. Myoelectric impulses generated from tens of thousands of muscle fibers superimpose, which results in the complex interference pattern where the behaviours of individual MUs are buried within the overall waveform (Day & Hulliger, 2001; Keenan et al., 2005; Farina, Fosci, & Merletti, 2002; Farina et al., 2010). Anatomical low-pass filtering of the signal as it transmits through fat, fascia, and skin prior to detection at the electrode surface compounds the problem further (De Luca, 1997).

The limitations outlined above may be circumvented by inserting an electrode into the muscle to record motor unit action potentials (MUAPs) directly. Unfortunately,

needle electrodes record from a limited volume of tissue that includes only a small percentage of the total number of MUs (Podnar & Mrkaic, 2003; Podnar, 2004). Multiple insertions around the muscle are then required to obtain a representative sample, which is not always feasible (Podnar et al., 1999). Muscle compartmentalization also opens the possibility to record from an area of the muscle not directly involved in the task (Segal et al., 1991; English, Wolf, & Segal, 1993; Hannam & McMillan, 1994; Carrasco & English, 1999).

Over the past two decades there have been new developments in the application of signal processing methods to analyze the sEMG interference pattern to provide insight into MU behaviours. Such techniques seek to exploit the global, non-invasive nature of surface recording while providing similar information about MU activity as obtained by indwelling methods (Zwarts, Drost, & Stegeman, 2000; Christie et al., 2009). Wavelets (von Tscharner, 2000; Wakeling et al., 2001), recurrence quantification analyses (Liu et al., 2004; Fattorini et al., 2005; Del Santo et al., 2007), and spike shape analysis (Gabriel et al., 2007) are examples of such techniques. The focus of this thesis is on spike shape analysis, which attempts to provide greater precision than other methods in describing MU behaviour (Gabriel et al., 2007).

Spike shape analysis was developed to detect changes in the sEMG signal associated with different MU activity patterns (Gabriel, 2000; Gabriel et al., 2007). While the activity of an individual MU may be buried within the overall interference, the behaviour of a population of MUs, as manifested in the superposition of action potentials, results in an interference that is quantitatively different for each type of activity pattern. This difference is reflected in the average shape of individual spikes (Magora & Gonen,

1970; Gabriel, 2000). Five measures are used to describe the average shape of individual spikes within the interference pattern. These five measures are: mean spike amplitude (MSA), mean spike frequency (MSF), mean spike slope (MSS), mean spike duration (MSD) and mean number of peaks per spike (MNPPS). A pattern classification table is used to identify alterations in MU discharge rate, recruitment, and/or synchronization based on distinct patterns of changes between the five measures (Calder, Gabriel, & McLean, 2009; Gabriel et al., 2011; Gabriel, 2011).

1.2. Statement of the Problem

The relationship between indwelling EMG spike shape measures and the different MU activity patterns has been established (Magora & Gonen, 1970; Magora & Gonen, 1972; Magora & Gonen, 1975; Magora, Blank, & Gonen, 1980; Shochina et al., 1984). Unfortunately, correlating MU and surface EMG variables present a number of difficulties that include the following: decomposing the indwelling signal at high levels of MVC, a complex relationship between recruitment threshold and discharge rate, and amplitude cancellation (Christie et al., 2009). As a result, validation of spike shape analysis of the surface EMG signal has been limited to demonstrating deterministic changes associated with the force gradation process, which has known MU activity patterns (Gabriel et al., 2007). Therefore, an intermediate step is necessary to further validate the use of spike shape analysis on the sEMG signal. This involves investigating the relationship between spike shape measures obtained on both indwelling and surface EMG recorded simultaneously.

1.3. Purpose

The purpose of this thesis is to investigate the relationship between indwelling and surface EMG spike shape measures in the tibialis anterior during isometric dorsiflexion contractions at 20, 40, 60, 80 and 100 % maximal voluntary contraction (MVC).

1.4. Hypothesis

It is hypothesized that indwelling and surface EMG spike shape measures will exhibit similar changes while isometric dorsiflexion force increases, which will be demonstrated by similar statistical trend components. To date, there are only two studies that have recorded surface and indwelling EMG activity with the specific purpose of comparing how measures extracted from the two interference patterns change with increasing force (Philipson & Larsson, 1988; Preece et al., 1994). Both investigative groups report that surface and indwelling measures change in a similar manner however the relationships were not quantified.

1.5. Significance

Indwelling EMG has great diagnostic value but is invasive, painful, and not appropriate for monitoring isotonic contractions as occur in human movement (Jan, Schwartz, & Benstead, 1999; Disselhorst-Klug et al., 2000; Finsterer, 2004; Brown, Bruce & Jakobi, 2009). Spike shape analysis of the sEMG signal responds to the call for non-invasive EMG measures for the detection of neuromuscular disorders (Zwarts et al., 2000; Meekins, So, & Quan, 2008), and has proven reliable to use during human movement (Gabriel, 2000). It has also been shown that sEMG spike shape analysis was equivalent to traditional quantitative analysis of indwelling motor unit action potentials for diagnosing repetitive strain injury (Calder et al., 2008; Calder et al., 2009). Given its

diagnostic potential, further validation is necessary for general acceptance as a clinical tool (Zwarts et al., 2000).

1.6. Assumptions

1. The interference pattern recording from surface electrodes represents motor unit activity in a deterministic way,
2. Ankle dorsiflexion is predominantly achieved with the tibialis anterior and there is minimal co-contraction from the gastrocnemius and soleus,
3. Serial contractions with sufficient rest intervals will not induce fatigue,
4. Performance of the subjects is assumed to always be optimal.

1.7. Delimitations

1. This study is delimited to a population that is (a) college-aged (18-25 years old), (b) absent of orthopaedic abnormalities, and (c) free of neurological disorder.
2. Participants will be right leg dominant.
3. Only isometric contractions will be performed.
4. The tibialis anterior will be the only muscle under analysis.
5. Muscle electrical activity will be measured only by root-mean-square amplitude, mean power frequency, and the five spike shape measures (MSA, MSF, MSD, MSS, and MNPPS) for surface and indwelling electromyograms.

1.8. Limitations

1. Since the participants will be healthy, college-age males and females, the findings may not apply to other age groups.
2. While the study is delimited to right-limb dominant individuals, it is expected that the results will generalize to the non-dominant limb.
3. Since only isometric contractions will be studied, the results may not apply to isotonic or isokinetic contraction types.
4. Only the tibialis anterior will be studied during isometric dorsiflexion so the findings may not apply to other muscles during more complex movements.
5. There are other measures of muscle electrical activity. The relationship between indwelling and surface EMG activity can only be generalized to the root-mean-square amplitude, mean power frequency, and the five spike shape measures (MSA, MSF, MSD, MSS, and MNPPS).

1.9. Definitions

Deterministic: Phenomena that can be predicted (i.e., non-random).

Electromyography (EMG): The measurement of muscle action potentials through the use of indwelling or surface electrodes.

Isometric contraction: The muscle generates tension without an appreciable change in length.

Isotonic contraction: The muscle changes length against a constant external load.

Mean spike amplitude: The average size of spikes within the EMG signal in a given period of time.

Mean spike frequency: The average number of spikes occurring within a given period of time.

Mean spike slope: The average rise time of the spikes within a time period, from the base of the spike to its highest peak.

Mean spike duration: The average time-difference between the base of the ascending and base of the descending sides of each spike within a given period of time.

Mean number of peaks per spike: The total number of peaks divided by the total number of spikes within a given time period.

Motor unit: A single alpha motor neuron and all the muscle fibers that it innervates.

Noise: Deflections in the EMG signal that are present before, between, and after spikes that do not themselves meet the following spike criteria.

Peak: Upward and downward deflection within a spike that does not qualify as a spike, however, a spike with a single peak are determined to be the same.

Spike: Composed of a pair of upward and downward deflections that both cross zero isoelectric baseline and are greater than the 95% confidence interval for baseline noise.

Chapter 2: Literature Review

2.1. Tibialis Anterior

The human tibialis anterior (TA) muscle is located on the anterior aspect of the lower leg directly lateral to the tibial shaft. It originates from the lateral condyle of the tibia and upper tibial shaft, traveling distally to its insertion at the medial cuneiform and the base of the first metatarsal in the foot. The overall muscle diameter decreases as it travels beneath the extensor retinaculum at the ankle (Biel, 2005) (Figure 1).

The TA is innervated by the descending pathways of 2-4 branches from the deep peroneal nerve (Reebye, 2004). Motor neuron terminal branches are largely populated in certain areas of the muscle, which are referred to as motor points. The number of motor points and their location in the TA vary between-subjects and within-subjects when comparing each leg (Bowden & McNulty, 2012). A motor point is located by direct superficial stimulation where the smallest twitch can be evoked. De Luca and Merletti (1988) detected 1 to 3 motor points in the TA for each participant with the most excitable one generally being located in the upper third of the muscle (Figure 2).

It is often assumed that the TA acts on the ankle only in the saggital plane. However, it has been shown that supination occurs during dorsiflexion and pronation occurs during plantar flexion (Isman and Inman, 1969). The TA serves two functions at the ankle and foot: 1) dorsiflexion; and 2) ankle inversion. These functions make it an important component of balance and gait where it stabilizes the ankle during the landing phase and lifts the forefoot during the swing phase. Marsh et al. (1981) used electrically evoked potentials to summarize the relationship between the TA, extensor hallucis

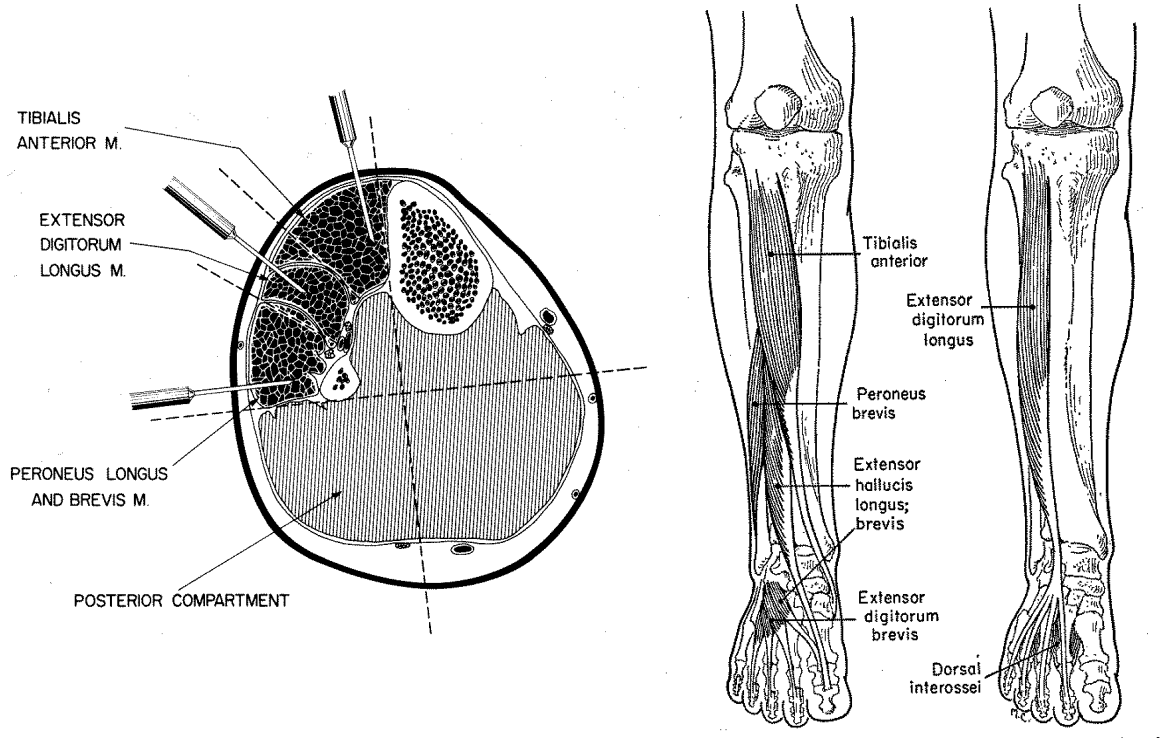

Figure 1. The diagram on the left illustrates the area distribution of the muscles and bones of the lower leg. Goodgold, J. (1984). *Anatomical correlates of clinical electromyography*. Baltimore, MD: Williams & Wilkins. The right shows a dissected illustration of the muscles working in synergy in the anterior compartment of the lower leg. Luttgens, K. and Wells, K. F. (1982). *Kinesiology: Scientific basis of human motion.* New York, NY: W. B. Saunders Company.

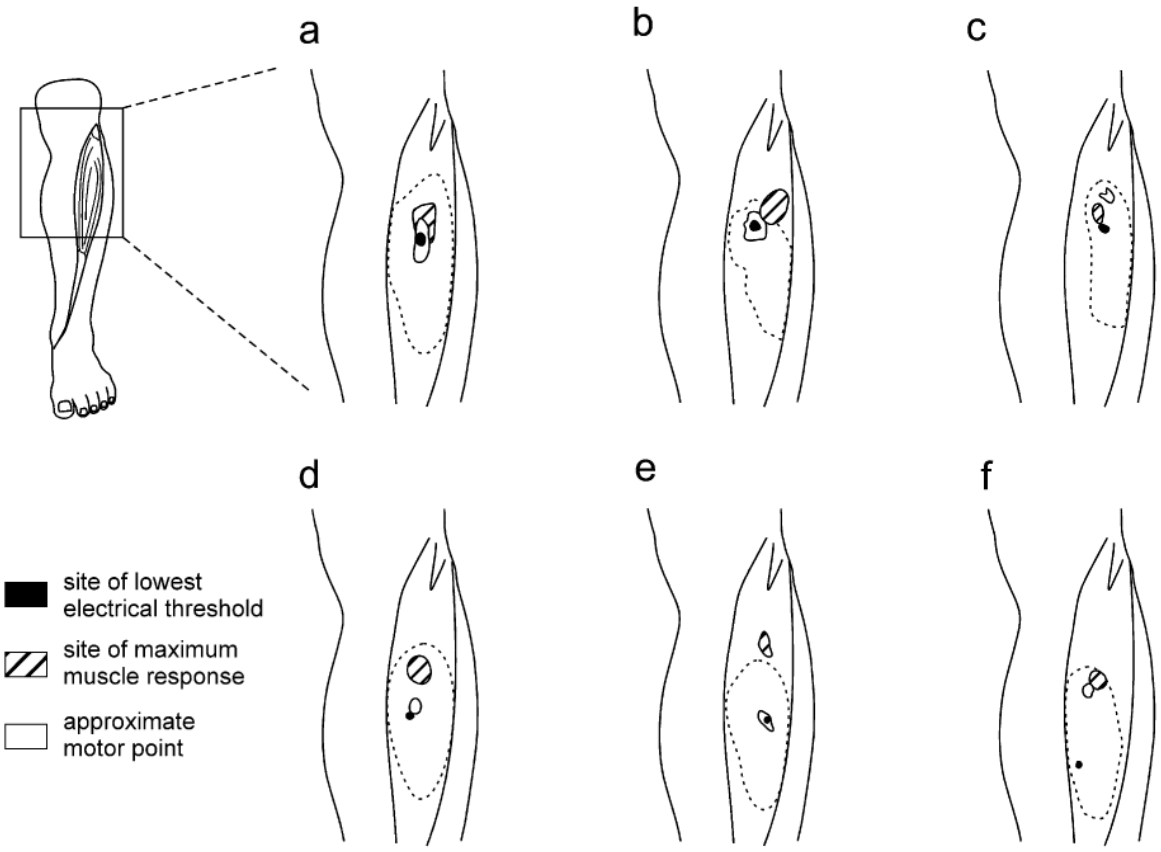

Figure 2. Tibialis anterior motor point locations. This illustration symbolizes the relationship between the regions of lowest electrical discharge threshold, maximum muscle response, and approximate motor point. The predominant motor point was generally found in the upper third of the TA. Bowden, J. L. and McNulty, P. A. (2012). Mapping the motor point in the human tibialis anterior muscle. *Clinical Neurophysiology*. 123, 386-392.

longus, extensor digitorum longus, and peroneus tertius, which all work in synergy to dorsiflex the foot. Dorsiflexion torque generated by the TA was 42% of the total dorsiflexion torque, which indicates that the synergist muscles contribute to dorsiflexion torque more than expected. Biomechanically, two components determine whether the TA can be maximally activated: the TA tendon moment arm, and the length-tension relationship, which refers to the length of the muscle at rest.

During an isometric dorsiflexion contraction, there is a change in the TA tendon action line and the center of joint rotation shifts distally (Maganaris, Baltzopoulos, & Sargeant, 1999). A general linear trend exists between joint angle and maximal voluntary dorsiflexion force, such that an increase in joint angle from dorsiflexion to plantar flexion is reflected by an increase in dorsiflexion force (Marsh et al., 1981; Fukunaga et al., 1996; Frigon et al., 2007). Associated with the increase in joint angle is a 10 percent increase in muscle length, a 60 percent increase in specific tension of the TA (Fukunaga et al., 1996), and a 30 percent decrease in the TA tendon moment arm length (Maganaris, et al., 1999; Maganaris, 2000). There are changes in the biomechanical and physiological characteristics of the TA during isometric dorsiflexion contractions, regardless of joint angle. In comparing resting state to a maximal voluntary contraction (MVC), the TA fiber length decreases (Simoneau et al., 2012) and there is a concurrent 30-40% increase in TA tendon moment arm length (Maganaris et al., 1999; Maganaris, 2000; Maganaris et al., 2001).

The TA is a symmetrically bipennate muscle with each unipennate side contributing to 50% of its force generating capacity, assuming each side has equal volume (Maganaris & Baltzopoulus, 1999). Fiber orientation in skeletal muscle impacts

the length-force and force-velocity relationships. Fiber length and consequentially sarcomere length are shorter in a pennate muscle and as a result, a small change in muscle length can be disadvantageous to its length-tension relationship (Narici, 1996). Both at rest and during MVC the muscle fiber pennation angle decreases with a subsequent change in joint angle from plantar flexion to dorsiflexion. Pennation angle is larger during an MVC compared with resting state (Maganaris & Baltzopoulus, 1999; Simoneau et al., 2012).

Physiological cross-sectional area (PCSA) is a general representation of the number of sarcomeres arranged in parallel, which is directly proportional to the muscle's peak force generating capacity (Wickiewicz et al., 1984). The PCSA of the TA does not correspond directly to the anatomical CSA because it depends on muscle volume and the distance between the aponeuroses and the pennation angle (Narici, 1999). The average muscle volume and the PCSA are greater in the plantar flexors compared with the dorsiflexors, 5- and 12-fold, respectively (Fukunaga et al., 1996). With respect to the dorsiflexor muscle group specifically, the TA comprises 57 percent of the total CSA (Wickiewicz et al., 1984; Fukunaga et al., 1996; Nakagawa et al., 2005). At various peak torques, Holmback et al. (2003) used isotonic dorsiflexion contractions to show that a significant positive linear relationship exists between contractile CSA and strength.

Skeletal muscle is composed of type I slow twitch and type IIa and IIb fast twitch fibers. Biopsies of the TA have been analyzed for the number of muscle fibers per fiber type and percentage of CSA occupied by each fiber type (Nakagawa et al., 2005). In terms of the total number of fibers, type I fibers occupied 79.0 ± 1.6 percent of the TA muscle. However, if fiber size (i.e., cross-sectional area) is considered, that percent

composition is different. Type IIa fibers have the largest diameter and are 70% greater in cross-sectional area than Type I and Type IIb fibers. However, Type IIa fibers are still only 28% of the total cross-sectional area when considering size, and only 18% of the muscle when counting the absolute number of fibers.

With these considerations for voluntary isometric dorsiflexion contractions, joint angle should be fixed to some level of plantar flexion to maximize the TA torque generating capacity and its contribution to overall dorsiflexion. Researchers have used 100 degrees (Marsh et al., 1981; Kasai & Komiyama, 1990) and 120 degrees (Connelly et al., 1999; Kent-Braun et al., 2002; McNeil et al., 2005; Nakagawa et al., 2005) but 110 degrees appears to be the ideal location for eliciting a maximum twitch response and optimizing the length-tension relationship of the TA to obtain a true MVC (O'Leary, Hope, & Sale, 1997).

2.2. Motor Control

A complex network of efferent motor neurons descends from the central nervous system (CNS) to neuromuscular junctions for the regulation of skeletal muscle contractions (De Luca & Erim, 1994). A motor unit (MU) is a descending alpha motor neuron and all of the muscle fibers that it innervates (Basmajian & DeLuca, 1985) (Figure 3). Motor unit number estimates have been performed on the TA using decomposition-enhanced spike-triggered averaging from sEMG and the results showed that the TA contains 150 ± 43 MUs (McNeil et al., 2005). The spike-triggered averaging technique is not as effective at high force levels (Taylor, Steege, & Enoka, 2002), so it is

not surprising that Feiereisen and colleagues (1997) recorded 302 MUs in the TA during an MVC.

During a voluntary contraction, MUs are recruited in an orderly fashion according to the amplitude of the twitch force generation (Milner-Brown, Stein, & Yemm, 1973; Andreassen & Arendt-Nielsen, 1987). Once a motor unit is recruited, the rate at which it discharges is modulated during the force gradation process. A population of MUs discharge in unison as a function of time and force, which indicates that the nervous system controls discharge rates of a *pool* of α-motorneurons rather than *individual* MUs (De Luca, 1985). Referred to as 'common' drive of the MU pool, the CNS regulates the activation patterns in different pools of α-motorneurons corresponding to the intended muscle output (De Luca & Erim, 1994). *Henneman's size principle* states that smaller motor neurons are recruited first in the force gradation process, which contributes to the orderly modulation of skeletal muscle contraction and relaxation from a common source (Henneman & Olsan, 1965). Feiereisen and colleagues (1997) had five subjects perform maximal voluntary isometric dorsiflexion contractions to determine the contribution of individual motor units during force development. Over 300 motor units were recorded from the TA, all of which were recruited from 1% to 88% of MVC, and the mean motor unit force was 98.3 ± 93.3 Nm.

During a linear increase in force there is a subsequent increase in MU discharge rates that follows a negative exponential function (De Luca & Contessa, 2012). Erim and colleagues (1996) monitored MU discharge rates in the TA during isometric actions of the dorsiflexors from 0 to 100% MVC and observed three phases of change. During the initial part of the contraction from 10 to 20% MVC, the MU discharge rate exhibited a

rapid increase. The second phase was characterized by a slower rate of increase while force continued to rise until 70% MVC. From 70% MVC onward, there was then another sharp increase in MU discharge rate. High threshold MUs recruited later have shorter duration and higher amplitude twitch-forces, which, teleologically, should give rise to higher discharge rates than low threshold MUs. However, initially recruited lower threshold MUs tend to have higher discharge rates than higher threshold motor units, termed the 'onion skin' phenomenon (DeLuca & Erim, 1994). When the MVC was held for a length of time *without* fatigue the MU pool tended to converge towards a maximum discharge rate, greater than 35 pulses per second (Erim et al., 1996).

All muscles follow *Henneman's size principle* (Henneman & Olsan, 1965) during contraction, but the range of force levels (i.e., 0-100% MVC) over which new MUs are recruited differs, depending on the size of the muscle. That is, each muscle has a different "recruitment range". Smaller muscles generally used for fine motor control recruit new MUs up until 50% MVC. Force is then further modulated by discharge rate (Bigland-Ritchie et al., 1983; Seki & Narusawa, 1996). Force modulation by discharge rate is termed "rate coding" (Kukulka & Clamann, 1981; Seki & Narusawa, 1996). Larger muscles such as the TA recruit new MUs up to 88-90% and rate coding progresses up to 100% MVC (Feiereisen et al., 1997; Christie et al., 2009). The adaptability of rate coding has been demonstrated in the TA by an increase in maximal discharge rate of MUs after a training program (Van Cutsem, Duchateau, & Hainaut, 1998).

From the onset of the contraction until a steady force level has been achieved, MUs can discharge twice with a short interpulse interval (< 10 ms), termed a "doublet". Doublet firings have been observed in the TA preceding a noticeable increase in force by

95 milliseconds, suggesting that there is a causal relationship between doublet firing and a rapid increase in force (Broman, De Luca, & Mambrito, 1985). Training-related increases in the rate of force development result in a higher probability of a doublet firing (Van Cutsem et al., 1998; Garland & Griffin, 1999). It is postulated that the greater rate of force development associated with doublets is due to a greater Ca^{2+} concentration in the cytoplasm, increasing the likelihood of the Ca^{2+} being used again before its uptake (Garland & Griffin, 1999).

Motor units can also fire simultaneously, more often than can be attributed to random occurrence, termed MU "synchronization". This MU synchronization pattern has been shown in all skeletal muscles with a greater prominence in the distally located muscles, including the TA (Kim et al., 2001; Fling, Christie, & Kamen, 2009). Similar to doublet firings, synchronization is more prominent in trained individuals (Hayes, 1978; Fling et al., 2009). Fling and colleagues (2009) found that synchronization was more prominent at higher strength contractions (80% versus 30% MVC) in the biceps brachii and first dorsal interosseous muscles.

2.3. Electromyography

Activation of the α-motorneuron results in the propagation of action potentials that reach the motor endplate (Figure 3). The synapse at the neuromuscular junction is chemically driven by the release of a neurotransmitter, called acetylcholine (ACh). When the action potential reaches the terminal branch, voltage-gated Ca^{2+} channels open, allowing for calcium to enter the cell while ACh is released into the synaptic cleft. The ACh binds to nicotinic receptors on the muscle cell membrane creating a depolarization

of the cell membrane. The result is a muscle fiber action potential (MFAP), which propagates bi-directionally along the muscle fibers (Masuda, Miyano, & Sadoyama, 1983). The motor unit action potential (MUAP) is created by the summation of MFAPs from each muscle fiber belonging to that particular MU (Figure 4). A sequence of multiple MUAPs, with various discharge rates and areas, represents a motor unit action potential train (MUAPT) (De Luca, 1975; Stulen & De Luca, 1978). The algebraic sum (superimposing) of the constituent MUAPTs make up the basic components of the EMG interference pattern (Figure 5) (Basmajian & De Luca, 1985; Kamen & Caldwell, 1996; Day & Hulliger, 2001). The resulting interference pattern recorded from within the muscle (indwelling electrodes) or from the skin surface (surface electrodes) is quantified in both the amplitude and frequency domains.

2.3.1. Amplitude

The amplitude of the interference pattern has long been used as a general measure of neural drive to the muscle (Farina et al., 2010). In a static voluntary contraction the spikes can be combined into bins to create a frequency-distribution histogram of amplitude values. The distribution of the histogram generally follows a *Gaussian* (normal) curve, especially for contractions lower than 70% MVC (Kaplanis et al., 2009). Electrodes detect the algebraic sum of all the action potentials; like phases increase while opposite phases decrease the overall amplitude when superimposed. The presence of cancellation reduces the rectified signal amplitude (Day & Hulliger, 2001; Keenan et al., 2006; Keenan & Valero-Cuevas, 2008). Keenen et al. (2005) used computer simulations to quantify the effects of amplitude cancellation and showed a 62% reduction at maximal activation. With greater activation, the number of active motor units and the duration of

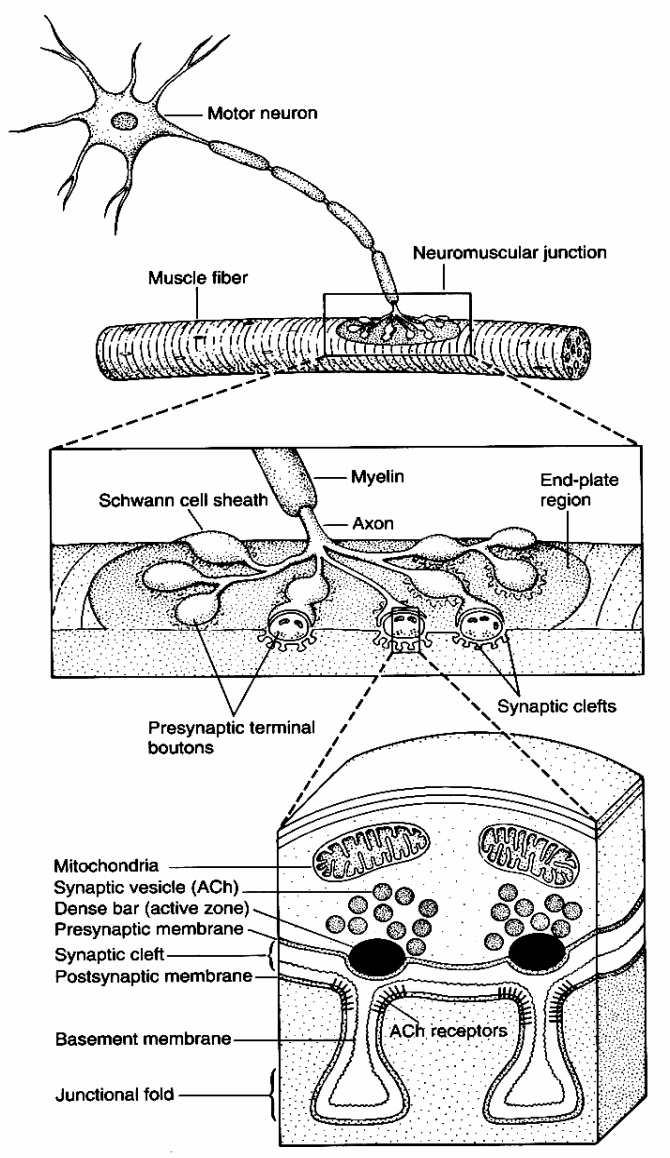

Figure 3. Action potential propagation and transmission. Depiction of the process by which the action potential travels along the α-motorneuron to the neuromuscular junction. The chemically driven synapse experiences a release of acetylcholine from the pre-synaptic cell, which binds to the nicotinic receptors on the muscle fiber. This causes the action potential along the muscle fiber that drives the contraction. Kandel, E. R., Schwartz, J. H., and Jessell, T. M. (2000). *Principles of neural science. Fourth Edition.* Toronto, ON: McGraw Hill.

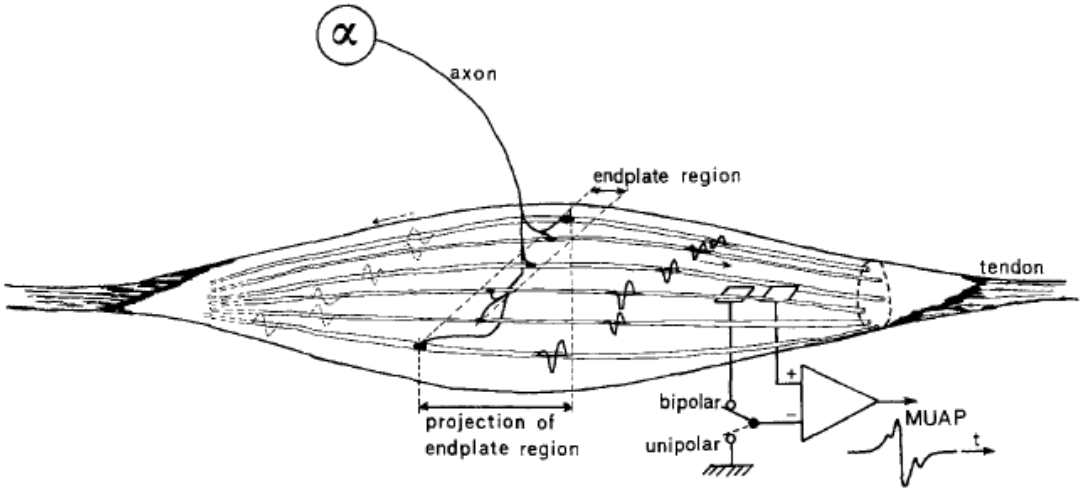

Figure 4. For each motor unit, the alpha motor neuron (α) innervates several muscle fibers throughout the muscle. The complex interference pattern is composed by the algebraic summation of all active motor unit action potential trains (shown on the right). Griep, P. A. M., Boon, K. L., and Stegeman, D. F. (1978). A study of the motor unit action potential by means of computer simulation. *Biological Cybernetics*. 30, 221-230. Figure 1a, page 222.

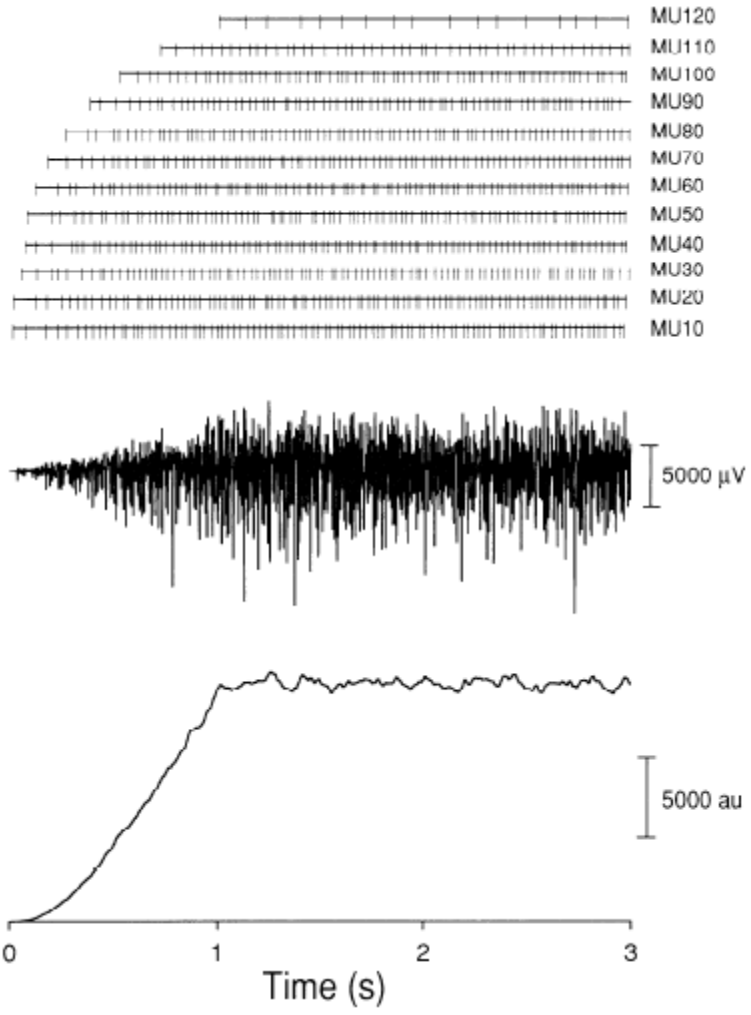

Figure 5. Each of the constituent MUAPTs are algebraically summed, where all trains are superimposed on one another, generating the EMG interference pattern. Fuglevand, A. J., Winter, D. A., and Patla, A. E. (1993). Models of recruitment and rate coding organization in motor-unit pools. *Journal of Neurophysiology*. 70 (6), 2470-2488. Figure 4, page 2477.

the action potentials resulted in greater overlap between phases with opposite polarities.

2.3.2. Frequency

The frequency content of an EMG signal provides physiological information including muscle fiber conduction velocity (MFCV) and motor unit discharge rates (Lindstrõm & Magnusson, 1977; Lago & Jones, 1977; Lago & Jones, 1981). It also contains non-physiological information from which unwanted noise can be identified (Sinderby, Lindstrõm, & Grassino, 1995; Baratta et al., 1998; Mello, Oliveira, & Nadal, 2007). The frequency content of any signal is determined by Fourier analysis, which calculates the constituent sine and cosine waveforms that can reconstruct the original signal in a least squares sense. If the frequency of each sinusoid is plotted in relation to its weighting coefficient (i.e., relative contribution to the overall signal) the result is a spectrum of frequencies in the signal. The sum of the squared weighting coefficients is signal power (or, energy) (Muthuswamy & Thakor, 1998; Harris, 1998).

In the case of EMG, the frequency distribution of a signal can provide important information about active MUs. For example, MUs generally fire between 10 and 40 Hz which may be observed as a spike in this region of the power spectrum, depending on the contraction level (Lago & Jones, 1977; Lago & Jones, 1981; van Boxtel & Schomaker, 1984; Weytjens & van Steenberghe, 1984). The overall shape of the power spectrum, which is positively skewed, is representative of the power spectrum of the MUs contributing to the contraction (Figure 6) (De Luca, 1975; Lindstrom & Magnusson, 1977; Tanzi & Taglietti, 1981; Myers et al., 2003; Dimitrova & Dimitrov, 2003). Ultimately, anything that affects MFCV, also affects the spread of frequencies in the

EMG signal (Stegeman & Linssen, 1992). The power spectrum exhibits a shift to the right with increases in force as higher threshold MUs are recruited (Moritani & Muro, 1987; Bilodeau et al., 1990; Bilodeau et al., 1995; Christie et al., 2009). However, local muscular fatigue results in a slowing of MFCV and a shift to the left of the power spectrum (Moritani, Muro, & Nagata, 1986; Krogh-Lund & Jørgensen, 1992; Krogh-Lund & Jørgensen, 1993; Lowery, Nolan, & O'Malley, 2002). Fast-twitch MU drop-out may also be a contributing factor (Peters & Fuglevand, 1999; Carpentier, Duchateau, & Hainaut, 2001; Adam & DeLuca, 2005; Christie & Kamen, 2009). Thus, there is an interrelationship between MFCV, MU-type, and the overall spread of frequencies, which is difficult to disentangle (Weytjens & van Steenberghe, 1984; Hermens et al., 1992). Fortunately, we know that the overall shape of the power spectrum reflects that of the MU, so we also know that there is no physiological information beyond 400-450 Hz for the surface signal (Zipp, 1978; van Boxtel, 2001; DeLuca & Hostage, 2010; Backus et al., 2011), 1000 Hz for the indwelling signal from wire electrodes (Backus et al., 2011), and 1500 Hz for needle electrodes (Christensen & Fuglsang-Frederiksen, 1986; Fuglsang-Frederiksen & Rønager, 1988) when considering the overall interference pattern.

Muscle fiber action potentials are affected by both physiological and technical factors, such as: muscle fiber diameter, conduction velocity, electrode configuration, and fiber position relative to the electrodes (Stashuk, 2001). The shape of the constituent MUAP waveforms of the EMG signal is dependent on the configuration of the detection electrodes and recording location relative to the muscle fibers. And, they ultimately affect the amplitude and frequency content of the signals.

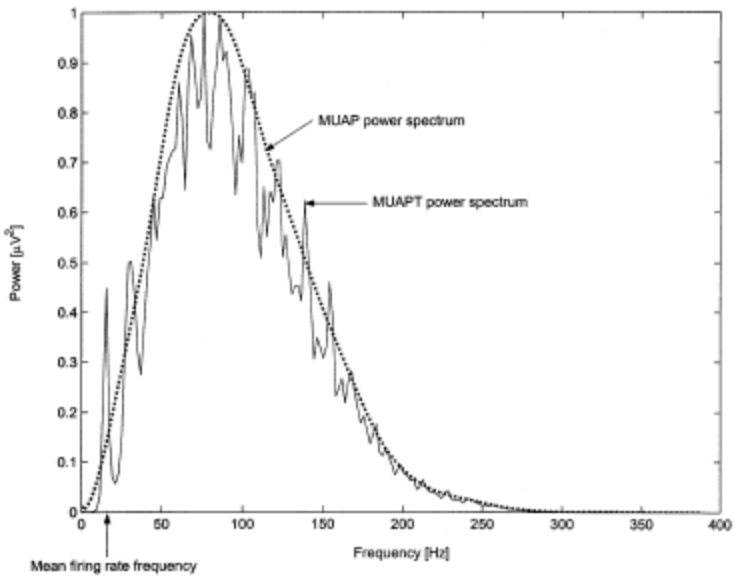

Figure 6. When both spectra are normalized to their maximum values, the MUAPT power spectrum has a similar shape to the individual MUAP power spectrum. Myers, L. J., Lowery, M., O'Malley, M., Vaughan, C. L., Heneghan, C., St Clair Gibson, A., Harley, Y. X. R., and Sreenivasan, R. (2003). Rectification and non-linear pre-processing of EMG signals for cortico-muscular analysis. *Journal of Neuroscience Methods*. 124, 157-165. Figure 2, page 159.

2.3.3. Physiological Factors Affecting the EMG Signal

2.3.3.1. Sex differences

Some of the physiological factors that affect the EMG signal manifest themselves through sex differences. The mean and median power frequencies of the sEMG signal show greater increase with increasing force, in males compared to females (Bilodeau et al, 1992; Cioni et al., 1994; Pincivero et al., 2001). However, differences in frequency characteristics from spectral analysis vary based on the muscle under examination (Bilodeau et al., 1994; Pincivero et al., 2000; Backus et al., 2011). For the TA, median power frequency is lower in women than in men (Cioni et al., 1994; Lenhardt, McIntosh, & Gabriel, 2009). Some proposed mechanisms underlying these sex related differences in the sEMG spectral parameters include: differences in skinfold thickness (De la Barrera & Milner, 1994; Nordander et al., 2003; Gabriel & Kamen, 2009; Bartuzi, Tokarski, & Roman-Liu, 2010), fiber type characteristics (Moritani, Muro, & Kijima, 1985; Kupa et al., 1995; Gerdle, Wretling, & Henriksson-Larsén, 1988; Gerdle et al., 1991; Gerdle et al., 1997), and fiber diameter (Lindstrom & Magnusson, 1977; Sadoyama et al., 1988; Kupa et al., 1995).

Greater skinfold thickness in women has been correlated to a reduced level of EMG magnitude and frequency content because subcutaneous tissue has been argued to act as either a low-pass filter (DeLuca & Merletti, 1988; Gath & Stålberg, 1978; Lowery et al., 2004) or modelled as a purely resistive medium (Griep et al., 1982; Stegeman et al., 2000; Tracey & Williams, 2011). Dimitrova et al. (2002) have suggested that the low-

pass filtering only affects the propagating components of the MUAP and not the muscle-tendon end-effects (or, terminal waves).

Moritani et al. (1985) summarized the characteristics of type II fast twitch fibers as having greater ATPase activity, leading to an increased rate of Ca^{2+} release and uptake. This results in faster conduction velocities, shorter action potential rise times, and a more efficient T-system and sarcoplasmic reticulum. There are no significant differences for fiber type distribution between men and women (Gerdle et al., 1997; Staron et al., 2000); however, there is a significant difference in the cross-sectional area of all fiber types between sexes (Kupa et al., 1995). During a contraction, fast twitch muscle fibers display greater initial values of median power frequency and MFCV than slow twitch fibers. As the contraction progresses these values decrease at a greater rate in fast twitch fibers (Kupa et al., 1995). Muscle biopsies have confirmed that the mean power frequency (MPF) is significantly correlated with the proportion of type I fibers during low-level contractions (Gerdle et al., 1988; Gerdle et al., 1997) and with the proportion of type II fibers at high-level contractions (Gerdle et al., 1997). The relationship can be described by an increase in MPF with a decrease in the percentage of type I muscle fibers, which is accompanied by a greater percentage of type II fibers (Gerdle et al., 1988; Gerdle at al., 1991).

Greater relative area of fast twitch fibers results in greater conduction velocities due to less axial resistance to the flow of charge (Sadoyama et al., 1988). This can be manifested in the power spectrum of the sEMG signal by a shift towards higher frequency content (Lindstrom & Magnusson, 1977). In terms of diameter, the TA muscle

fibers are smaller in females than males (Henriksson-Larsén, 1985). This provides insight on why the mean power frequency of the sEMG signal is greater for males.

2.3.3.2. Fatigue and/or Serial Contractions

Muscle fatigue is defined as a decrease in maximal force-generating capacity of muscle or the muscle's inability to regenerate a previously attained force alongside an increase in perceived exertion (Kent-Braun, 1999; St. Clair Gibson, Lamnert, & Noakes, 2001; Dimitrova & Dimitrov, 2003). Muscle fatigue is divided into two general components: peripheral and central muscular fatigue. Kent-Braun (1999) defined peripheral fatigue as an inhibition of excitation-contraction coupling due to an accumulation of intramuscular metabolites. Some factors include: lactate production, which causes proton accumulation increasing cell acidity; calcium accumulation from decreased ability of sarcolemmal uptake/release; and decreased sodium-potassium gradient on the cell membrane rendering action potential propagation less probable. Central fatigue is a reduction in neural drive during efferent activation of the muscle, causing decreased force production or tension development (St. Clair Gibson et al., 2001).

Three methods for measuring central drive failure were used in a study on fatiguing isometric ankle dorsiflexion (Kent-Braun, 1999). The first method was the central activation ratio, which is a ratio between peak MVC and peak total force. The second measure compared the decline in MVC with declining tetanic force. Decreases in this ratio indicate central activation failure. The third measure showed a failure in central drive when there was a reduction in the integrated EMG amplitude, barring a reduction in

the compound muscle action potential. The results of this study indicated that central activation failure plays a significant role during fatiguing isometric MVCs. Central drive failure contributed to approximately 20% of fatigue developed.

The physiological responses to muscle fatigue manifest themselves in the power spectrum of the sEMG signal. There is a shift in the power spectrum towards lower frequencies due to a linear decrease in conduction velocity (Arendt-Nielsen & Mills, 1985; Moritani et al., 1986; Broman, Bilotto, & De Luca, 1985; Merletti, Knaflitz, & De Luca, 1990). However, other physiological factors also play a role in the spectral shift (Bigland-ritchie, Donovan, & Roussos, 1981). A change in the shape (left shift) of the EMG power spectrum towards a more positively skewed curve with fatigue can also result from derecruitment of previously active MUs (dropout) and the recruitment of new MUs with lower discharge rates (Lloyd, 1971; Peters & Fuglevand, 1999; Carpentier et al., 2001; Adam & DeLuca, 2005; Christie & Kamen, 2009).

During a sustained MVC, MU discharge rate decreases by about 50% (Bigland-Ritchie et al., 1983; Peters & Fuglevand, 1999). The change in discharge rate is thought to resist fatigue in two ways. First, the reduction in discharge rate is designed to match the slower twitch contraction speeds as fatigue progresses. Second, the lower discharge rate is thought to be minimally sufficient for tetanus and delays conduction failure. This phenomenon, termed “muscle wisdom”, is designed to maintain force over a longer duration while forestalling the onset of fatigue (St. Clair Gibson et al., 2001). At present, the muscle wisdom hypothesis has only partial support in the literature, as there are other mitigating factors (i.e., potentiation) that complicate the relationship between MU discharge rates and MU contractile properties (Garland & Gossen, 2002; Fuglevand &

Keen, 2003). Nevertheless, a decrease in MU discharge rates could also result in spectral compression towards the lower frequencies (Moritani et al., 1985).

2.3.3.3. Temperature Homeostasis

Regardless of whether subjects are performing fatiguing or non-fatiguing contractions it is important to monitor skin temperature to ensure that it remains unchanged throughout the protocol. Ion channel kinetics are affected by temperature, which affects the propagation of action potentials. With cooling there is a net increase in ion flow across the cell membrane because the Na^+ channels remain open longer due to slower kinetics (Rutkove, 2001).

The massed action potential (M-wave) evoked by electrical stimulation of the peripheral nerve represents all the active motor units with the associated muscle when the peak-to-peak amplitude is at maximum. A reduction in temperature affects the M-wave of the signal in the following ways. Slower depolarization and repolarization of the action potential causes it to propagate more slowly and remain under the electrodes for a longer period of time. As a result, the M-wave appears longer. The net increase in Na^+ produces a larger amplitude response (Hodgkin & Katz, 1949; Buchthal, Pinelli, & Rosenfalck, 1954; Troni, DeMattei, & Contegiacomo, 1991). Finally, the subsequent increase in the refractory period also prevents reactivation of the membrane for a prolonged period (Delbeke, Kopec, & McComas, 1978). The opposite effects occur with an increase in temperature such that there is a positive relationship between temperature and conduction velocity (Troni et al., 1991) but an inverse relationship with both amplitude and duration (Rutkove, 2000).

The changes in M-wave characteristics with temperature manifest themselves in the overall EMG interference pattern. Winkel and Jørgensen (1991) recorded sEMG signals from the soleus muscle of six human subjects at ambient temperatures of 30°C and 14°C. Cooling the skin temperature almost doubled sEMG signal amplitude with a subsequent decrease in MU discharge rate. These findings were supported by Bell (1993) who further demonstrated reduced signal amplitude in hot environments. The frequency content of the sEMG signal is also affected by temperature. There is a positive linear relationship between temperature and MPF of the sEMG signal (Madigan & Pidcoe, 2002). Alterations in MPF are consistent with how conduction velocity alters the shape of action potentials, which is also the main determinant of the power spectrum. Thus, a lack of methodological controls for temperature can cause misinterpretation of the sEMG spectral characteristics.

Physiological responses or elevated environmental temperature can cause the individual's body temperature to increase, causing a sweat response during a testing protocol. When sweat is present on the skin surface it has a dampening effect on the amplitude of the sEMG signal. No significant differences were found for the MPF between dry and wet conditions (Abdoli-Eramaki et al., 2012). Surface electrodes are subject to greater movement artifact contamination of the sEMG signal when the skin is wet from perspiration. Sweat can also cause a loss of contact with the skin surface, which reduces the amplitude of the sEMG signal (Roy et al., 2007).

Bigard et al. (2001) performed analyses on body weight, muscle performance, blood chemistry, and EMG spectral parameters during fatiguing contractions to determine the relationship between dehydration and the sEMG power spectrum. Dehydration

resulted in an earlier onset of fatigue and a shift in the power spectrum towards lower frequencies, but there were no specific dehydration effects on the sEMG signal. Furthermore, Evetovich et al. (2002) showed no differences in the amplitude and frequency content during non-fatiguing isometric contractions between euhydration and dehydration states. Thus, hydration status does not appear to impact spectral changes in the sEMG signal, other than determining the onset of normal fatigue-related changes.

2.3.4. Technical Factors Affecting the EMG Signal

2.3.4.1. Electrodes

The main goal of analysing the EMG signal is to evaluate neuromuscular function. There are physical factors that alter the EMG signal independent of neuromuscular function that can result in a misinterpretation of data. Electrode type and configuration are amongst the first contributing factors to alterations in signal amplitude and frequency content based on pick-up volume. For sEMG, a monopolar configuration has the recording electrode over the innervation zone and the reference electrode over the distal tendon of the corresponding muscle, and is primarily used for evoked potentials (Roeleveld & Stegeman, 2002; Bromberg & Spiegelberg, 1997; Nandedkar & Barkhaus, 2007). A bipolar electrode configuration is most often used in non-clinical applications (Hermens et al., 2000). Both electrodes should be placed at least 1 cm distal to the electrically identified motor point and avoid straddling the innervation zone, which alters the amplitude and frequency content due to the cancellation associated with differential recording (Vigreux, Cnockaert, & Pertuzon, 1979; Li & Sakamoto, 1996; Rainoldi, Melchiorri, & Caruso, 2004; Mesin, Merletti, & Rainoldi, 2009). A more distal location

also minimizes signal distortion associated with changes in shape of the muscle during contraction (Mesin, Merletti, & Rainoldi, 2009).

Beck et al. (2007) evaluated the sEMG-force relationship with monopolar and bipolar recordings. There were significant differences between the two electrode configurations with respect to mean amplitude value (MAV) and MPF of the EMG signal but the overall relationship with force was the same when the values were normalized. The monopolar interference pattern has a higher amplitude (Beck et al., 2007; Stock et al., 2010; Gabriel, 2011), is lower in frequency content (Beck et al., 2007; Gabriel, 2011), and is more sensitive to changes in force (Gabriel, 2011). Several factors have been suggested to contribute to a greater amplitude for the monopolar sEMG signal: greater pick-up volume (Andreassen & Rosenfalck, 1978; Roeleveld et al., 1997), the influence of the "fiber-end effect" on monopolar EMG (Merletti et al., 1999a; 1999b), and lack of common mode rejection (Winter & Webster, 1983; Tucker & Türker, 2005; Tucker & Türker, 2007). However, if the examination room is electrically isolated, a monopolar configuration is more desirable for sEMG recording to preserve important information in the EMG signal (Gabriel, 2011). Zipp (1978) suggests that a monopolar electrode configuration is also beneficial because a variation in electrode position or contact area presents no significant variation on the bandwidth of the EMG signal.

Electrode type is important when recording muscle activity because surface and indwelling needle electrodes measure electrical activity from different volumes of tissue, referred to as "pick-up volume". The pick-up volume is generally accepted to be a spherical volume of tissue with a radius the same distance as the inter-electrode distance (Lynn et al., 1978). Pick-up volume therefore determines the selectivity of the recordings.

The larger inter-electrode distances (IED=1- 2 cm) associated with surface electrodes will have a pick-up volume that represents a much larger proportion of the muscle than indwelling needle electrodes (25-50 μm). Surface recordings are therefore less selective than indwelling needle electrodes, as they detect the interference pattern from a large number of MUs within muscle and potentially neighbouring muscle through volume conduction (Gath & Stålberg, 1977; De Luca & Merletti, 1988; Dumitru & DeLisa, 1991; Dumitru, 2000; Roloveled et al., 1997). The smaller IED for needle electrodes is selective enough to record MUAPs from within the muscle itself (Gath & Stålberg, 1976).

2.3.4.2. Volume Conduction

Volume conducted electrical activity from neighbouring muscle is referred to as "cross-talk". Solomonow et al. (1994) showed clear evidence of cross-talk by recording electrical activity in a denervated muscle when a nearby muscle was active. They also demonstrated that a layer of subcutaneous fat below the recording surface resulted in greater cross-talk contamination. The interference pattern is affected by the fiber-electrode distance, which is partially determined by the amount of subcutaneous tissue. There is a decrease in the overall signal magnitude but there are differential effects upon the two components of the MUAP: the propagating versus non-propagating (muscle-tendon end-effects) portions. Figure 7 illustrates the two components of the MUAP. Both components of the MUAP decrease in overall magnitude but the propagating wave exhibits a dramatic reduction "relative" to the non-propagating portion. The result is an increase in high frequency content of the sEMG associated with the nonpropagating portion of the MUAP as it dominates the signal. Thus, the farther away the electrode is from the signal source, the greater the cross-talk is in form of high frequency components

(Dimitrova & Dimitrov, 2006; Farina et al., 2002). These potentials are often referred to as “far field potentials” and are due to volume conduction (Dumitru & King, 1992).

Cross-talk has been explored in human subjects in vivo to determine how much a desired signal may be contaminated by the activity of neighbouring muscles. Mogk and Keir (2003) placed surface electrodes around the forearm to measure EMG of all the muscles involved in rotation and gripping tasks. A cross-correlation function was used to determine how much ‘common signal’ existed between the electrodes. Results confirmed the presence of cross-talk such that adjacent electrodes possessed the greatest percentage of common signal (33-41%) and a larger distance between electrodes (6-9 cm) resulted in less common signal (2-10%). Methods to reduce cross-talk include: mathematical differentiation (van Vugt & Dijk, 2000), decreasing the cross-sectional area of electrodes (Winter, Fuglevand, & Archer, 1994; De Luca et al., 2012), decreasing interelectrode distance (Zipp, 1982), and placing the electrodes away from the muscle boarder (Winter et al., 1994). Cross-talk is an important consideration when using a monopolar configuration because the discrimination index is 5-10% lower than bipolar recording (Zipp, 1982). To minimize the cross-talk while using monopolar recordings, the recording electrode (G1) should be placed at the source of greatest signal strength in the endplate region of muscle (Dimitrov et al., 2003).

Technically surface and indwelling electrodes will record all potentials within the finite volume of the limb. The radial detection volume underneath the surface electrodes or surrounding the indwelling electrodes based on IED distance is meant to encapsulate meaningful signal energy from neighboring motor units. Meaningful signal is based on MUAP amplitude in comparison to background noise. For example, one operational

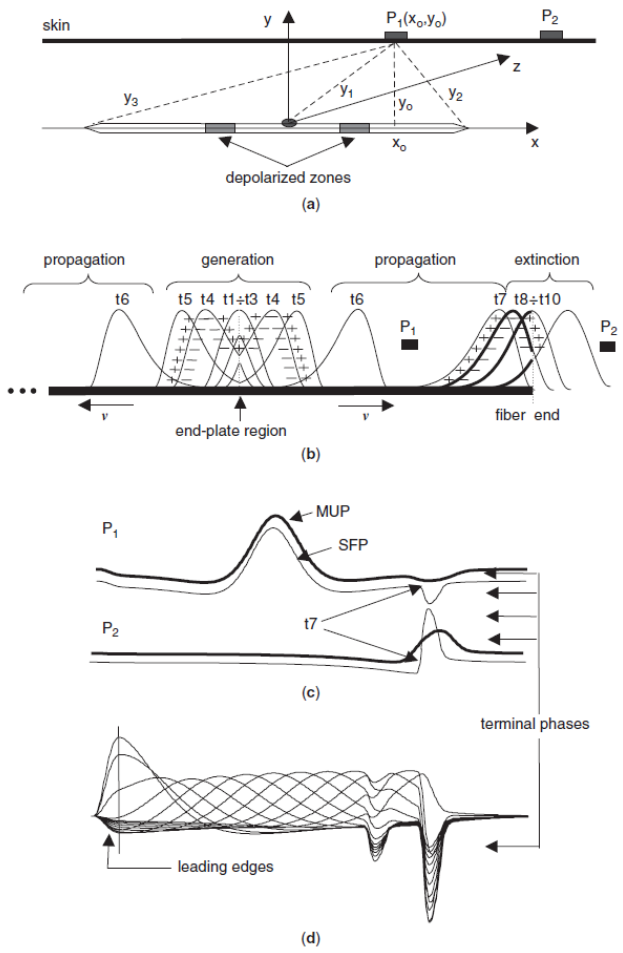

Figure 7. (a) Differences in detection from the surface electrode (P_1) as a result of varying distance. The observation is different between the actual distance (Y_o), the distance to the end-plate region (Y_2), and the distance to the fiber-ends (Y_2 and Y_3). (b) Action potentials are generated at the end-plate region and propagate bi-directionally along the fiber until extinction at the fiber end. (c) Single-fiber (thin lines) and motor unit (thick lines) potentials detected from above the fibers (P_1) and behind the ends of the fibers (P_2). (d) Single-fiber potentials generated from a fiber with an end-plate region that is not centered with respect to the fiber ends. Positive charge is downward on the current figure.

Dimitrova, N. A. and Dimitrov, G. V. (2006). Electromyography (EMG) modeling. *Wiley Encyclopedia of Biomedical Engineering*. Figure 3, page 3.

definition is based on radial isoelectric zones where the farthest distance for a muscle fiber is one that contributes less than 1/100 of the signal energy of a muscle fiber at 1 mm depth, directly beneath the surface electrode (Farina et al., 2002; Fuglevand et al., 1992). Likewise, for indwelling electrodes, the farthest radial distance is the point at which the peak-to-peak amplitude of the MUAP is attenuated by 90% (Gath & Stålberg, 1978). It is important to keep in mind that the operational definitions also depend on technical aspects related to the electrode detection system.

In practicality, the number of MUs that may be identified from highly selective indwelling quadrifilar needle recordings ranges from 5 to 11 MUs during contractions up to 80% MVC (Nawab, Wotiz, & De Luca, 2008). Quadrifilar surface electrodes have recently been developed and can detect MUAPs from the skin surface. Initial research has identified 16 to 40 MUs during contractions up to 100% MVC (Nawab, Chang, & De Luca, 2010; Farina et al., 2008). Even though considerably more MUs may be detected by surface electrodes, simulation work estimates that 20 to 22% of the total MU pool of a muscle is detected by a bipolar versus a monopolar configuration (Farina et al., 2008).

2.3.4.3. Compartmentalization

Muscle compartmentalization also has an impact on selectivity. Cadaver studies have shown that descending nerves to human muscles (flexor carpi radialis, extensor carpi radialis longus, lateral gastrocnemius, and biceps brachii) have divisional innervation to multiple compartments of the muscle (Segal et al., 1991; Segal, 1992). In vivo, fine wire electrodes have been inserted into multiple sites of the gastrocnemius muscle, demonstrating that activity from each partition in the muscle is selectively

different depending on the motor task (Wolf, Segal, & English, 1993). Compartmentalization is especially important for indwelling needle recordings, which selectively sample only a small portion of the overall MU pool due to the small IED. When using indwelling needle electrodes, multiple needle insertions and adjustments may be required for optimized MU sample size to represent the entire muscle (Christensen & Fuglsang-Frederiksen, 1986; Podnar & Mrkaic, 2003; Podnar, 2004).

Surface EMG recordings are dominated by the superficial muscle fibers where the signal energy is the greatest (Lynn et al., 1978). Previous research has demonstrated that a correlation exists between amplitude and the area between surface and needle recordings (Stålberg, 1980). Knight and Kamen (2005) recorded muscle activity at various depths using indwelling needle EMG to demonstrate that larger MUs are found closer to the surface and smaller MUs are located deeper in the muscle. The larger MUs generally constitute fast twitch fibers, which can create a recording bias that alters the interference pattern according to the properties of these fibers (Stålberg, 1980).

2.4. Measures of Electromyography

2.4.1. Traditional Measures

The traditional measure used to evaluate the amplitude of the EMG signal is the root-mean-square (RMS) amplitude (Appendix D). The RMS amplitude value depends on the power of the signal, which means it is affected by the number and discharge rates of MUAPTs. It is not however, affected by cancellation, making it a better measure than the average rectified value (ARV) for looking at EMG activity across various force levels (see Figure 8) (De Luca & Vandyk, 1975; Keenan et al., 2005). If the following

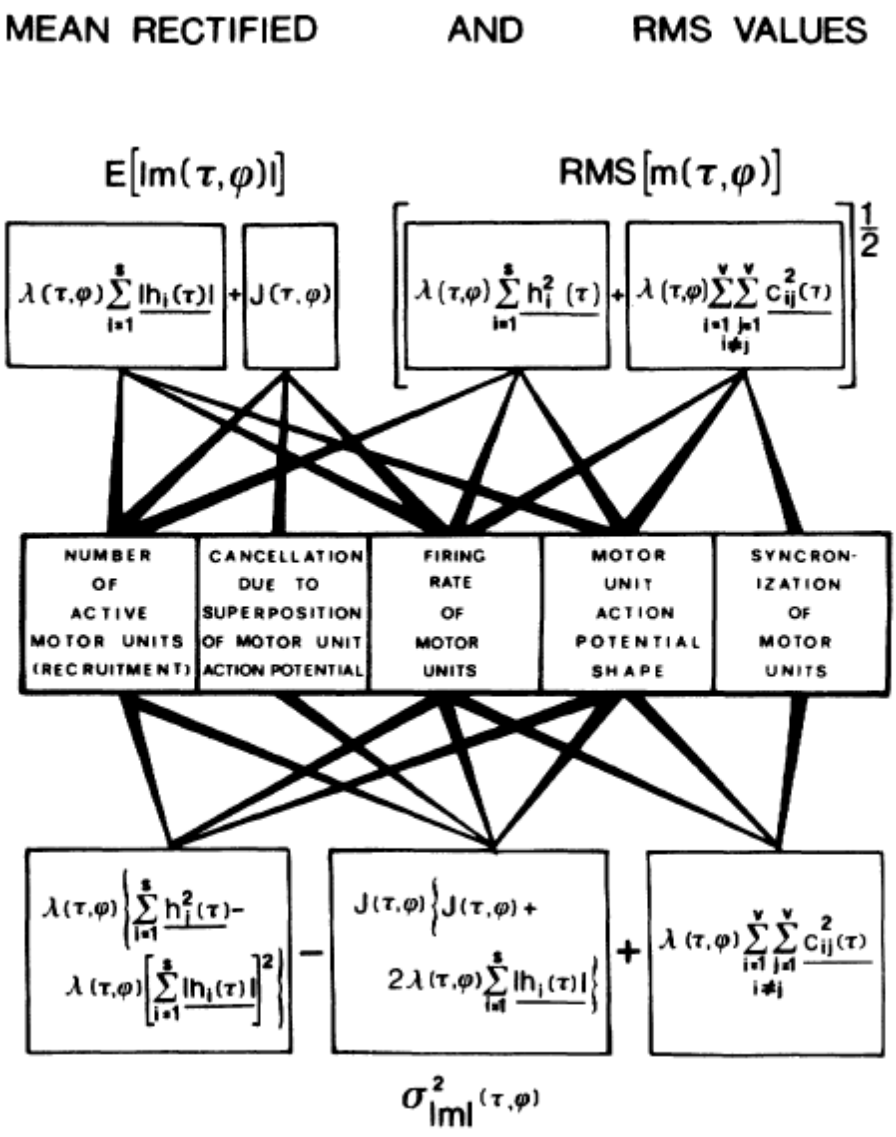

Figure 8. This diagram illustrates the theoretical correlations between the physiological characteristics of a contracting muscle and the traditional measures of the myoelectric signal. De Luca, C. J. (1979). Physiology and mathematics of myoelectric signals. *IEEE Transactions on Biomedical Engineering*. BME-26 (6), 313-325. Figure 6, page 322.

assumptions are acknowledged, the RMS measure is directly proportional to the square root of the generalized discharge rate: 1) with no change in force there is no recruitment, 2) MUAP area does not change, and 3) MUAPTs are not cross correlated (De Luca, 1979).

Two common frequency measures are used to characterize the power spectrum of the signal: mean power frequency (MPF) and median power frequency (MDF) (Stulen & De Luca, 1981). These measures are located on the positively skewed power spectrum such that the mean is greater than the median (Farina & Merletti, 2000). Appendix D shows how to calculate the power spectral density (PSD) function, as well as the MPF and MDF measures in the frequency domain. Bilodeau et al. (1992) showed that a somewhat non-linear relationship exists between both the MPF and MDF and force for the anconeus muscle. There are contradicting viewpoints in the literature with respect to the relationship between frequency measures and force, which is likely due to the strong relationship with fiber type (Gerdle et al., 1988). Researchers have demonstrated that physiological properties can manifest themselves in the power spectrum, which is seen as shifts in the MPF and MDF measures. For example, fatigue is associated with a decrease in these frequency measures (Arendt-Nielsen & Mills, 1985; Moritani et al., 1986; Broman et al., 1985; Merletti et al., 1990). Other physiological factors related to MU discharge characteristics play a role in spectral shifts but are still under investigation (Lloyd, 1971; Peters & Fuglevand, 1999; Carpentier et al., 2001; Adam & DeLuca, 2005; Christie & Kamen, 2009).

2.4.2. Non-traditional sEMG measures

Non-traditional quantification of the sEMG interference pattern has evolved through similar work on the indwelling recordings as a means to identify neuromuscular disorders (Finsterer, Mamoli, & Fuglsang-Frederiksen, 1997). A large number of quantification measures have been proposed and the reader is directed to the following reviews for a complete analysis on the subject (Fuglsang-Frederiksen, 2000; Finsterer, 2001). The current review will be delimited to those measures obtained from both surface and indwelling recordings.

Traditional measures are based on the power spectral characteristics of the EMG signal. In contrast, interference pattern analysis uses discrete measures extracted from the signal to quantify some aspect of its shape. It has been demonstrated in different patient populations (Magora & Gonen, 1970; Magora & Gonen, 1972; Toulouse et al., 1992) and during the force gradation process in able-bodied participants (Komi & Viitasalo, 1976; Gabriel, 2000; Gabriel et al., 2007), that different types of MU activity patterns result in distinctly different interference patterns as quantified by its shape. The indwelling and surface interference patterns have been quantified in the following ways: zero crossings, turns, and the number of spikes (Finsterer, 2001).

2.4.2.1. Zero Crossings

Background muscle electrical activity at rest determines a threshold that the signal must exceed to count as a baseline crossing. The number of times the signal crosses this baseline over a specific interval constitutes the “zero crossings” per unit time (Finsterer, 2001). Interference pattern analysis from a needle EMG signal has demonstrated that there is a continuous increase in the number of zero crossings per 100 ms during a

gradual increase in force up to 50% MVC (Christensen et al., 1984). During evaluation of the sEMG signal, Kaplanis and colleagues (2009) found a linear increase in the number of zero crossings per second from 10% to 100% MVC in able-bodied males and females. Wave duration is another type of zero crossing because the "wave" is measured by a signal deviation from baseline (positive or negative) until its return to baseline (Fusfeld, 1971; Sica, McComas, & Ferreira, 1978). Wave duration increases in proportion to the number of zero crossing (Fusfeld, 1971). Wave duration, determined from the number of zero crossings per unit time, has been studied in patients suffering from denervation neuropathies and myopathies. The pathological interference pattern obtained by a needle electrode had higher count rates and shorter wave durations, leading the authors to conclude that this measurement technique is a possible diagnostic tool (Fusfeld, 1971; Fusfeld, 1972; Sica et al., 1978; Vatine et al., 1990).

Differences between the indwelling and surface signal in the number of zero crossings have been observed: 177 versus 100 zero crossings per second for indwelling and surface EMG, respectively (Fusfeld, 1971; Grabiner & Robertson, 1985; Robertson & Grabiner, 1985). Unfortunately, the two 1985 studies by Grabiner and Robertson report the number of zero crossing as a percentage of MVC while Fusfeld (1971) gives an absolute force level, making a comparison of the two studies rather tenuous. Preece et al. (1994) recorded the number of zero crossings per second from surface and indwelling needle EMG in the TA and rectus femoris muscles. The average number of zero crossings per second was similar between needle and surface for the TA, 272 versus 267, respectively. However, Preece et al. (1994) demonstrated that the findings may be muscle

dependent as the zero crossings per second obtained by needle was higher (224) compared to surface EMG (139) in the rectus femoris muscle.

2.4.2.2. Number of Spikes

Similar to zero crossings, an isoelectric baseline is used to establish a threshold. The positive and negative turning points of the interference pattern that surpass the threshold are summed to provide the number of spikes per unit time (Finsterer, 2001). There is a positive linear relationship between muscle force and total action potential (spike) count. However, action potential (spike) count does not provide insight into the underlying MU activity patterns that result in an increase during the force gradation process (Close, Nickel, & Todd, 1960; Komi & Viitasalo, 1976; Grabiner & Robertson, 1985; Robertson & Grabiner, 1985). The number of spikes per unit time is, however, affected by both fatigue and neuromuscular disorders. There is a marked decrease in the frequency of spikes per second under conditions of muscle fatigue (Shochina et al., 1984; Shochina et al., 1986; Vatine et al., 1990) while higher spike counts are found in myopathic disorders compared with normal controls (Fusfeld, 1971).

The number of spikes counted depends on recording technique, data window length, and threshold criteria used by the researcher. There is also the difficulty of reporting absolute force versus percent MVC to make comparisons across studies. For example, Close and colleagues (1960) reported action potential (spike) counts from needle recordings ranging from 150 to 1800 per ten seconds of data with increases in absolute force. In contrast, the number of spikes per one second of data ranged from only 5 to 40 as force increased from 0 to 100% MVC for sEMG (Komi & Viitasalo, 1976;

Viitasalo & Komi, 1977). The threshold level for spikes detection affects the sensitivity of the relationship between spike counts and force; that is higher thresholds reduce the correlation between spike counts and force (Robertson & Grabiner, 1985; Grabiner & Robertson, 1985). It was concluded that there was a poor relationship between spike counts and the level of muscle activation as measured by sEMG.

2.4.2.3. Turns

Turns amplitude analysis requires a given threshold (~100 μV) that must be attained between the preceding and following turning points of signal for a turn to be counted. Several variables have been created from this measure (Jørgensen & Fuglsang-Frederiksen, 1991; Finsterer, 2001); turns/second, amplitude/turn, the ratio between these two variables, and duration between turns (Jørgensen & Fuglsang-Frederiksen, 1991; Finsterer, 2001). During the force gradation process, the number of turns per 100 milliseconds for indwelling needle EMG increases gradually until 40-50% MVC and then there is no further change with increasing force (Christensen et al., 1984). The number of zero crossings also increases simultaneously with the number of turns (Christensen et al., 1984; Nandedkar, Sanders, & Stålberg, 1991). Differences in the number of turns between healthy individuals and patients with neuromuscular disorders have been shown to have high diagnostic value (Kurca & Drobny, 2000). Higher turns/second and lower amplitude/turn in the TA was evident in individuals with myopathies (Dioszeghy et al., 1996). Using a concentric needle electrode, Christensen and Fuglsang-Frederiksen (1986) showed a relationship between the high/low frequency ratio of the power spectrum and turns, suggesting that these measures may reveal differences between controls and patients with neuromuscular disorders.

Turns analysis has also been performed on the surface electromyogram for the masseter muscle where the average number of turns for 500 milliseconds of data was reported to range from approximately 100 to 175 (Junge, 1993). During the simultaneous recording of surface and needle EMG, Preece et al. (1994) demonstrated that the number of turns per second is also muscle dependent. In the TA, values averaged 417.2 turns per second for surface and 490.2 for needle EMG, whereas in the rectus femoris values averaged 260.9 turns per second for surface and 425.5 in needle EMG.

Philipson and Larsson (1988) evaluated the EMG-force relationship with surface and indwelling needle electrodes. Both turns and zero crossings for sEMG increased linearly up to 50% MVC, plateauing at 75% MVC. Qualitatively, inspection of the figures presented in the paper indicates that turns and zero-crossings for the indwelling EMG followed the same pattern as observed for the surface EMG. Unfortunately, the spread of scores for indwelling activity, as assessed by the overall standard deviation at each force level, resulted in a pattern that was too diffuse to allow for EMG-to-force prediction. Therefore, differences in the variability of measures obtained for surface versus indwelling EMG recordings may be an issue when attempting to compare the methods.

2.4.2.4. Spike Shape

The measures described in the preceding paragraphs do not always accurately represent the same characteristic of the MU. For example, the duration of a spike can vary based on MU superposition and the degree of summation or cancellation, and as a result do not always reflect the duration of the individual MU. Magora and Gonen (1970)

explained that "*the characteristic of a MU still preserved in a full interference pattern is the shape, as demonstrated by its peaks. Each of these spikes has a certain number of peaks, representing the active, superimposed MUs*." A spike was defined as a pair of upward and downward deflections that cross baseline and a peak was defined as a pair of upward and downward deflections that do not cross the isoelectric baseline.

Magora and Gonen (1970; 1972) used concentric needle electrodes to evaluate the characteristics of spikes in the electromyogram. The number of peaks per spike (NPPS) provides information about the active MU by accounting for all superimposed MUs. The greatest portion of spikes contain one peak in normal subjects (~ 50%) followed by ~25% with two peaks and so on. Occurrences of more than ten peaks per spike are very rare and the greatest percentages of spikes contain five or fewer peaks (Magora & Gonen, 1970; 1972). In these Magora and Gonen studies, controls were compared to those with nerve degeneration. As expected, a loss of MUs was evident in the nerve degeneration population by 70-80% of spikes containing one peak, reflecting an increase in synchronization and summation. Comparisons were also performed between normal and myopathic individuals and the opposite was seen in the NPPS values with only about 25% of spikes containing one peak, many multi-peaked spikes, and spikes containing more than ten peaks were common in the myopathic population (Magora & Gonen, 1970). In the case of myopathic individuals, muscle fiber drop-out requires existing MUs to discharge at greater frequencies for a given force level. The activity pattern of MUs is therefore asynchronous. Compensatory recruitment of additional MUs at a given force level would also result in an increase in the NPPS, which is evident as a fuller interference pattern at lower force levels (Kimura, 1989, p 270).

Magora and Gonen (1975) again examined spike shape with concentric needle electrodes, to examine the amplitude characteristics of the spikes. Average spike amplitudes were 400 to 600 μV reaching magnitudes as high as 1000 and 2000 μV. Individuals with a neuropathy displayed a large portion of giant spikes in various different muscles. The increase in amplitude is a result of anatomic reorganization of denervated muscle fibers through axonal sprouting and enlarging MU territories and/or synchronous discharges of multiple MUs (Kimura, 1989, p 269). Although spike shape amplitude is helpful for diagnosing neuromuscular diseases, Magora and Gonen (1975) recommended this technique in combination with other more pertinent electrophysiological findings.

Viitasalo and Komi (1975) conceptualized the "average motor unit potential", or AMUP of differentially recorded sEMG obtained at the motor point wherein spikes exceeding a certain threshold (120 μV) were averaged, similar to the spike triggered averaging of indwelling motor unit action potentials developed by Lang (1971). The AMUP is not equivalent to a spike triggered MUAP. Rather, it is the triggered average of individual spikes within the interference pattern. Peak-to-peak amplitude, rise time, duration, and number of spikes (individual MUPs) per second were used to evaluate alterations in MU activity patterns with increases in force (Komi & Viitasalo, 1976) and fatigue (Viitasalo & Komi, 1977).

Komi and Viitasalo (1976; 1977) made theoretical connections between alterations in the AMUP and MUs contributing to the interference pattern. For example, it is known that high threshold MUs have greater amplitudes, shorter durations, and shorter rise times than low threshold MUs. The AMUP increased in amplitude, had a shorter rise

time, and occurred in greater number with increasing force levels, suggestive of high threshold MU recruitment (Komi & Viitasalo, 1976; Viitasalo & Komi 1977). Alterations in the number of spikes per second were attributed to either an increase in discharge rate of active MUs and/or due to the recruitment of new MUs (Viitasalo & Komi 1977). The authors cautioned that the validity of such conclusions would require more extensive work, presumably using simultaneous surface and indwelling needle recordings. However, the AMUP measures were sensitive to alterations in force and the onset of muscle fatigue.

A thesis by Mark Flieger (1983) completed under the direction of Dr. Walter Kroll at the University of Massachusetts, combined the indwelling EMG measures advocated by Magora and Gonen (1970) with the sEMG measures of the AMUP developed by Viitasalo and Komi (1975) but replaced rise time with slope. The goal of the thesis was to document alterations in MU activity patterns during practice of maximal isotonic elbow flexion at different percentages of forearm inertia, in both males and females. Using standard bipolar surface recordings over the belly of the muscle, Flieger (1983) extracted five measures from the sEMG interference pattern data window: mean spike amplitude (MSA), mean spike frequency (MSF), mean spike slope (MSS), mean number of peaks per spike (MNPPS), and mean spike duration (MSD), see Appendix C for formulas. The different measures were “theoretically” linked with distinct patterns of MU activity. The MNPPS measured synchronous versus asynchronous discharge patterns (Magora and Gonen, 1970) while MSA, MSF, MSS, and MSD were used to indicate recruitment (Viitasalo and Komi, 1975). Viitasalo and Komi (1977) acknowledged that MSF and MSD could also be related to discharge rate. It is interesting to note that

Viitasalo and Komi (1977) showed that MSF could also change independently of MSD. This may be due to that fact that MSF was obtained by the number of spikes per second from the interference pattern whereas the MSD was obtained from the AMUP where the spike averaging may have affected the outcome.

Gabriel (2000) recognized the potential to study MU activity patterns while using sEMG, a non-invasive technique. First, the reliability of the five spike measures developed by Flieger (1983) was established. The sEMG activity from the biceps brachii was recorded during non-resisted, maximal isotonic elbow flexion. The measures were found to be highly reliable (R = 0.85-0.93) over multiple test sessions spanning two-weeks, and they exhibited systematic changes with increases in elbow flexion torque. The study was significant because it showed that sEMG could be reliably recorded during dynamic muscle contractions, which are typically problematic (Farina, 2006). The sensitivity of the five spike measures to experimental manipulation was then evaluated. The goal was to determine if the changes in the five spike measures could reveal "known" MU activity patterns during established experimental conditions, such as local muscular fatigue and increasing levels of force. In both cases, alterations in the five spike measures were consistent with predictions for MU activity patterns based on indwelling recordings (Gabriel et al., 2001; Gabriel et al., 2007).

The five spike measures described by Flieger (1983) have thus far been used in clusters independent of each other based on their original conceptions by Magora and Gonen (1970) and Viitasalo and Komi (1975). However, systematic patterns of changes in the five spike measures simultaneously, consistent with known MU activity patterns for fatigue and force gradation, motivated the development of a pattern classification

Table 1. Pattern classification table demonstrating the expected changes in each of the five sEMG spike shape measures representing MU firing patterns. Gabriel, D. A. (2011). Effects of monopolar and bipolar electrode configurations on surface EMG spike analysis. *Medical Engineering and Physics*. 33, 1079-1085. Table 1, page 1080.

Motor unit firing pattern	Five sEMG spike measures				
	MSA	MSF	MSS	MSD	MNPPS
Increased firing frequency	-	↑	-	↓	-
Increased recruitment	↑	↑	↑	↓	↑
Increased synchronization	↑	↓	↑	↑	↓

table (Gabriel et al., 2007; see Table 1). The pattern classification table required the evaluation of all five measures be used simultaneously to better discriminate between types of MU activity patterns underlying the sEMG signal. The original idea by Magora and Gonen (1970) that different MU activity patterns result in spike shapes that are quantitatively different from one another is still preserved. Independently, Komi and Viitasalo (1976) also refer to the "sharpness" of the AMUP sEMG spike as indicating the recruitment of high threshold MUs. Thus, the pattern classification table developed by Gabriel et al. (2007) has been referred to in the literature as "spike shape analysis" for the sEMG signal.

Traditional amplitude and frequency analyses (RMS and MPF, respectively) suffer from the problem that different MU activity patterns can result in similar changes in both measures simultaneously. For example, MPF can increase due to an increase in MU discharge rates or the recruitment of higher threshold MUs (Van Boxtel & Schomaker, 1983; Moritani & Muro, 1987; Gamet & Maton, 1989). Similarly, the RMS amplitude may also increase due to increases in MU discharge rates or the recruitment of higher threshold MUs (Moritani & Muro, 1987; Fuglevand, Winter, & Patla, 1993). The pattern classification table for spike shape analysis of the sEMG signal is a significant development because no two patterns of MU activity can produce the same changes in all five measures simultaneously. Furthermore, each measure is theoretically linked to a different physiological aspect of MU activity.

To date, spike shape analysis for the sEMG signal has only indirect support by changing in a predictable manner in response to experimental conditions with well-known MU activity patterns. Work is now focused on more direct assessments of

validity, which is an ongoing process of converging evidence from multiple sources (Messick, 1995). Simultaneous surface and indwelling needle EMG recordings on patients suffering from specific neuromuscular disorders with well-known compensatory MU activity patterns is a powerful validation technique (Muro et al., 1982; Hermens, Boon, & Zivold, 1984; Blanchi & Vila, 1985; Toulouse et al., 1992). Calder et al. (2008; 2009) obtained simultaneous surface and indwelling needle EMG recordings of the flexor carpi radialis in normal controls, patients with repetitive strain injury, and a sample at risk for the disorder, during ramp isometric contractions from 0 to 70% MVC. Spike shape analysis of the sEMG signal not only identified the underlying MU activity patterns but also discriminated between the three separate groups.

Gabriel et al. (2011) recently combined both experimental and modelling techniques to evaluate spike shape analysis of the sEMG signal during ramp isometric contractions of the elbow flexors from 0 to 100% MVC. Modelling and simulation was used because it is methodologically difficult (but, not impossible) to obtain indwelling recordings of motor unit action potentials over 80% MVC. Experimentally obtained indwelling MU recordings were used as inputs to the model (Christie et al., 2009). The observed sEMG was then used to solve the inverse problem. That is, to ensure that the simulated MU activity patterns resulted in synthetic sEMG signals that are comparable to those obtained experimentally.

The spike shape measures extracted from the synthetic and experimentally obtained sEMG signals followed the same patterns of change with increases in isometric force. The alterations were consistent with predicted MU activity patterns obtained by indwelling needle EMG during the same experiment (Christie et al., 2009). The sEMG

model allowed a sensitivity analysis for the amount of subcutaneous tissue; it affected the absolute magnitude of the five spike shape measures. The change in MSF, MSD, and MNPPS increased with force. Since modeling and simulation work have indicated that the amount of subcutaneous tissue may be a threat to validity of spike shape analysis of the sEMG signal, the present thesis work will compare the sensitivity of five spike shape measures from, surface versus indwelling EMG, with increases in isometric force during step contractions from 0 to 100% MVC.

Chapter 3: Methods

3.1. Participants

A convenience sample of university students (24 males and 24 females) ages 18-25 from Brock University was recruited for the present study. Participants reviewed and signed an assessment of physical health status (Physical Activity Readiness Questionnaire; PAR-Q) and an informed consent document that included approval from the Brock University Research Ethics Board (#12-027) (see Appendix A). Participants varied in physical training experience but right-leg dominance was required, and free of orthopaedic abnormalities and neurological disorders.

3.2. Experimental Setup

All testing was completed within a grounded Faraday cage. Participants were seated in a testing chair so that the hip and knee were fixed at 90 degrees with the ankle fixed at 20 degrees of plantar flexion (Figure 9). A padded bar secured on top of the foot across the distal metatarsal region allowed participants to perform isometric actions of the dorsiflexors. A restraint was lowered on top of the knee to prevent extraneous movement, minimize activity from synergistic muscles, and isolate the tibialis anterior muscle. Restraints were also fastened across the participant's lap and chest for further security. Force was recorded from a load cell (JR3 Inc., Woodland, CA) secured to the foot plate beneath the distal metatarsals.

An oscilloscope (Tetronix, TDS 460A, Beaverton, OR) was used to provide real-time feedback about the quality of the EMG signal from the needle electrode. A speaker

(Advent, 1002, Lake Mary, FL) was connected to the oscilloscope to relay auditory feedback to further evaluate EMG signal quality (Spitzer et al., 1992; Okajima et al., 2000; Daube & Rubin, 2009). Both visual and auditory feedback is important for determining the correct location inside the muscle to maximize the signal-to-noise ratio. The investigator made micro-adjustments of the needle electrode to hone in on a sharp signal providing a good representation of motor unit activity within the muscle (Stashuk, 2001). A second oscilloscope (Hitachi, VC-6525, Woodbury, NY) was displayed to the participant providing real-time feedback of his/her force, which ensured that contractions were performed at the desired percentage of maximum voluntary contraction.

3.2.1. Subject Information and Anthropometric Measurements

Participants provided demographic information including age, weight, height, and training and physical activity background. Anthropometric measurements of the lower leg were then collected as follows: lower leg length (fibular head to lateral malleolus), lower leg circumference (mid-calf), whole foot length (calcaneus to distal first digit), lateral malleolus to bottom of foot length, lateral malleolus to metatarsals length, and calcaneus to metatarsals length (see Appendix B).

3.2.2. Surface Electromyography

Small areas of the tibialis anterior and patellar tendon were shaved, lightly abraded (NuPrep®; Weaver and Company, Aurora, CO, USA), and cleansed with alcohol. The motor point was then electrically identified as the area where the lowest voltage produced a minimally visible twitch of muscle fibers beneath the skin. Conductive electrode gel (Signal Gel®; Parker Laboratories, Fairfield, NJ, USA) was applied to Ag/AgCl

electrodes (Grass F-E9, Astro-Med Inc., West Warwick, RI), placed in a monopolar configuration on the tibialis anterior. This means the recording electrode was placed over the motor point and a second electrode (reference electrode) was placed over the distal tendon of the muscle. A 5 cm ground electrode (CF5000; Axelgaard Manufacturing CO., LTD, Fallbrook, CA) was placed on the lateral malleolus. Skin-electrode impedance was measured pre and post testing session with an impedance meter (Grass EZM5; Astro-Med Inc., West Warwick, RI) ensuring that the value was below 10 kΩ.

3.2.3. Indwelling Electromyography

The skin surface around the surface electrode was further sterilized with ChloraPrep® One-Step (Chlorhexidine Gluconate 2% w/v and isopropyl 70% v/v solution). A ground electrode was placed on the patella. An intramuscular 1.5 inch, 25 gauge quadrifilar needle electrode with a reference electrode inside the cannula (Viasys Healthcare UK; Surrey, England) was inserted at a 30-45 degree angle. Auditory feedback was used to determine when the electrode has passed through the fascia entering into the muscle. Within the needle cannula there were four 50μm diameter platinum-iridium wires epoxied in a side port that allowed for several MUs to be detected. This electrode remained in the muscle for the duration of the testing protocol. Needles underwent 24-hour ethylene oxide gas sterilization before reuse.

3.2.4. Signal Collection Equipment

Muscle electrical activity recorded by the passive surface and needle electrodes was passed to an amplifier (Grass P511; Astro-Med Inc., West Warwick, RI). The surface EMG signal was band-pass filtered between 3 and 300 Hz and the needle EMG signal

was band-pass filtered between 1 and 10 kHz (Brownell & Bomberg, 2009; Brown et al., 2010). For each signal the gain was determined accordingly for the target contraction level in order to maximize the resolution on the 16 bit analogue-to-digital converter (NI PCI-6052E; National Instruments, Austin, TX, USA) for storage on a Dell Pentium 4 Processor (Dell; Round Rock, TX, USA). Force and EMG signals were sampled at 25.6 kHz using a computer-based data acquisition system (DASYLab; DASYTEC National Instruments, Amherst, NH, USA). Data was saved with .ASCII and .I32 file formats for off-line reduction and analysis.

3.3. Experimental Protocol

Participants (N = 48) were asked to attend the Electromyography and Kinesiology Laboratory for two sessions separated by a minimum of 24 hours. The first session was a familiarization session and the second session was the testing protocol.

3.3.1. Familiarization Day

During this first day, participants read the information letter outlining study requirements, potential risks and benefits, and provided informed consent for their voluntary participation. They then read and signed the PAR-Q survey. The investigator then collected anthropometric measurements as outlined above. Finally, the participants were seated in the testing chair and performed 2-3 contractions at 20, 40, 60, 80, and 100% MVC to become familiar with the task. Instructions were to "pull up hard and fast against the bar, **while not using your toes**, hold, and then completely relax when instructed at the end."

3.3.2. Test Day

Participants were prepared for recording electrical activity from the tibialis anterior with surface and needle electrodes, as outlined in 3.2.2. and 3.2.3. The testing chair was adjusted according to the participant's size to secure them in the desired position for isometric dorsiflexion contractions. Once all electrodes were in position, the participant was asked to perform three 5-second maximal voluntary contractions separated by three minutes of rest. Participants performed three consecutive five-second contractions (trials) at each percent (20%, 40%, 60%, and 80%) MVC. There was three minutes of rest between each contraction. The corresponding force levels were displayed on the real time feedback oscilloscope, with two horizontal lines positioned at ± 2.5% of the target. The order of presentation of the submaximal conditions was balanced across subjects. The protocol ended with an additional three MVCs with the same work-to-rest ratio to test for the presence of fatigue (Figure 10).

3.4. Data Reduction and Analysis

The impedance and temperature measures recorded from the beginning and end of the testing sessions were analyzed using a paired *t*-test to observe any changes over the course of the protocol. Similarly, mean maximum force, RMS, and MPF for sEMG activity for the first versus second presentation of the 100% MVC conditions were analysed using a paired *t*-test to detect the presence of fatigue.

Surface and indwelling EMG signals were reduced in Matlab (The Mathworks Inc.; Natick, MA, USA) to determine the traditional measures (root-mean-square amplitude, mean power frequency, and median power frequency) and the five spike shape measures

(MSA, MSF, MSD, MSS, and MNPPS). The measures were calculated from a 1-second window centred at the most stable portion (± 2.5%) of the contraction (Figure 11).

All data were first screened for the presence of outliers as defined by a value 3 standard deviations greater or less than the mean. Skewness, kurtosis and normal probability plots were used to test for the assumption of normality. Mauchley's test for sphericity was performed as part of the repeated mesasures analysis of variance models to determine if there was a significant difference between the differences in variance between conditions (Field & Miles, 2010).

Several preliminary split-plot factorial ANOVAs were performed. The first model had one between groups factor (males versus females) and two within groups repeated measures factors (contraction levels and trials). The goal was to determine if the data for males and females could be collapsed across trials to simplify the analysis. These analyses were carried out for each surface and indwelling measure. The final split-plot factorial ANOVA was used to compare each criterion measure for surface versus indwelling EMG. There was one between groups factor (electrode type) and one repeated factor within groups (contraction levels). Orthogonal polynomials were used to compare changes in criterion measures across force levels between the two electrode types. The focus was on a comparison of trends (linear, quadratic, cubic, and/or quartic) in the means across force levels between electrode types. Statistical procedures were performed in SAS® (SAS Institute Inc.; Cary, NC, USA) with alpha set at the 0.05 probability level.

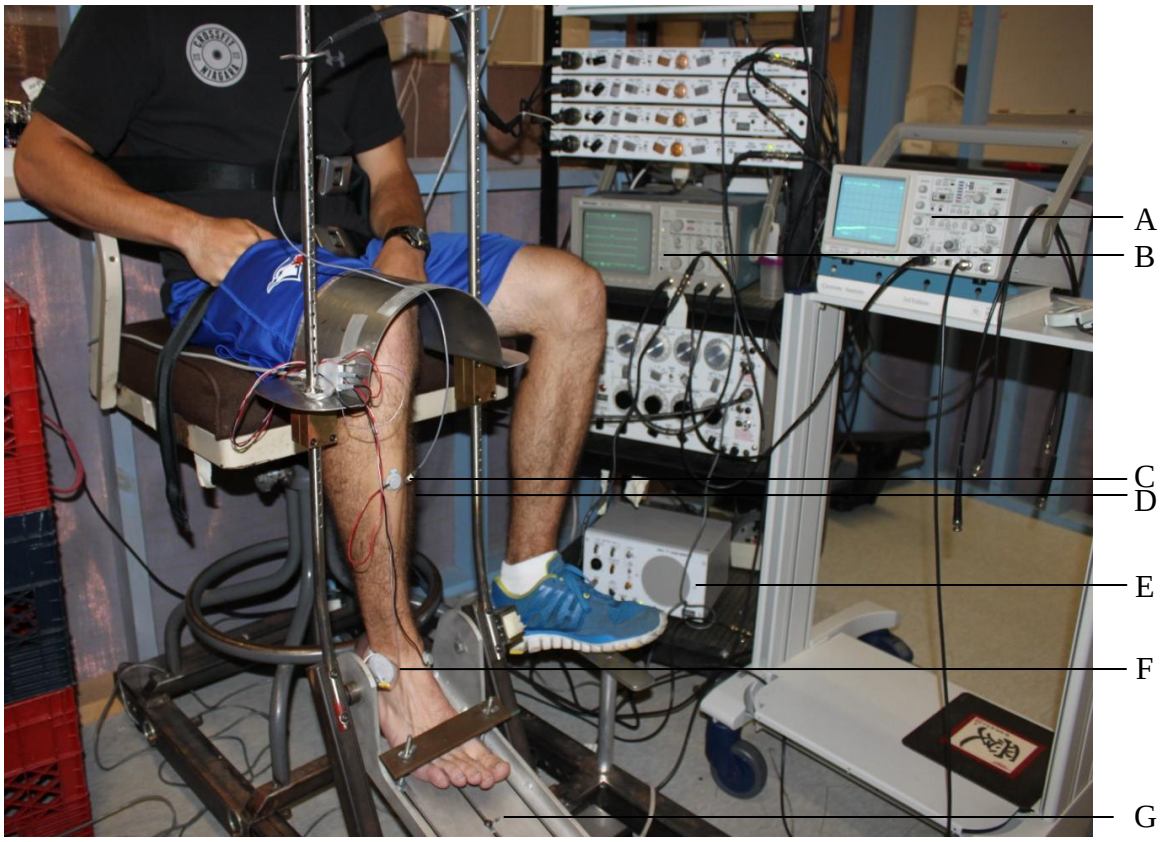

Figure 9. Experimental set up. Subjects were seated in the testing chair with real-time feedback of their force from the oscilloscope (A). A second oscilloscope (B) and a speaker (E) were used as real-time feedback for the experimenter to hone in on motor units. Surface, needle, and ground electrodes are shown as C, D, and F respectively. The load cell is located beneath the metal foot plate (G).

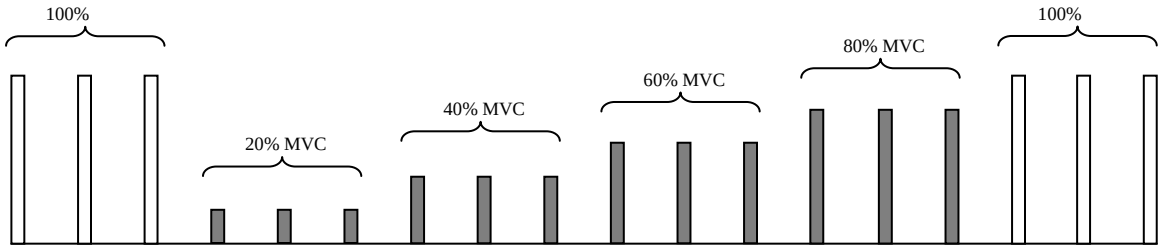

Figure 10. Experimental protocol. Each block represents a 5-second contraction at a given level of MVC (20, 40, 60, 80, or 100%) and the space between blocks represents 3 minutes of rest between contractions. Grey blocks were performed in a balanced order across subjects.

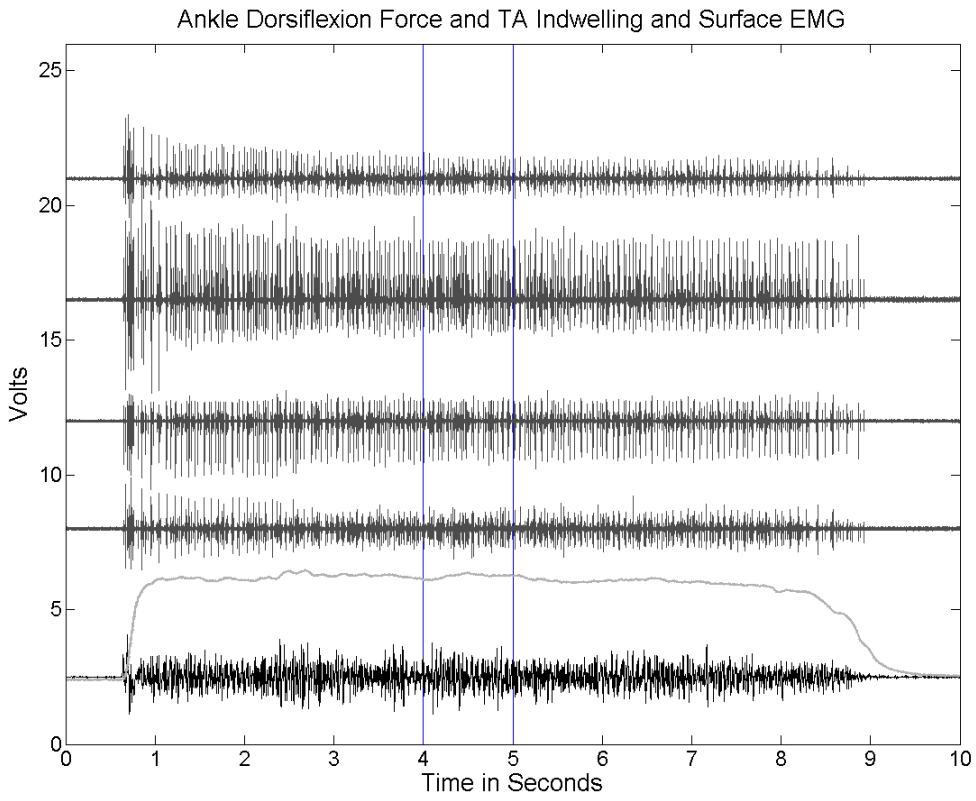

Figure 11. Single trial depiction of force and EMG data at 100% MVC. The top four EMG channels represent the muscle electrical activity recorded from each channel of the quadrifilar needle electrode. The bottom channel represents the muscle electrical activity recorded from the monopolar surface electrodes. Force is shown over the surface EMG channel.

Chapter 4: Results

4.1. Participants

Participant (Females: N=24; Males: N=24) characteristics are presented in Table 2. Skin impedance and temperature were recorded from the TA before and after the testing protocol. The average skin impedance decreased by 0.83 kΩ (Δ11%). No practical significance can be placed on small changes in impedance below 10 kΩ, which is well within the accepted range for sEMG (Hewson et al., 2003). The average skin temperature increased 0.31 degrees Celsius (Δ1%). While the change was small, it was statistically significant (p<0.05). It could be argued that a comparably small change might alter the sEMG signal (Winkel & Jørgensen, 1991; Rutkove, 2000); however, a balanced presentation of experimental conditions ensures that there was no order effect associated with a change in muscle temperature.

Table 2. Means and standard deviations for participants' age and physical characteristics.

Participant Characteristics	**Mean ± SD**
Age (years)	21.77 ± 1.88
Height (cm)	170.50 ± 26.72
Weight (kg)	71.46 ± 16.28
Low Leg Length (cm)	37.92 ± 2.68
Calf Circumference (cm)	37.42 ± 2.59
Foot Length (cm)	25.08 ± 1.74
Malleolus to bottom of foot (cm)	7.64 ± 1.01
Malleolus to metatarsal (cm)	12.26 ± 1.74
Calcaneus to metatarsal (cm)	16.15 ± 2.04

4.2. Data Screening

The data were analyzed for agreement with the statistical assumptions prior to running the repeated measures analysis of variance (ANOVA). Means and standard deviations were calculated for each variable and plotted to show distribution characteristics. There were no values outside of 3 standard deviations from the means. The normal probability plots supported the skewness and kurtosis measures for each cell, all of which were under 3. Mauchly's test of sphericity showed that the assumption of homogeneity of variances was violated ($p < .05$). As with any statistical test, power depends on sample size. Large deviations from sphericity can be non-significant with a small sample size while small deviations can be significant (Field & Miles, 2010). Thus, the results must be interpreted within the sample size context. In the case of the present study, the variance of indwelling measures was on average 6 times greater than that observed for the surface measures. When the numbers between groups are equal and the sample size is large, the *F*-test is robust to even extreme violations in these assumptions (Glass, Peckham, & Sanders, 1972). Further, polynomial trend testing was used as a primary evaluation tool which is the recommended approach when the homogeneity of variances is violated (Tabachnik & Fidell, 2007).

All trials recorded using indwelling EMG had a minimum of three bipolar channels, some had up to four. Each of the first three channels changed in the same way across force for each measure. As a result, the three indwelling EMG channels were averaged across force and the resultant measures were used for data analysis.

4.3. Gender

A split-plot factorial ANOVA was performed on each criterion measure for all channels to test for an interaction between males and females. There were no significant interactions for all but the following: MSS (p = 0.005). Given the sample size and the observed probability values, the observed interaction was deemed to be trivial since males and females exhibited the same statistical trends (Figure 12). In general, the relationship between males and females followed the same trends as those described by Lenhardt et al. (2009), who found no differences between the groups in relation to sEMG. Therefore, the data were collapsed into one group for analysis.

4.4. Fatigue

The data were analyzed for the presence of fatigue from beginning to end of the testing protocol. Force was averaged for the first three trials and the final three trials, which were all performed at 100 percent of MVC. There was a 7 N (Δ 4%, t = 2.22; p = 0.03) decrease in MVC force while RMS (Δ 5%, t = 1.39; p = 0.17) and MPF (Δ 2%, t = -1.33; p = 0.19) for surface recordings remained unchanged. Similar findings were observed for the indwelling EMG. The small magnitude of the observed changes are considered trivial, which is consistent with previous findings wherein a similar number of isometric contractions at different percentages of 100 percent MVC are present within the same test session in balanced order (Gabriel et al., 2007). Overall, EMG data did not exhibit the classic signs of muscle fatigue: a decrease in MPF and an increase in RMS amplitude (Arendt-Nielsen & Mills, 1985, Moritani et al., 1986).

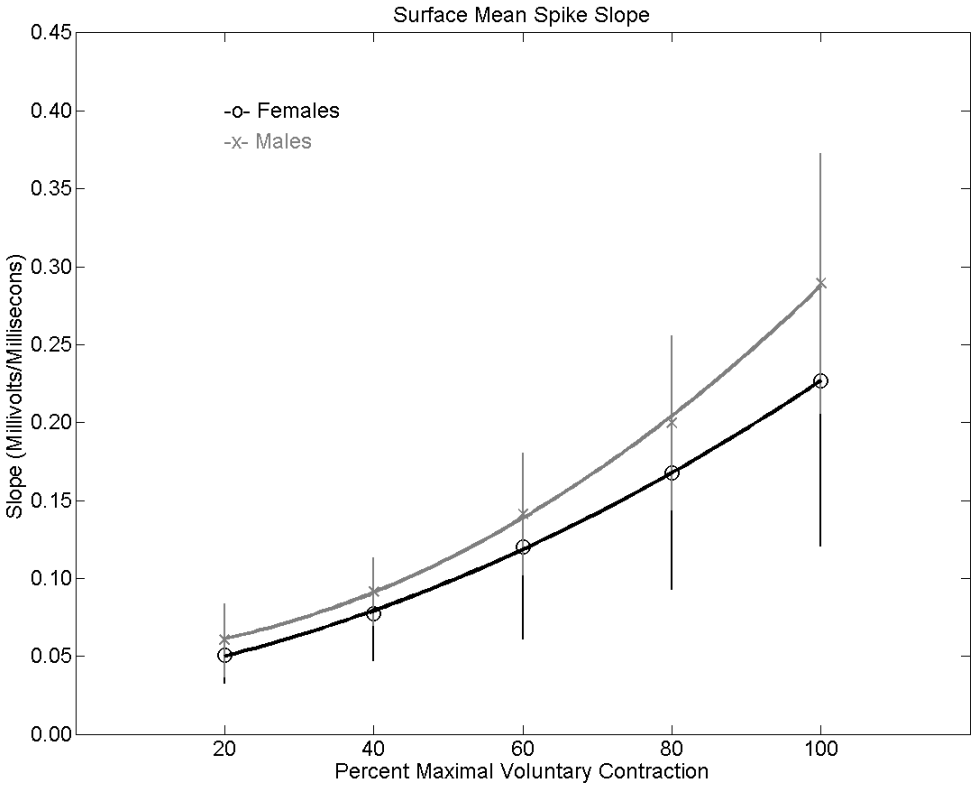

Figure 12. The interaction term for MSS of the third indwelling EMG channel between males and females was significant; however the means followed the exact same quadratic increase with increasing force. This was the only channel of each of the measures than showed a significant interaction.

4.5. Surface versus Indwelling EMG

Figures 13 through 17 show the indwelling needle and surface EMG activity with increasing force from 20 to 100% MVC, in succession. Preliminary analysis of the plots indicated that the criterion measures for each of the three channels followed the same trends. All three indwelling channels were therefore averaged to generate one mean value at each force level for each measure to be compared with the sEMG means. A split-plot factorial ANOVA was then performed on the means for the surface and indwelling EMG. There was one between grouping factor (electrode type) and one within (force levels). Orthogonal polynomial testing was used to compare changes in criterion measures across force levels between the two electrode types.

4.5.1. Amplitude

Root-Mean-Square Amplitude

There was a significant interaction between electrode types ($F_{(4,376)} = 154.39$, $p < .0001$). Orthogonal polynomial testing further revealed significant differences for the linear and quadratic trends. Figure 18 depicts the means and standard deviations for RMS across force levels for both electrode types. Table 3 presents the trend analysis associated with Figure 18. While force increased, there was an overall significant linear increase in RMS amplitude for both surface and indwelling EMG. The linear trend component accounted for the greatest portion of variance in means across force levels; it was 96% and 100% for surface and indwelling, respectively. The RMS amplitude for sEMG also exhibited a quadratic increase (4%).

Mean Spike Amplitude

There was a significant interaction between electrode types ($F_{(4,376)} = 127.78$, $p <$ .0001). Orthogonal polynomial testing further revealed significant differences for the linear and quadratic trends. Figure 19 depicts the means and standard deviations for MSA across force levels for both electrode types. Table 4 presents the trend analysis associated with Figure 19. There was an overall significant linear increase in MSA for both electrode types with increases in force. The linear trend component accounted for the greatest portion of variance in means across force levels; it was 95% and 86% for surface and indwelling, respectively. The MSA for sEMG also exhibited a significant quadratic increase (4.7%) while indwelling EMG did not.

4.5.2. Frequency

Mean Power Frequency

There was a significant interaction between electrode types ($F_{(4,376)} = 46.33$, $p <$ .0001). Orthogonal polynomial testing further revealed significant differences for the linear and cubic trends. Figure 20 depicts the means and standard deviations for MPF across force levels for both electrode types. Table 5 presents the trend analysis associated with Figure 20. While force increased, there was an overall significant linear decrease in MPF for both electrode types. The linear trend component accounted for the greatest portion of variance in means across force levels; it was 67% and 94% for surface and indwelling, respectively. However, the actual pattern of decrease was different between the two electrode types. The MPF for sEMG exhibited a quadratic reduction (28.2%) while indwelling EMG followed a cubic decrease (3.4%).

Mean Spike Frequency

There was a significant interaction between electrode types ($F_{(4,376)} = 117.68$, $p < .0001$). Orthogonal polynomial testing further revealed significant differences for the linear, quadratic, and cubic trends. Figure 21 depicts the means and standard deviations for MSF across force levels for both electrode types, while Table 6 presents the trend analysis associated with the figure. Both electrode types exhibited a different overall relationship with force. The quadratic trend component accounted for the greatest portion of variance (89.9%) for sEMG which exhibited an increase from 20-60% of MVC followed by a subsequent decrease until 100% MVC. In contrast, a linear increase accounted for 95.6% of the indwelling EMG variance. Furthermore, the secondary trend components were not the same. The increase in indwelling EMG MSF was highly curvilinear, plateauing at 80% MVC so that both quadratic (2.6%) and cubic (1.6%) trend components were significant.

Mean Spike Duration

There was a significant interaction between electrode types ($F_{(4,376)} = 6.76$, $p < .0001$). Orthogonal polynomial testing further revealed significant differences for the linear and quadratic trend components. Figure 22 depicts the means and standard deviations for MSD across force levels for both electrode types, while Table 7 presents the trend analysis associated with the figure. There was an overall significant linear increase in MSD for both electrode types with increases in force. While linear trend accounted for the greatest portion of the variance for indwelling EMG (93.2%), it was less than half the variance for sEMG (41.8%). The remaining portion of the variance in

sEMG MSD was accounted for by a quadratic trend (58.1%) component. In contrast, indwelling EMG followed a cubic (6.2%) increase across force levels.

4.5.3. Other Spike Shape Measures

Mean Spike Slope

There was a significant interaction between electrode types ($F_{(4,376)} = 5.35$, $p = 0.0003$). Orthogonal polynomial testing further revealed significant differences for the linear and quadratic trends. Figure 23 depicts the means and standard deviations for MSS across force levels for both electrode types. Table 8 presents the trend analysis associated with Figure 23. Only the sEMG MSS exhibited significant increases with force. The linear trend component accounted for the greatest portion of variance (97.4%) while the rise was slightly quadratic (2.6%).

Mean Number of Peaks Per Spike

There was a significant interaction between electrode types ($F_{(4,376)} = 4.75$, $p = 0.001$). Orthogonal polynomial testing further revealed significant differences for the linear and cubic trends. Figure 24 depicts the means and standard deviations for MNPPS across force levels for both electrode types. Table 9 presents the trend analysis associated with Figure 24. Both electrode types exhibited a different overall relationship with force. The linear trend component accounted for the greatest portion of variance (80.5%) for sEMG which exhibited a decrease with force. In contrast, the linear trend component account for only 46.1% of the indwelling EMG variance but the means increased. Furthermore, the secondary trend components were not the same. The decrease in

MNPPS for sEMG follows a quadratic pattern (17.5%) while the increase for indwelling EMG was cubic (53.3%).

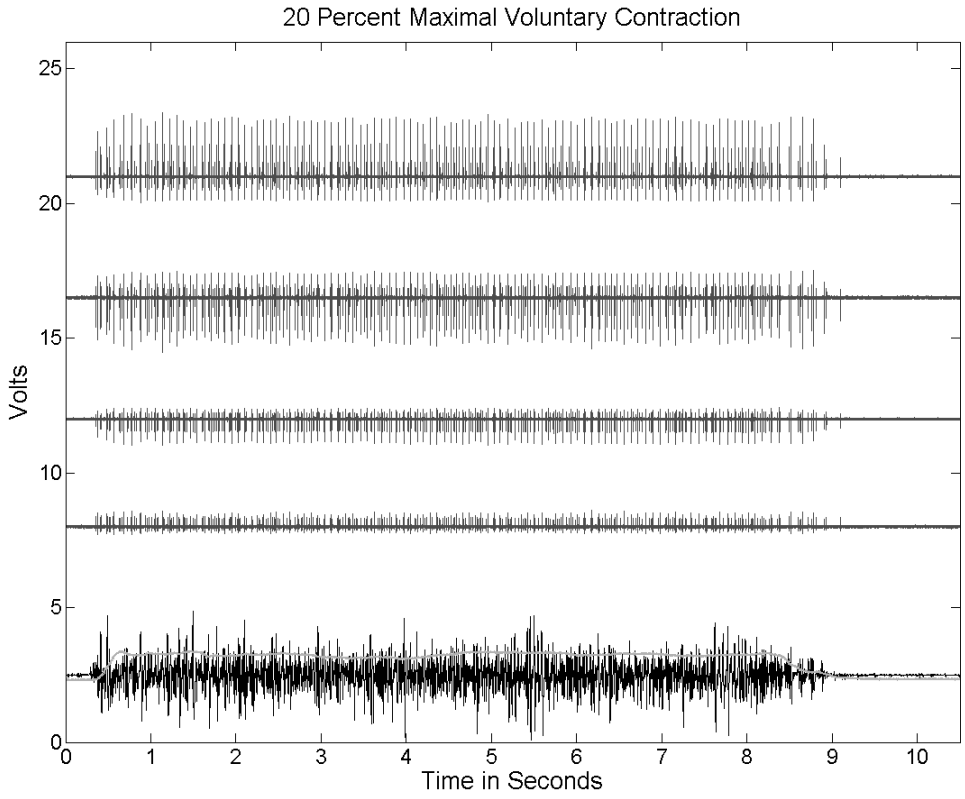

Figure 13. Single trial depiction of force and EMG data at 20% MVC. The top four EMG channels represent the muscle electrical activity recorded from each channel of the quadrifilar needle electrode. The bottom channel represents the muscle electrical activity recorded from the monopolar surface electrodes. Force is shown over the surface EMG channel.

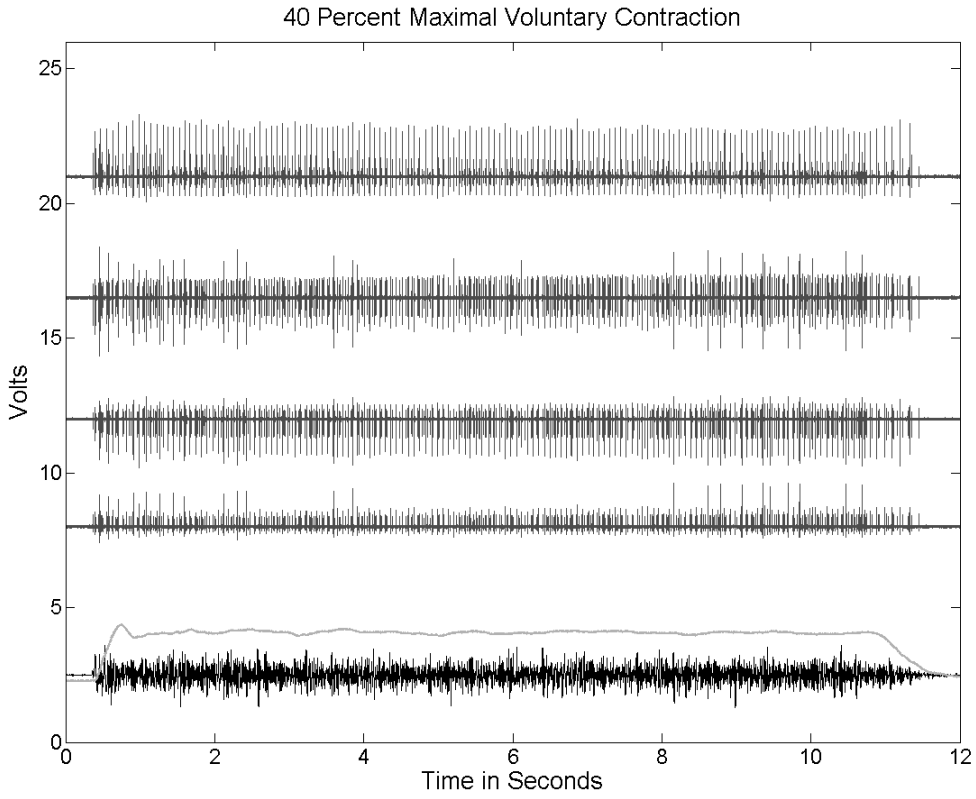

Figure 14. Single trial depiction of force and EMG data at 40% MVC. The top four EMG channels represent the muscle electrical activity recorded from each channel of the quadrifilar needle electrode. The bottom channel represents the muscle electrical activity recorded from the monopolar surface electrodes. Force is shown over the surface EMG channel.

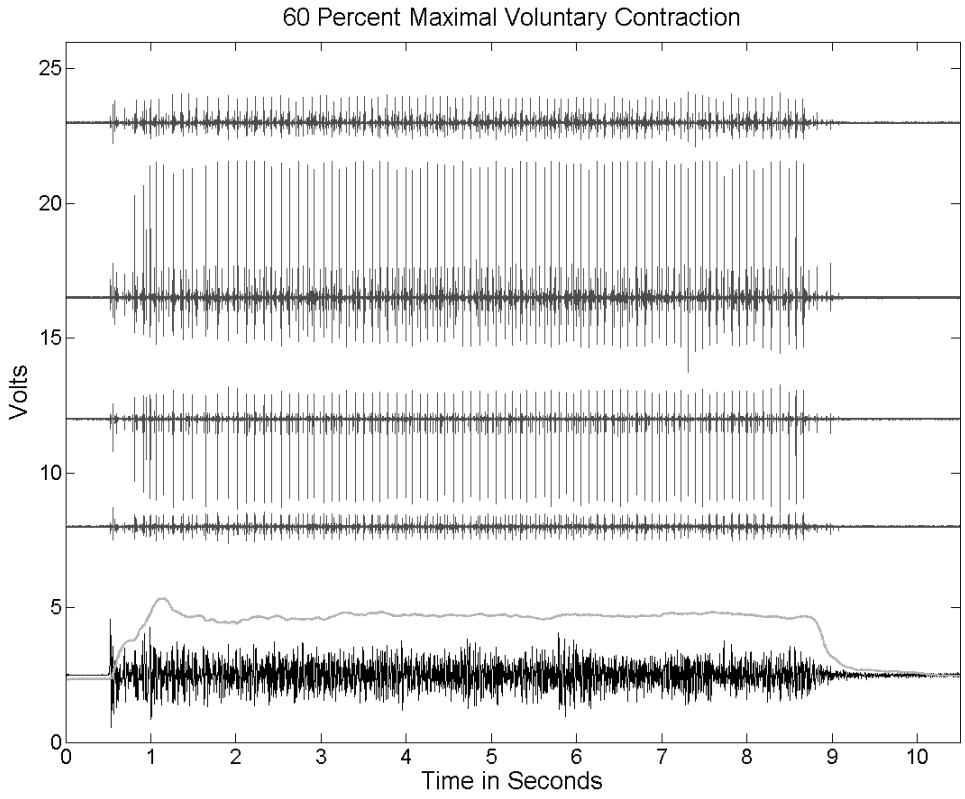

Figure 15. Single trial depiction of force and EMG data at 60% MVC. The top four EMG channels represent the muscle electrical activity recorded from each channel of the quadrifilar needle electrode. The bottom channel represents the muscle electrical activity recorded from the monopolar surface electrodes. Force is shown over the surface EMG channel.

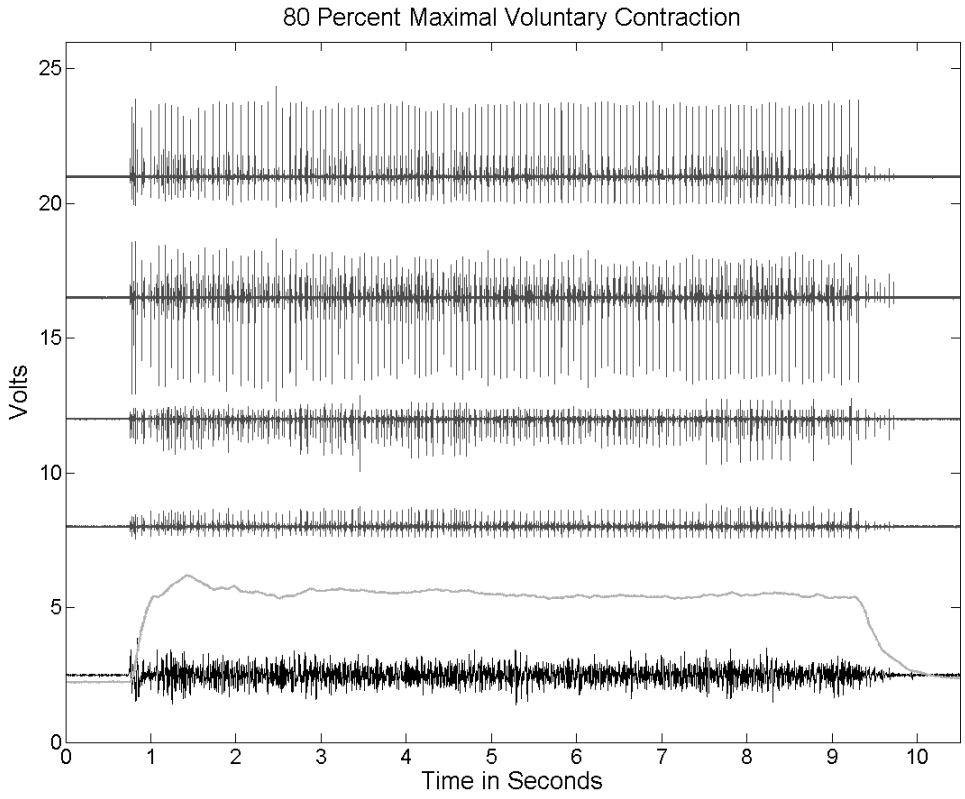

Figure 16. Single trial depiction of force and EMG data at 80% MVC. The top four EMG channels represent the muscle electrical activity recorded from each channel of the quadrifilar needle electrode. The bottom channel represents the muscle electrical activity recorded from the monopolar surface electrodes. Force is shown over the surface EMG channel.

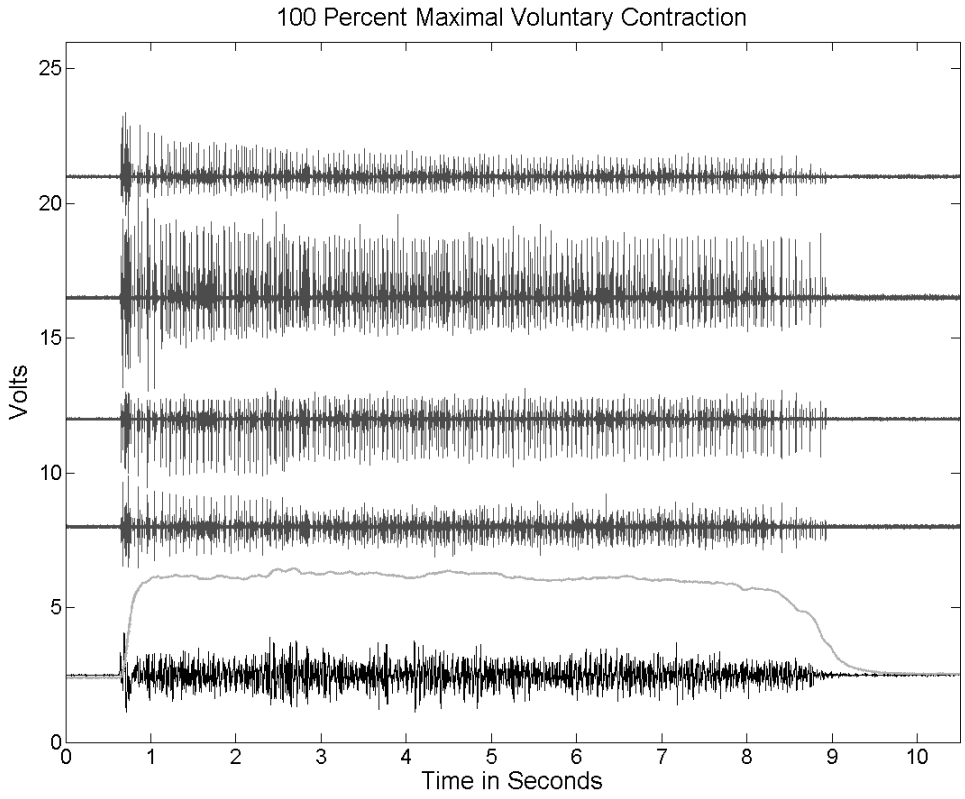

Figure 17. Single trial depiction of force and EMG data at 100% MVC. The top four EMG channels represent the muscle electrical activity recorded from each channel of the quadrifilar needle electrode. The bottom channel represents the muscle electrical activity recorded from the monopolar surface electrodes. Force is shown over the surface EMG channel.

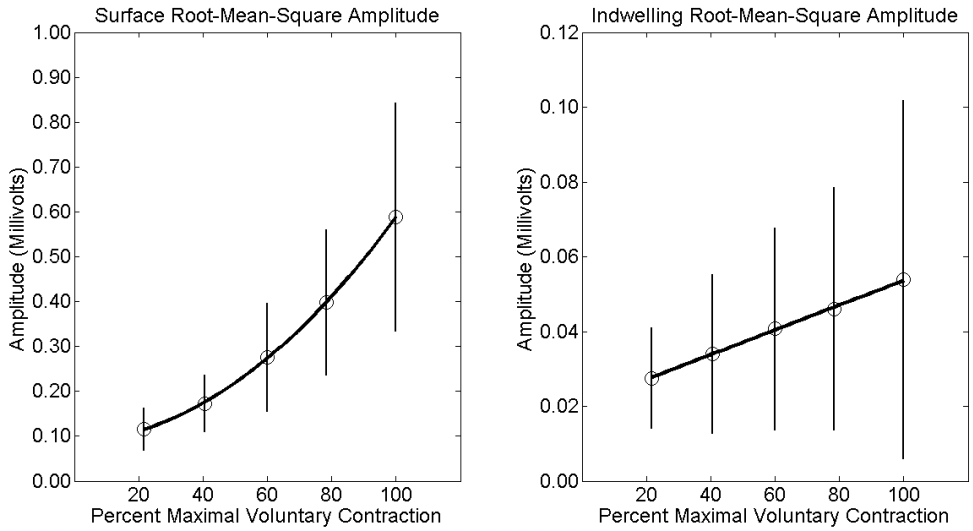

Figure 18. Surface (left) versus indwelling (right) root-mean-square amplitude averaged across participants at each force level.

Table 3. Analysis of variance of RMS. The first row represents the significance of the interaction term between electrode types across trend components. For each proceeding row, the first column shows the significance between electrode types for that particular trend component. The next two columns represent how much of the variance is accounted for (%VAR) by the polynomial trend for surface and indwelling, respectively.

RMS			
		Surface	Indwelling
	p-value	% VAR	% VAR
Interaction (surface × indwelling)	<.0001		
1 Linear	<.0001	95.89%**	99.76%**
2 Quadratic	<.0001	4.02%**	0.03%
3 Cubic	0.2957	0.03%*	0.11%
4 Quartic	0.1053	0.05%**	0.10%

*$p < .05$
**$p < .001$

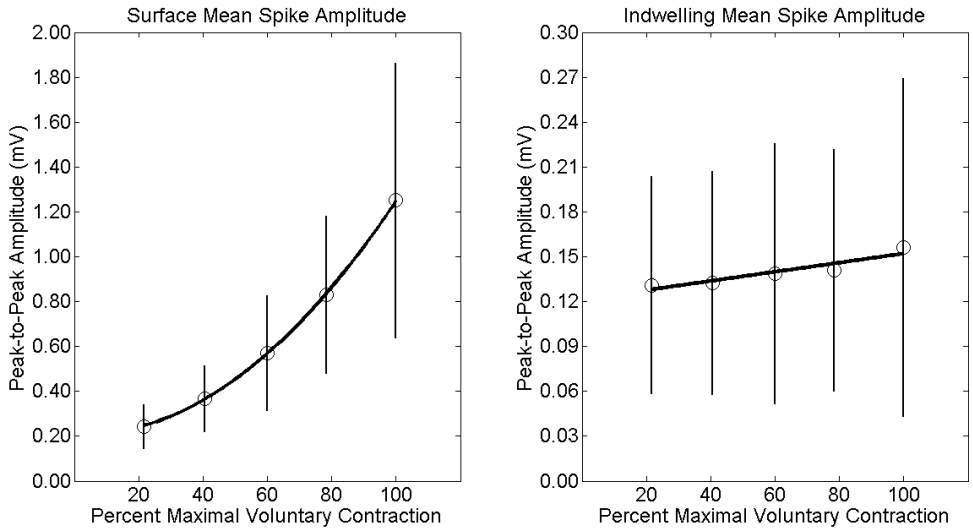

Figure 19. Surface (left) versus indwelling (right) mean spike amplitude averaged across participants at each force level.

Table 4. Analysis of variance of MSA. The first row represents the significance of the interaction term between electrode types across trend components. For each proceeding row, the first column shows the significance between electrode types for that particular trend component. The next two columns represent how much of the variance is accounted for (%VAR) by the polynomial trend for surface and indwelling, respectively.

	MSA		
	Trends*EMG	Surface	Indwelling
	p-value	% VAR	% VAR
Interaction (surface × indwelling)	<.0001		
1 Linear	<.0001	95.21%**	85.95%*
2 Quadratic	<.0001	4.65%**	10.14%
3 Cubic	0.1302	0.10%	1.82%
4 Quartic	0.2216	0.04%	2.09%

*$p < .05$
**$p < .001$

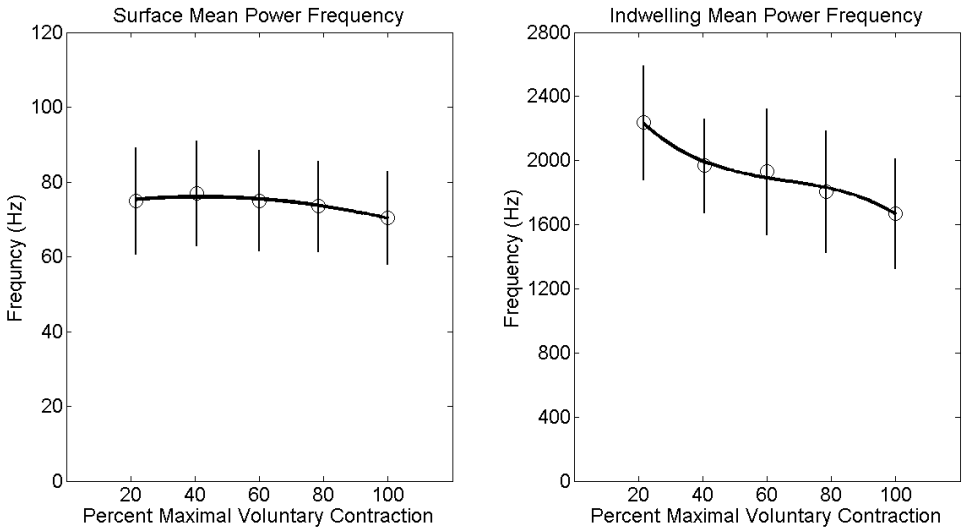

Figure 20. Surface (left) versus indwelling (right) mean power frequency averaged across participants at each force level.

Table 5. Analysis of variance of MPF. The first row represents the significance of the interaction term between electrode types across trend components. For each proceeding row, the first column shows the significance between electrode types for that particular trend component. The next two columns represent how much of the variance is accounted for (%VAR) by the polynomial trend for surface and indwelling, respectively.

	MPF		
	Trends*EMG	Surface	Indwelling
	p-value	% VAR	% VAR
Interaction (surface × indwelling)	<.0001		
1 Linear	<.0001	66.56%*	94.16%**
2 Quadratic	0.1729	28.18%**	1.28%
3 Cubic	0.0019	2.70%	3.36%*
4 Quartic	0.047	2.56%	1.20%

*$p < .05$
**$p < .001$

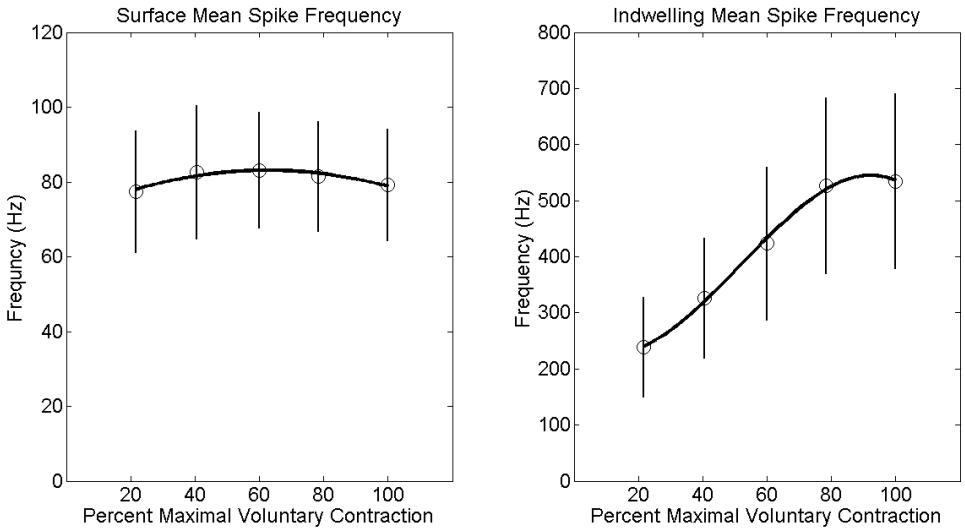

Figure 21. Surface (left) versus indwelling (right) mean spike frequency averaged across participants at each force level.

Table 6. Analysis of variance of MSF. The first row represents the significance of the interaction term between electrode types across trend components. For each proceeding row, the first column shows the significance between electrode types for that particular trend component. The next two columns represent how much of the variance is accounted for (%VAR) by the polynomial trend for surface and indwelling, respectively.

	MSF		
	Trends*EMG	Surface	Indwelling
	p-value	% VAR	% VAR
Interaction (surface × indwelling)	<.0001		
1 Linear	<.0001	2.31%	95.56%**
2 Quadratic	0.0054	89.87%**	2.60%*
3 Cubic	0.0005	7.81%	1.63%**
4 Quartic	0.1906	0.01%	0.21%

*$p < .05$
**$p < .001$

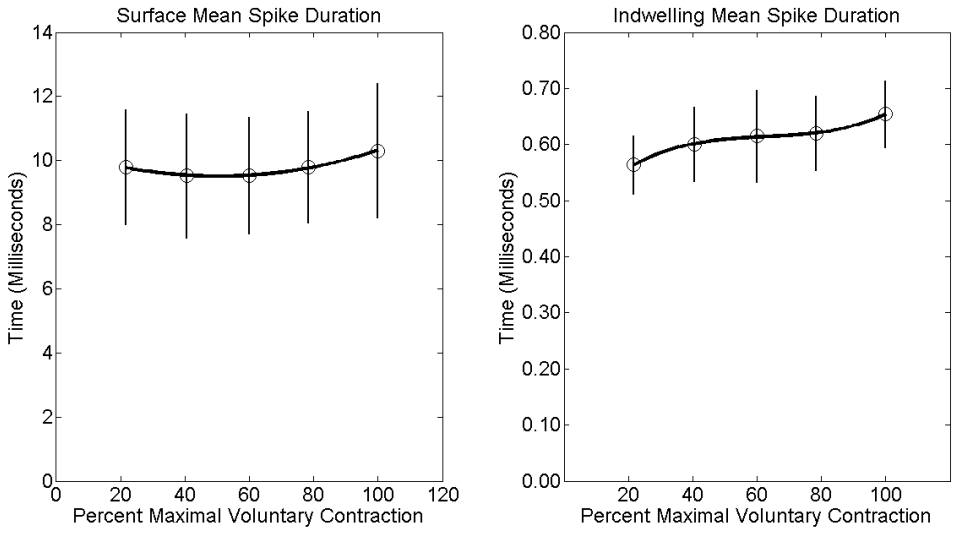

Figure 22. Surface (left) versus indwelling (right) mean spike duration averaged across participants at each force level.

Table 7. Analysis of variance of MSD. The first row represents the significance of the interaction term between electrode types across trend components. For each proceeding row, the first column shows the significance between electrode types for that particular trend component. The next two columns represent how much of the variance is accounted for (%VAR) by the polynomial trend for surface and indwelling, respectively.

	MSD		
	Trends*EMG	Surface	Indwelling
	p-value	% VAR	% VAR
Interaction (surface × indwelling)	<.0001		
1 Linear	0.0493	41.82%*	93.17%**
2 Quadratic	<.0001	58.12%**	0.36%
3 Cubic	0.7392	0.05%	6.18%*
4 Quartic	0.9624	0.01%	0.29%

*$p < .05$
**$p < .001$

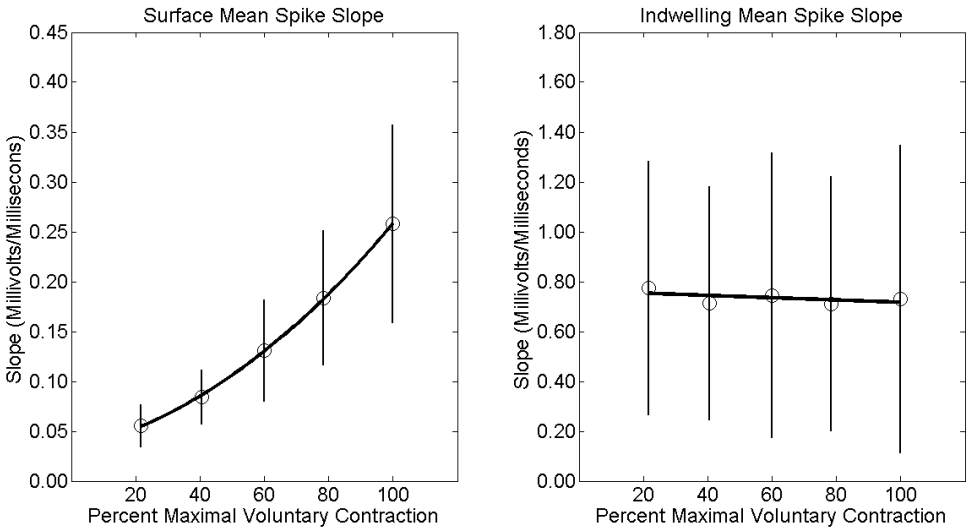

Figure 23. Surface (left) versus indwelling (right) mean spike slope averaged across participants at each force level.

Table 8. Analysis of variance of MSS. The first row represents the significance of the interaction term between electrode types across trend components. For each proceeding row, the first column shows the significance between electrode types for that particular trend component. The next two columns represent how much of the variance is accounted for (%VAR) by the polynomial trend for surface and indwelling, respectively.

	MSS		
	Trends*EMG	Surface	Indwelling
	p-value	% VAR	% VAR
Interaction (surface × indwelling)	0.0004		
1 Linear	<.0001	97.37%**	29.29%
2 Quadratic	0.9966	2.59%**	24.07%
3 Cubic	0.5893	0.01%	6.10%
4 Quartic	0.3732	0.03%	40.54%

*$p < .05$
**$p < .001$

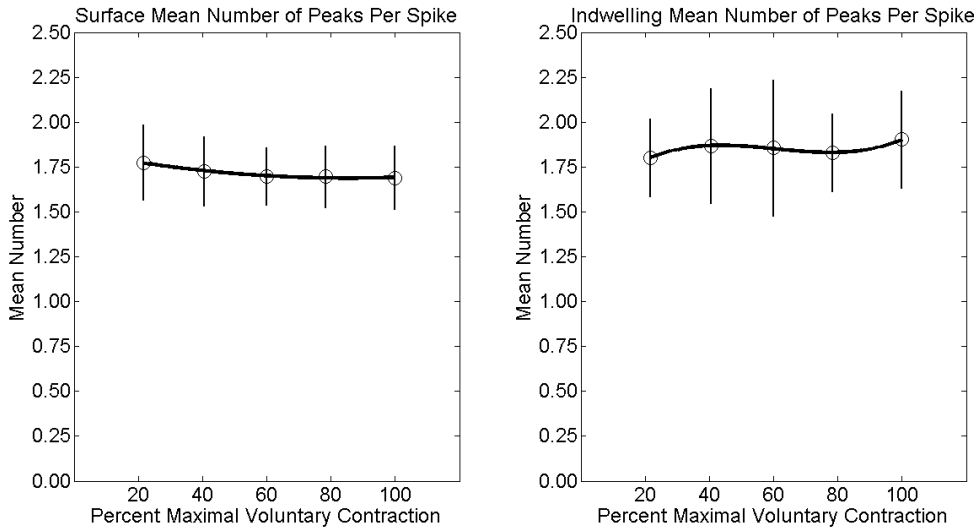

Figure 24. Surface (left) versus indwelling (right) mean number of peaks per spike averaged across participants at each force level.

Table 9. Analysis of variance of MNPPS. The first row represents the significance of the interaction term between electrode types across trend components. For each proceeding row, the first column shows the significance between electrode types for that particular trend component. The next two columns represent how much of the variance is accounted for (%VAR) by the polynomial trend for surface and indwelling, respectively.

	MNPPS		
	Trends*EMG	Surface	Indwelling
	p-value	% VAR	% VAR
Interaction (surface × indwelling)	0.001		
1 Linear	0.0019	80.53%*	46.05%*
2 Quadratic	0.4536	17.50%*	0.01%
3 Cubic	0.0116	1.39%	53.31%*
4 Quartic	0.6086	0.58%	0.64%

*$p < .05$
**$p < .001$

Chapter 5: Discussion

The purpose of this study was to investigate the relationship between indwelling and surface EMG spike shape measures in the tibialis anterior during isometric dorsiflexion contractions at 20, 40, 60, 80, and 100% of MVC. Participants were required to perform a series of three isometric dorsiflexion contractions at each of the desired force levels. Monopolar sEMG and quadrifilar needle EMG measured tibialis anterior activity simultaneously. It was hypothesized that surface and indwelling EMG spike shape measures would exhibit similar trends with increasing isometric force.

The discussion will begin by comparing the present study's 100% MVC values with those obtained in the literature. The comparison will show that the force and EMG methodology resulted in acceptable data. The discussion will show that any differences in absolute magnitude were due to reasonable differences in experimental technique. Next, the EMG-force relationship for traditional measures extracted from the surface and indwelling recordings will be reviewed with respect to findings in the extant literature. The hypothesized parallel between surface and indwelling EMG did not manifest itself. Differences were explained in the interaction between the physical characteristics of the electrode-detection system and volume conduction theory. The discussion will then conclude with "The Good, The Bad, and The Ugly" of interpreting EMG data followed by specific recommendations for future work.

5.1. Comparison with Literature Values

5.1.1. Force

Averaged across male and female participants, maximal isometric dorsiflexion was 170.31±53 N. MacIntosh and Gabriel (2012) reported a nearly identical value (177.67±24.52 N) for maximal isometric dorsiflexion strength averaged across 21 male and 19 female participants, using the same experimental set-up. Maximum isometric dorsiflexion strength for males (200±46 N) in the present study was similar to Green et al. (In Press), 238±58 N using an identical experimental setup, and lower than reports by Lenhardt et al. (2009), 269 ± 61 N, Kent-Braun and Ng (1999), 262±19 N, and Patten and Kamen (2000), 251±8 N. In contrast, average maximum strength for females in this study was 129±38 N, similar to that observed by both Kent-Braun and Ng (1999) and Patten and Kamen (2000), 136±15 N and 150 ±4.2 N, respectively. Lenhardt et al. (2009) showed slightly higher average female force at 191±50 N. Overall, males were 35% stronger than females with respect to maximum isometric dorsiflexion force in this study. This is in agreement with previous evidence supporting that muscle cross-sectional area is the primary determinant of dorsiflexion strength (Miller et al., 1993; Holmbäck et al., 2003). On average, the muscle cross-sectional area is about 20% greater in males (Jaworowski et al., 2002; Holmbäck et al., 2003).

5.1.2. Traditional Measures

The surface RMS amplitude was 0.558±0.254 mV and MPF was 70±12 Hz at 100% MVC. Green, Parro, and Gabriel (In Press) used the same experimental set-up with the exception of a bipolar electrode configuration and reported a RMS amplitude of 0.242±0.063 mV and MPF of 123±27 Hz. Similarly, Lenhardt et al. (2009) reported these measures separately for males and females using a bipolar sEMG configuration. They showed comparable RMS values for males (0.524±0.363 mV) and females (0.508±0.277

mV). The MPF values for males (115±27 Hz) and females (102±27 Hz) were slightly higher. The differences are most likely due to the selectivity of bipolar electrodes with a small (1 cm) inter-electrode distance. The bipolar electrode detection system is sensitive to the most superficial Type II fibers (Sinderby et al., 1996; Lynn et al., 1978, Zipp, 1978; 1982). In contrast, the present study used a monopolar surface electrode configuration. Cioni et al. (1994) is the only other comparable study that used isometric dorsiflexion contractions. Although they did not report average values, based on estimations from their figures, the maximum RMS and MPF magnitudes at 100% MVC for a monopolar sEMG configuration are very similar to those reported here. For the present study, the male and female EMG data were collapsed for analysis because it failed to demonstrate any sex-related differences in the EMG measures, except for MSS which was deemed to be trivial.

There are a limited number of studies that have reported on traditional and spike shape measures obtained from indwelling recording and all have used a concentric needle. Indwelling needle electrode configuration has a significant impact in terms of selectivity and the number of motor units within the pick-up volume (Gath & Stålberg; 1976; 1979; Merletti & Farina, 2009). As a result the magnitudes may not be directly comparable. Data do exist for discrete parameters measured from the motor unit action potential for the tibialis anterior and other muscles (Akaboshi, Masakadi, & Chino, 2000; Brownell & Bromberg, 2007; Boe et al., 2009; 2010), but this is different from the quantification of the interference pattern generated by a bipolar electrode recording needle.

In the present study, indwelling RMS amplitude was 0.054±0.048 mV and MPF was 1670±343 Hz at 100% MVC. The RMS amplitude is much lower than the mean amplitude value (MAV) of 0.987±0.08 mV observed at 80% MVC by Christensen et al. (1984). Liguori, Dahl, and Fuglsang-Frederiksen (1992) reported biceps brachii MAV, of 1.31±0.27 mV for males and 1.04±0.22 mV for females at 60% MVC. The authors stated that there were no appreciable differences in MAV of indwelling concentric needle EMG between the biceps brachii and the tibialis anterior. Christensen et al. (1995) reported on isometric contractions of the biceps brachii at approximately 10% MVC and observed an RMS of 0.159±0.045 mV. The MPF was not reported in a table, but was approximately 200±10 Hz as estimated from their Figure 1, page 31.

The differences in the amplitude and frequency characteristics of the indwelling EMG signal between concentric and bipolar needle electrodes is very similar to the differences that exist between surface electrode configurations. Dumitru, King, Nandedkar (1997) showed that the recording territory of a concentric needle electrode was a sphere similar to macro-EMG electrode and is functionally similar to a monopolar needle. Higher amplitude and lower frequency potentials may therefore be expected (Andreassen & Rosenfalck, 1978). Andreassen and Rosenfalck (1978) studied monopolar versus bipolar needle electrode recordings in the tibialis anterior; they further evaluated the effects of orientation (parallel versus perpendicular) while manipulating inter-electrode distance (25–200 μm). Bipolar needle electrodes with an inter-electrode distance of 50 μm resulted in peak-to-peak amplitude (0.25–0.69 mV) and frequency values consistent with the present observations. A peak power of 2800 Hz was reported for a bipolar parallel orientation and 1800 Hz for perpendicular orientation. The present

study's MPF of 1670±343 Hz observed at 100% MVC is reasonably within this bandwidth (Lateva, Dimitrov, & Dimitrova, 1990). Christensen and Fuglsang-Frederiksen (1986) evaluated the power spectrum and turns of the indwelling EMG interference pattern obtained with a concentric needle electrode. Participants performed isometric contractions of the elbow flexors from 10 to 80% MVC. The MPF at 140 Hz and 1400 Hz was calculated and the ratio of high frequency-to-low frequency (HF/LF) was the main criterion measure. As will be discussed later, increases in force were accompanied by a decreased in the HF/LF ratio. Thus, the MPF observed in the present study is within the main bandwidth of the power spectrum reported by Christensen and Fuglsang-Frederiksen (1986). This research group has demonstrated that relative power at 1400 Hz is a key diagnostic variable in neuromuscular disorders, with very little power at either 2800 or 4200 Hz. (Fuglsang-Frederiksen & Rønager, 1988; Rønager, Christensen, & Fuglsang-Frederiksen, 1989).

The MAV reported by the research is not a true arithmetic MAV. It was calculated as the mean amplitude between pulses divided by the number of turns, which is analogous to MSA in the present study. Both measures are mathematically related to RMS and expectedly larger in magnitude, where $V_{rms}=V_{pp}/\sqrt{2}$. A true mathematical MAV is generally 10% larger than the RMS (Clancy & Hogan, 1999), and is most likely a minor factor. The fact that the bipolar and concentric needle EMG amplitudes are very different but the frequencies are on the same order of magnitude suggests another possible intervening factor. Vertical position relative to the active motor units (Nandedkar, Sanders, & Stålberg, 1988), and longitudinal position away from the innervation zone (Brownell & Bromberg, 2007) both have significant effects on

amplitude but not necessarily the duration of the potentials, which is a key component affecting the power spectrum (Andreassen & Rosenfalck, 1978). Position relative to active motor units influences signal strength (Nandedkar et al., 1988) whereas longitudinal position relative to the motor point determines the degree of temporal dispersion (Brownell & Bromberg, 2007). In the present study, the surface electrode was placed directly over the electrically identified motor point. The needle was then placed close to the edge of the surface electrode, away from the motor point. Anecdotal evidence from participants in past studies indicated that needle insertion close to the motor point is more painful than other locations (Strommen & Daube, 2001).

5.1.3. Spike Shape Measures

No study to date has reported surface EMG spike shape measures for the tibialis anterior, and comparative indwelling data is also limited. Since the biceps brachii and tibialis anterior generate EMG magnitudes that are generally within the same order of magnitude (Christensen et al., 1984; Liguori, Dahl, & Fuglsang-Frederiksen, 1992), data for the biceps brachii will also be used to provide basis of comparison.

The surface MSA was 1.25±0.61 mV at 100% MVC. Gabriel et al. (2007; 2011) studied spike shape measures for ramp (N=8) and step (N=96) isometric contractions of the elbow flexors with a 100% MVC target and reported a MSA of 2.32±0.97 mV and 3.07±1.52 mV, respectively. The values were averaged across male and female participants in near equal numbers. The difference in amplitude between the two studies on the biceps brachii is of the same order of magnitude as the difference between the current findings and the ramp study. Large differences between studies even on the same

muscle are not surprising. It is well-known that there are a myriad of technical and physiological factors that can affect surface EMG amplitude, which makes a direct comparison between studies often difficult (Disselhorst-Klug, Schmitz-Rode, & Rau, 2009).

The surface MSF was 79.2±14.8 Hz at 100% MVC. Mean spike frequency was more comparable than the MSA; it was 86±27 Hz for ramp (Gabriel et al., 2011) and 79.0±11.2 Hz for step (Gabriel et al., 2007) isometric contractions. Mean spike duration is used to calculate MSF, so there is a direct inverse relationship between the two measures. As a result, the MSD observed in the present study of 10.3±2.1 ms is nearly identical to the 10.9±1.6 ms reported by Gabriel et al. (2007). Mean spike slope is similar to MSA in that it is linked with the recruitment of higher threshold motor units (Gabriel et al., 2007; Gabriel et al., 2011). Since MSA for the tibialis anterior was smaller than that for the biceps brachii (Gabriel et al., 2007), it is not surprising that the MSS for the tibialis anterior (0.258±0.099 mV/ms) is smaller than previously reported for the biceps brachii (0.630±0.320 mV/ms). Normal values for the MNPPS at 100% MVC appear to be relatively consistent across studies. The present work observed 1.69±0.27 peaks/spike compared to 1.33±0.10 (Gabriel et al., 2007) and 1.24±0.34 (Gabriel el al., 2011).

Indwelling MSA at 100% MVC was 156±113 μV. This value is lower than 566±444 μV biceps brachii at 100% MVC (Magora & Gonen, 1975) but closer in magnitude to 206±138 μV for 20% MVC (Blank, Gonen, & Magora, 1980). The difference in magnitudes can reasonably be expected due to two interacting factors: (1) the greater selectivity of bipolar versus concentric needle recordings, and (2) the threshold method used to detect EMG spikes themselves.

In comparison to the concentric electrode configuration, bipolar detection records from a smaller volume of tissue encompassing fewer fibers (Nandedkar et al., 1988; Andreassen & Rosenfalck, 1978; Gath & Stålberg, 1976). The bipolar configuration itself also results in lower amplitude and higher frequency signals (Andreassen & Rosenfalck, 1978). Magora and Gonen (1975) used a threshold value of 40 μV, above which an indwelling EMG spike was detected. The present study used a threshold value based on the 95% confidence interval for baseline noise, which on average was 20 μV. Hirose and Uno (1985) studied the effect of threshold level on the quantification of indwelling EMG spikes and showed a precipitous rise in the number of detected spikes as the threshold decreased from 40 to 20 μV. Histograms of the number of motor units within each amplitude and recruitment threshold bin (i.e., frequency counts) are very positively skewed. That is, there are an extraordinarily large number of low-threshold, small amplitude motor unit action potentials compared to high threshold, large amplitude motor units (Stålberg, 1980; Boe, Stashuk, & Doherty 2007; Feiereisen, Duchateau, & Hainaut, 1997; Hogrel, 2003). Magora and Gonen (1975) further demonstrated the same histograms for MSA. A lower threshold, as used in the present study, would therefore include far more low amplitude motor unit action potentials in the calculated averages.

Further comparisons of spike shape measures with the foundational papers of Magora and Gonen (1975) are not straightforward due to experimental methodology and reporting conventions unique to clinical neurology. Further, there are no studies on the tibialis anterior by these investigators. Mean spike frequency was 526.44±157.07 Hz at 100% MVC in the current study. However, a MSF of 238.48±88.63 Hz was observed at 20% MVC, which is comparable to 329±132 Hz at 20% MVC for the biceps brachii

(Magora, Blank, & Gonen, 1980). Another paper by the Magora and Gonen research group reported MSA of 200 μV and a MSF of 185.8 Hz for isometric contraction of the biceps brachii at 50% MVC (Shochina et al., 1989). Mean spike duration was 0.56±0.05 ms at 100% MVC. In separate studies, a MSD of 1.77±0.56 ms (Magora, Blank, & Gonen, 1980) and 1.91±0.84 ms (Blank, Magora, & Gonen, 1980) were reported at 20% MVC for the biceps brachii. The MSD at 20% MVC was 0.60±0.07 ms for the current study. The shorter MSD observed in the present study may be expected as it is used to calculate MSF, which was shown to be higher than previously reported. Mean spike slope was 0.731±0.618 mV/ms at 100% MVC in the current study. Unfortunately, indwelling MSS has not previously been reported in the literature. The MNPPS was 1.90±0.27 at 100% MVC in the current study. At 20% MVC, the MNPPS was 1.80±0.22. The 20% MVC value is nearly identical to 1.82±0.24 reported from the biceps brachii at 20% MVC (Blank, Gonen, & Magora, 1980) and slightly lower than a separate finding of 1.91±0.27 (Magora, Blank, & Gonen, 1980).

5.2. The EMG-Force Relationship

5.2.1. Amplitude

The pattern of amplitude results across force levels in the current study are identical to the findings of Philipson and Larson (1988) who compared surface and indwelling (concentric needle) EMG activity of the biceps brachii during step isometric contractions from 0 to 100% MVC. The surface EMG amplitude measures followed a quadratic increase across force levels while indwelling EMG amplitude measures exhibited a linear increase.

Consistent with previous work, both the RMS and MSA exhibited the same relationship with force (Gabriel et al., 2001; 2011). The EMG-force relationship is affected by both the electrode detection system and physiological factors related to the gradation of force specific to the muscle (Farina et al., 2004; Lawrence & De Luca, 1983). For example, recruitment range is the percent MVC beyond which no more motor units are activated; rate coding is then responsible for the remaining increases up 100% MVC (Lawrence & De Luca, 1983). Muscles with a narrow recruitment range (40-60% MVC) depend on rate coding for the gradation of muscle force and have a non-linear sEMG-force relationship (Fuglevand et al., 1993; Zhou & Rymer, 2004; Keenan et al., 2005). Muscles with a broad recruitment range (80-90% MVC) rely primarily upon the recruitment of additional motor units for the gradation of force and have a more linear sEMG-force relationship (Fuglevand et al., 1993; Zhou & Rymer 2004; Keenan et al., 2005).

The tibialis anterior has a recruitment range of 90% MVC (Feiereisen et al., 1997), so a linear relationship with force might be expected. However, physiological data indicates that motor unit size increases exponentially (Hogrel, 2003; Keenan et al., 2005). The size of motor unit action potentials would therefore increase dramatically towards the end of the recruitment range, as these motor units correspond to higher threshold type II fibers closest to the skin surface (Kamen & Caldwell, 1996; Hogrel, 2003; Mesin et al., 2010). The quadratic surface EMG-force relationship therefore reflects the bias towards type II motor units as the percent MVC increases. Modelling studies have demonstrated that the rate of increase in surface EMG amplitude beyond the recruitment range is also dependent upon motor unit discharge rates and/or the level of synchronization within the

motor unit pool. High discharge rates and synchronization levels can increase the temporal overlap between potentials resulting in greater surface EMG amplitude (Fuglevand et al., 1993; Zhou & Rymer, 2004; Gabriel & Kamen, 2009). However, it has yet to be demonstrated experimentally, which of the two motor unit behaviors is operative. Further, there is evidence that changes in the intracellular action potential can occur independent of alterations in muscle fiber conduction velocity, but can alter the sEMG interference pattern in the same way as synchronization (Arabadzhiev et al., 2010). Described in greater detail in the next section, increased attention is now being given to potential peripheral mechanisms.

The quadratic increase in surface EMG amplitude appears to be a robust finding for the tibialis anterior and has been demonstrated for both monopolar (Cioni et al., 1994) and bipolar electrode configurations (Cioni et al., 1994; Lenhardt et al., 2009). It is tempting to suggest the surface EMG-force relationship for amplitude is mostly explained by anatomical and physiological factors. For example, the biceps brachii is similar to the tibialis anterior in that it has a mixed muscle fiber-type composition (Jaworowski et al., 2002) with a recruitment range up to 90% MVC (Christie et al., 2009). The surface EMG RMS for the biceps also exhibits non-linear increases with force (Philipson & Larson, 1988; Smyth et al., 1990; Pérot et al., 1996; Sbricolli et al., 2003; Hogrel, 2003; Gabriel et al., 2011). The quadratic increase observed for the tibialis anterior was however more pronounced than reported for the biceps; this is consistent with a higher innervation ratio (329 versus 209) as reported by Gath and Stålberg (1981).

Root-mean-square amplitude and MSA for indwelling EMG also mirrored each other across force levels. However, indwelling EMG amplitude exhibited a linear

increase with force. This finding is in agreement with Christensen et al. (1984) who used a concentric needle electrode to investigate the EMG-force relationship up to 100% MVC in the tibialis anterior. The linear increase in indwelling EMG amplitude is most likely a result of two factors. First, the indwelling needle electrode has a bipolar inter-electrode distance of 50 μm. The result is a small pick-up volume that only includes an estimated 5 to 11 motor units contributing to the recorded signal (Nawab et al., 2008). Second, the sampled motor units are deeper within the muscle, which correspond to lower threshold motor units in which changes in size are more linear (Lexell, Downham, & Sjöström, 1986; Knight & Kamen, 2005; Keenan et al., 2005). In contrast, the much larger pick-up volume for the monopolar surface electrode has a conservative estimate of up to 40 motor units of more diverse size contributing to signal energy (Farina et al., 2008; Nawab et al., 2010). A fundamental figure by Fujimoto and Nishizono (1993, Figure 1, page 248) clearly illustrates the effect of the pick-up volume on surface versus indwelling EMG amplitude changes with increasing force. The indwelling EMG increased steadily, while the surface EMG rose dramatically towards the later portion of the ramp increase in force. The effect of pick-up volume is reinforced because Fujimoto and Nishizono (1993) used indwelling wire electrodes with a greater inter-electrode distance and larger pickup volume than a bipolar needle electrode.

5.2.2. Frequency

When examining the frequency content of the EMG signal across force levels, a number of different factors affect the interpretation of the results. The factors include: (1) the gradation of muscle force through neural strategies, (2) technical factors, and (3) issues related to the algorithm used to extract individual spikes from the interference

pattern (Gabriel et al., 2011). The presence of these factors was evident in the pattern of change in MPF versus MSF across force levels. In general, the surface EMG data were consistent with earlier findings for the biceps brachii using a ramp isometric contraction to 100% MVC (Gabriel et al., 2011). Mean power frequency was relatively stable until 60% MVC, and then it exhibited a curvilinear decrease until 100% MVC. In contrast, MSF was more parabolic, increasing to 60% at the apex and then decreasing with continued force.

The findings for MSF follow the conduction velocity data reported by Lange, Van Weerden, and Van der Hoven (2002). Lange et al. (2002) measured muscle fiber conduction velocity with increases in isometric elbow flexion force. Recall, the biceps brachii has the same recruitment range as the tibialis anterior. A steady increase was observed until 50 to 60% MVC. The values stabilized between 60 and 80% MVC, after which there was a decrease until 100% MVC. Lange et al. (2002) also showed that the higher firing rates of lower threshold motor units had a significant impact on the muscle fiber conduction velocity data obtained beyond 50% MVC. As a result, it is reasonable to argue that by 50% MVC, the firing rates of already active motor units have increased to a degree that temporal overlap within the motor unit pool also masks frequency changes associated with newly recruited high threshold motor units (Fuglevand et al., 1993; DeLuca & Erim, 1994).

A number of investigators have reported spectral compression in the surface EMG signal as force progresses towards 100% MVC (Bilodeau et al., 1990; 1992; Sanchez et al., 1993; Sbriccoli et al., 2003; Hagberg and Ericson, 1982; Gerdle et al., 1990; Rainoldi et al., 1999; Beck et al., 2005; Ollivier et al., 2005). Rate-coding of higher threshold

motor units beyond the recruitment range may increase temporal overlap enough to actually decrease the overall frequency content of the surface EMG signal (Fuglevand et al., 1993; Gabriel & Kamen, 2009). Alternatively, modelling studies have suggested that synchronization may be a plausible explanation (Yao, Fuglevand, & Enoka, 2000; Gabriel & Kamen, 2009). In support, there is experimental data which shows an increased tendency for greater levels of motor unit synchronization at 80% MVC but there is not data at higher force levels (Fling, Christie, & Kamen, 2009).

Increased attention is being given to how changes in the intracellular action potential are manifested in the surface EMG signal. In the present study, repeated isometric contractions of the tibialis anterior could have resulted in post-activation potentiation (PAP) of the muscle (Inglis et al., 2011). Arabadzhiev, Dimitrov, and Dimitrov (In Press) have pointed out that post-tetanic potentiation is known to increase the resting free intracellular Ca^{2+} which lengthens the intracellular action potential (IAP) negative afterpotential. The authors suggest that the same could be assumed for PAP. It was shown that the lengthened IAP negative afterpotential could produce the same increases in surface EMG signal as synchronization (Arabadzhiev et al., 2010). Thus, peripheral effects associated with repeated isometric contractions, even in the absence of fatigue, cannot be ignored.

Unlike MPF, calculation of MSF included a threshold criterion. Mean spike frequency is therefore more sensitive to changes in force than MPF because only distinct spikes are used for analysis. As a result, the inclusion of all potentials in the MPF signal exacerbated the effects of temporal overlap on masking changes in the high frequency content of the surface EMG signal until 60% MVC. Rate-coding by higher threshold

motor units and/or synchronization towards the end of the recruitment range increased temporal overlap enough to effect a change in MPF between 60 and 100% MVC. It could be argued that, while the threshold explanation is appealing, other studies have showed that MPF is sensitive to the gradation of muscle force below 60% MVC. Cioni et. al (1994) reported a progressive increase in tibialis anterior MDF during isometric contractions from 10 to 100% MVC using both monopolar and bipolar electrodes. Lenhardt et al. (2009) reported a more mild increase in tibialis MPF during isometric contractions from 20 to 80% MVC, with spectral compression at 100% MVC. The issue is resolved when another study is considered. Gabriel et al. (2011) showed that MPF increased during ramp isometric contractions of the elbow flexors up almost 50% MVC, in agreement with other authors (Bilodeau et al., 1990; 1992; Sanchez et al., 1993; Sbriccoli et al., 2003; Hagberg and Ericson, 1982; Gerdle et al., 1990). However, the MSF was still more sensitive to changes in force because of the threshold criterion (Gabriel et al., 2011).

The comparison between surface and indwelling EMG activity will be discussed with respect to differences predicted by volume conduction theory (Dimitrov & Dimitrova, 1998; Dimitrova et al., 1999; 2002). The volume conduction model developed by Dimitrova and Dimitrov (1996) describes changes in motor unit action potentials as a result of the interaction between a finite volume conductor, the incorporation of non-propagating potentials, and physical characteristics of the electrode detection system. The model was later extended to incorporate neural strategies involved in the gradation of muscle force for step (Gabriel and Kamen, 2009) and ramp isometric contractions (Gabriel et al., 2011) so that changes in the whole EMG interference pattern may be

evaluated. The difference between surface and indwelling EMG is then described in terms of electrode-source distance where “near” recordings correspond to an “extra-territorial” electrode immediately above the muscle (0 mm). A surface electrode corresponds to “far” recordings with the electrode placed farther above the muscle (≥10 mm) to represent electrical activity at the skin surface.

The pattern of means across force levels for indwelling versus surface MPF followed the exact predictions for near versus far recordings, respectively. That is, the degree and pattern of curvature was “sculpted” by electrode-source distance (Gabriel & Kamen, 2009; Gabriel et al., 2011). The greater the electrode-source distance, the less the curvature in the pattern of means across force levels. Commonly referred to as “low-pass tissue filtering” effects, Dimitrova and Dimitrov (1996) have argued against the term. The investigators have demonstrated that alterations in motor unit action potentials associated with electrode-source distance are due to “resistive-capacitive” elements of the volume conductor. Muscle fiber membranes are capacitive while the volume conductor itself is purely resistive. As a result, increases in electrode-source distance disproportionally affect the propagating portion (lower-frequency component) of the motor unit action potential to a greater degree than the non-propagating terminal wave (higher-frequency). Thus, the sensitivity to changes associated with the recruitment of higher threshold motor units decreases the farther away from the muscle the electrode is placed.

In support, the surface MPF means were relatively stable until the upper end of the recruitment range where spectral compression becomes more pronounced. At this point, the higher threshold motor units begin rate-coding and the temporal overlap is

great enough to be detected at the skin surface (Gabriel and Kamen, 2009; De Luca and Erim, 1994). The indwelling MPF exhibited a progressive cubic reduction across force levels. Given the proximity to motor units within the tissue, it might be expected that indwelling recordings would be very sensitive to the temporal overlap of motor unit action potentials due to both rate-coding and recruitment until approximately 60 to 80% MVC. Thereafter, rate-coding and/or synchronization of higher threshold motor units would dominate beyond the recruitment range until 100% MVC. The idea that temporal overlap is responsible for spectral compression is reinforced by more recent contributions to the volume conduction theory (Arabadzhiev et al., 2010). Based on the geometry of the source along the muscle fiber and electrode location (near versus far), recordings within close proximity are "insensitive" to alterations in the intracellular action potentials associated with fatigue. Force and surface EMG at 100% MVC before and after the series of contractions further demonstrated the absence of fatigue, and any lengthening of the intracellular action potential associated with fatigue would not be observed by indwelling recordings.

There is no doubt that electrode-source distance is the main factor involved in differences observed between surface and indwelling EMG activity patterns. The effect of spatial filtering associated with electrode configuration (monopolar versus bipolar) must also play a role. Several investigators have demonstrated that inter-electrode distance has an effect on the curvature of the MPF-force curve, with larger inter-electrode distances resulting in an overall lower MPF and less sensitivity to changes in force (Gerdle et al., 1990; Bilodeau et al., 1994; Beck et al., 2005). Bilodeau et al. (1994) compared the triceps brachii MPF means across force levels for inter-electrode distances

of 6 versus 30 mm. The MPF obtained with a 6 mm inter-electrode distance was greater and it followed the identical cubic decrease observed for the indwelling MPF in the present study. Further still, the 30 mm inter-electrode distance showed very little change across force levels with spectral compression between 80 and 100% MVC, similar to the surface MPF. General high-frequency suppression associated with electrode spatial-filtering is a known factor (Lindström, 1977; Sinderby et al., 1996; Lynn et al., 1978, Zipp, 1978; 1982). However, the progressive decrease in MPF associated with the 6 mm inter-electrode distance was incorrectly interpreted as increased sensitivity to the recruitment of high-threshold motor units which are disproportionately affected by low-pass tissue filtering (Bilodeau et al., 1994). It is believed that low-pass tissue filtering has a disproportionate effect on the higher frequency components of the signal associated with the recruitment of high threshold motor units with higher conduction velocities (Bilodeau et al., 1992; 1994; 1995).

A shorter inter-electrode distance results in increased selectivity from a smaller pick-up volume (Gath & Stålberg, 1977; Lynn et al., 1978, Zipp, 1978; 1982; Nandekar et al., 1984; Nandedkar, Sanders, & Stålberg, 1985), which may reasonably translate to greater sensitivity to physiological changes. However, the cubic decrease in indwelling MPF is consistently an interaction between: (1) the exponential increase in motor unit size, (2) with many lower-threshold motor units discharging at higher rates, (3) superimposed upon the recruitment of fewer higher-threshold motor units that eventually start rate-coding as the force requirements increase (Christensen & Fuglsang-Frederiksen, 1986; Hogrel, 2003; Gabriel & Kamen, 2009; Gabriel et al., 2011). It is very likely that

another muscle with a more limited recruitment range or innervation ratio would result in a different pattern of decrease (Farina, Fosci, & Merletti, 2002; Zhou and Rhymer, 2004).

The difference between indwelling MPF and MSF was predicted in an earlier modelling study, and explained in the same way as the surface measures (Gabriel et al., 2011). The calculation of MSF includes a threshold criterion, which allows only distinct spikes to be used in the analysis. Since MPF includes all waveforms within the data window, potentials rejected by the MSF algorithm, could impact results. Thus, it is logical that indwelling MPF is more sensitive to temporal overlap of waveforms. In contrast, indwelling MSF only captures discrete spikes: overlapping waveforms below the 95% confidence interval for baseline noise would be excluded. In support, Willison turns and MSF are both highly related to the frequency content of the signal and they employ a threshold criterion (Christensen & Fuglsang-Frederiksen, 1986; Gabriel et al., 2001). The indwelling MSF followed the identical pattern of increase with force as observed by Nandedkar, Sanders, and Stålberg (1991) for turns. There was a quadratic increase in the frequency at which the spikes occur up until 80% MVC. The plateau in MSF between 80 and 100% MVC coincides with the recruitment range for the tibialis anterior.

Christensen and Fuglsang-Frederiksen (1986) basically arrived at a similar conclusion, but through a slightly different mechanism. The authors evaluated the power spectrum and turns of the indwelling EMG interference pattern obtained with a concentric needle electrode. Participants performed isometric contractions of the elbow flexors from 10 to 80% MVC. The MPF at 140 Hz and 1400 Hz was calculated and the ratio of high frequency-to-low frequency (HF/LF) was the main criterion measure. A

decrease in the ratio was observed and attributed to a decrease in the high frequency component of the ratio:

> *In contrast, using needle electrodes there is more and more interference and summation of action potentials with increasing force, resulting in cancellation of small spike components (Christensen et al., 1984) with a high frequency content. Thus increasing force associated with increasing summation of action potentials may give rise to a decrease in HF/LF amplitude ratio.*

Linking the number of zero-crossings with the frequency content of the signal, the earlier study in 1984 showed that the measure has a non-linear increase with force, similar to turns. The number of zero-crossings increased rapidly then started to decelerate between 40 and 60% MVC with a 100 μV threshold. The deceleration began earlier between 10 and 20% MVC with a 50 μV threshold. The authors concluded that the 50 μV threshold resulted in greater cancellation effects due to the inclusion of smaller spikes.

Surface MSD showed the same inverse relationship with surface MSF across force levels previously demonstrated for ramp (Gabriel et al., 2011) and step (Gabriel et al., 2007) isometric contractions of the elbow flexors. The relationship is to be expected because MSD is part of the algorithm for calculating MSF. The two separate measures were retained as part of spike shape analysis because MSD has been demonstrated to behave differently than MSF (Viitasalo and Komi, 1977). Indeed, this was the case for the indwelling measures for similar reasons outlined in the Literature Review (see page 47).

Understanding the interference pattern obtained by a needle electrode with an inter-electrode distance of 50 microns, is critical to explaining why indwelling MSD can increase at the same time as MSF. At lower force levels motor unit action potentials appear at lower discharge rates. The selectivity of the needle electrode records only a few motor units. There are relatively large intervals between potentials in the indwelling signal (see Figure 13). As force increases between 20 and 40% MVC, more motor units are recruited and already active motor units discharge more frequently. Motor unit action potentials superimpose to create longer duration, higher amplitude spikes. However, because of the selectivity of the recordings, the absence of more distant potentials means there are more discrete spikes per second. The recruitment and rate coding process continues between 40 and 80% MVC, but increases in MSD were more gradual because the absolute duration of each spike is small (see Figure 15). There was a distinct increase in MSD while MSF plateaued beyond the recruitment range (>80% MVC). At this point, the indwelling interference pattern appears very dense (see Figure 17). The temporal overlap is significant enough to lengthen the average duration of each spike so that there are no further increases in frequency. In support, the MSD and MSF for both experimental and simulated EMG (Gabriel et al., 2011) exhibited the trends observed in the present work. Below 20% MVC, the MSF increased while MSD duration remained unchanged. As force increased from 0 to 20% MVC, discrete motor unit action potentials populated the interference pattern with little to no temporal overlap. This effect is illustrated in Figure 1, page 259 in MacIntosh and Gabriel (2012). Individual motor unit action potentials in the tibialis anterior can be detected from the skin surface at very low

force levels, up to even 30% MVC using ordinary surface electrodes. The noise between the spikes would be rejected by the threshold criterion.

5.2.3. Other Spike Shape Measures

Mean spike slope is similar to MSA because it increases with the recruitment and rate-coding throughout the force gradation process for the same reasons (Gabriel et al., 2007; Gabriel et al., 2011). Likewise, results for MSS were also affected by differences in pick-up volume between surface and indwelling electrodes. The much larger pick-up volume for the monopolar surface electrode will have a greater number of motor units (≈40) of more diverse size contributing to signal energy (Farina et al., 2008; Nawab et al., 2010). Similar to MSA, there was a quadratic increase in MSS. In contrast, the small pick-up volume for the needle electrode includes only a small number of motor units (≈5-11) contributing to the signal (Nawab, Wotiz, & De Luca, 2008). The tissue deeper within the muscle most likely includes lower threshold motor units where changes in size might not be as great as towards the surface, closer to where the higher threshold motor units are located (Lexell et al., 1986; Knight & Kamen, 2005; Keenan et al., 2005). It is not surprising therefore that there was no appreciable change in indwelling MSS.

The MNPPS is based on the percent total number of spikes that have 1, 2, and 3 or more peaks (Magora & Gonen, 1970; 1975). The number of peaks per spike is determined by the unique "types" of superposition associated with different motor unit activity patterns: recruitment, rate-coding, and synchronization. The initial work was completed using indwelling needle (concentric) electrodes on patient populations (Shochina et al., 1992). The present work is the first to directly compare the surface and

indwelling measures. The MNPPS followed a quadratic decrease across force levels, which has been demonstrated for both maximal isometric (Gabriel et al., 2007; Gabriel et al., 2011) and isotonic (Gabriel, 2000) contractions of the elbow flexors. Modelling work suggested that the decrease in MNPPS with increases in force is due to temporal overlap between motor unit action potentials (superposition) associated with normal recruitment and rate coding throughout the force gradation process (Gabriel et al., 2011). While the underlying physiology may be correct, direct measurement of indwelling MNPPS indicates that physiology is not the only thing that affects the surface EMG signal.

The linear increase in the indwelling MNPPS is exactly consistent with the findings and expectations of Magora and Gonen (1975). Force gradation by recruitment and rate coding should increase the MNPPS, reflecting more asynchronous activity within the motor unit pool. Conversely, a decrease in the MNPPS would indicate more synchronous activity. Thus, it would appear that the surface MNPPS is subject to significant electrode-source distance effects, suppressing the higher frequency component of the signal (Lateva, Dimitrov, & Dimitrova, 1990). Modelling work by Gabriel et al. (2011) failed to reveal these effects as the near recordings were extraterritorial and still subject to high frequency suppression associated with the volume conductor, but to a much lesser degree than the simulated far recordings (Dimitrova & Dimitrov, 2002; Arabadzhiev et al., 2008a; 2008b).

5.3. The Good, The Bad, and The Ugly

It would appear that the pattern of means in the EMG-force relationship fit anatomical and physiological data too conveniently. The explanation provided is

parsimonious because it links both the amplitude and frequency data together, without having to incorporate separate theories. Moreover, the data follow the exact predictions for a finite volume conductor. When interpreting surface EMG data, the following quote must always be kept uppermost in mind: "*The most consistent finding in surface EMG is inconsistent findings*" (Gabriel & Kamen, 2008).

The relationship between electrode pick-up area and the relatively small number of recorded motor units was used to explain the linear relationship between indwelling EMG amplitude and force. Support was provided by Christensen et al. (1984) who also observed a linear increase in indwelling EMG amplitude obtained with a concentric needle and isometric dorsiflexion force from 10 to 100% MVC. However, Christensen et al. (1991) reported a quadratic increase in indwelling EMG amplitude for the tibialis anterior under identical conditions in a later study. There was a great deal of emphasis placed on how the quadratic increase in surface EMG magnitude is closely linked with the exponential increase in motor unit size in combination with rate-coding and/or some level of synchronization. Further evidence was given that it might be a more general finding because the same results have been obtained in the biceps brachii (another flexor) which has similarities related to motor unit size increase and recruitment range. Yet, Gabriel and Kamen (2009) and other investigators (Dupont, Gamet, & Pérot, 2000; Beck et al., 2005) have demonstrated a linear increase in biceps brachii surface EMG amplitude with force. Beck et al. (2005) even provided evidence that the linear increase also was independent of electrode spatial filtering. Both Pérot et al. (1996) and Dupont et al. (2000) did however show that the linear relationship between biceps EMG amplitude and elbow flexion force can be modified by muscle synergies associated with the addition of

wrist supination. Methodological controls over task performance should have prevented "trick" or "substitution" movements that would involve other muscles. Synergistic muscle activity (i.e., flexor digitorum longus) was not monitored directly in the present study, so it is possible that the data may reflect the coactivation of muscles not directly involved in the task.

Discrepancies between findings for the EMG-force relationship have also been attributable to the nature of the task: step versus ramp isometric contractions that encompass the same range of force levels (Bilodeau et al., 1991). Bilodeau et al. (1991) showed that the pattern of increase in MPF and MDF of triceps brachii and anconeus were different for ramp versus step increases in isometric force from 10 to 80% MVC.

Experiments that measured motor unit action potentials (Moritani and Mauro, 1987), muscle fiber conduction velocity (Roy, De Luca, & Schneider, 1986; Sbriccoli et al., 2003; Lange et al., 2002), and peripheral nerve stimulation of motor units according to size (Solomonow et al., 1990), have all demonstrated the MPF and/or the MDF were directly affected by the progressive recruitment of higher threshold motor units. It is therefore reasonable to believe that different patterns of increase in spectral characteristics of the EMG signals would suggest different recruitment strategies for step versus ramp contractions. However, in a later study, Bilodeau et al. (1994) failed to demonstrate any such differences between step and ramp isometric contractions for the gastrocnemius and soleus. Further, other studies have, for example, shown a quadratic increase in RMS EMG for both step and ramp contractions of the biceps brachii (Sbriccoli et al., 2003; Gabriel et al. 2011) and the tibialis anterior (Siegler et al., 1985; Philipson & Larsson, 1988). Siegler et al. (1985) also demonstrated that the degree of

curvature could also be affected by signal processing methods and the degree of digital low-pass filtering. In the present study, it was the use of noise rejection through a threshold criterion. Even if a consistent relationship can be shown, caution must be exercised when linking curve shape to neural control strategies without understanding the moderating effects of anatomical factors or volume conduction theory (Farina et al., 2002; Farina, Merletti, & Enoka, 2004; Dimitrova & Dimirov, 2003; Arabadzhiev et al., 2008a; 2008b).

Spike shape analysis has been in development for over 14 years, and the present study is the first attempt to validate the proposed relationships between the surface and indwelling EMG activity patterns (see Table 1). As a result the Electromyographic Kinesiology Laboratory has a deeply rooted interest in presenting only those results that are consistent with the theory. The following summary should demonstrate that this is not the case. The goal of the current work is to determine if surface and indwelling EMG measures followed the same pattern of change with increasing force levels. Root-mean-square amplitude and MSA were observed to have the same EMG-force relationship, but the surface and indwelling measures exhibited different patterns of change, quadratic versus linear, respectively. Surface mean spike slope increased quadratically while the indwelling measure remained unchanged. Independently, the surface and indwelling frequency measures behaved differently. Mean spike frequency was more sensitive to changes in force than MPF, exhibiting increases and decreases consistent with recruitment and rate-coding. Surface MPF remained stable until spectral compression was significant only at the highest force levels. Further still, the frequency measures of the surface EMG also behaved very differently compared to the indwelling. Indwelling MPF

exhibited a cubic decrease while MSF increased. The differences between traditional and spike shape measures were easily explained on the basis of a threshold criterion for the inclusion of muscle electrical activity in the analysis. Differences between surface and indwelling measures were easily explained on the basis of the interaction of: (1) the threshold criterion with (2) electrode pick-up area, and (3) electrode-source distance effects due to volume conduction. The three factors were most evident in the disconnection between MSD and MSF.

The recent modelling study suggested that there may be a problem with the MNPPS measure, and attributed the difficulty with the noise rejection portion of the threshold criterion (Gabriel et al., 2011). The present work indicated that the problem may be more serious than a computer algorithm. The MNPPS is the most critical measure with the greatest clinical application, indicating asynchronous versus synchronous motor unit behavior. First, interpretation of MNPPS is based on clinical data obtained on neuropathic versus myopathic patients who are known to have more "asynchronous" versus "synchronous" motor unit activity patterns. Interpretation of the MNPPS has not yet been validated through direct measurement. Further still, there is modelling work suggesting the observed EMG activity patterns may be due to peripheral changes within muscle itself associated with the flow of Ca^{2+}, not central adaptations in motor unit behavior (Arabadzhiev et al., 2008a; 2008b; 2010). Failure to observe the predictions for the MNPPS also revealed a weakness in the surface EMG modelling approach, as it did not account for "intraterritorial" EMG recording characteristics.

There are three factors that could have affected the results but were not under the control of the investigator. First, anxiety may have had an effect on the individual's

performance due to the presence of a needle electrode. This could have changed physiological factors that would affect the identification of muscle activity through surface electrodes. This could mean an increase in body temperature, an increase in perspiration, and other physical changes associated with anxiety (Jan et al., 1999; Strommen & Daube, 2001; Finsterer, 2004; Abdoli-Eramaki et al., 2012). Second, training history could have influenced the results; however, this information was collected using self-report and the level of detail and accuracy was not sufficient to include in the overall analysis of the EMG to force relationship. Third, body composition was also not included in the overall analysis. Although the TA is generally associated with a smaller amount of subcutaneous tissue, which is good for surface EMG recording, there may be value in performing this research on a smaller muscle (i.e. a hand muscle). The goal would be to eliminate a possible effect of body composition on the EMG to force relationship (De la Barrera & Milner, 1994; De Vito, McHugh, & Riches, 2003; Nordander et al., 2003; Bartuzi et al., 2010; Park & Ty Hopkins, 2011).

5.4. Recommendations for the Future

1. Modify the sEMG model to include “intraterritorial” recordings.

2. Directly assess the relationship between synchronization and MNPPS using surface and indwelling needle recordings.

3. Directly assess the relationship between changes in the intracellular action potentials and surface and indwelling spike shape measures.

4. Conduct simultaneous recordings using surface and indwelling bipolar wire electrodes. The main technical limitation to the present study was the highly selective needle electrode. The small pick-up volume limited the number of motor units involved in the recordings. Bipolar wire electrodes will still allow for the development of a full interference pattern while minimizing the electrode-source distance effects (Gabriel et al., 2004; Backus et al., 2011). A comparison of EMG activity for surface versus indwelling bipolar wire electrodes would therefore be more valid comparison of interference pattern measures.

References

Abdoli-Emramaki, M., Damecour, C., Christenson, C., and Stevenson, J. (2012). The effect of perspiration on the sEMG amplitude and power spectrum. *Journal of Electromyography and Kinesiology*. 22, 908-913.

Adam, A. and De Luca, C. J. (2005). Firing rates of motor units in human vastus lateralis muscle during fatiguing isometric contractions. *Journal of Applied Physiology*. 99, 268-280.

Adrian, E. D., and Bronk, D. W. (1928). The discharge of impulses in motor nerve fibres Part I. Impulses in single fibres of the phrenic nerve. *The Journal of Physiology*. 66(1), 81-101.

Akaboshi, K., Masakado, Y., and Chino, N. (2000). Quantitative EMG and motor unit recruitment threshold using a concentric needle with quadrifilar electrode. *Muscle & Nerve*. 23, 361-367.

Andreassen, S. and Rosenfalck, A. (1978). Recording from a single motor unit during strong effort. *IEEE Transactions on Biomedical Engineering*. BME-25 (6), 501-508.

Andreassen, S. and Arendt-Nielsen, L. (1987). Muscle fibre conduction velocity in motor units of the human anterior tibial muscle: a new size principle parameter. *Journal of Physiology*. 391, 561-571.

Arabadzhiev, T. I., Dimitrov, G. V., Chakarov, A. G., and Dimitrova, N. A. (2008a). Effects of changes in intracellular action potential on potentials recorded by single-fiber, macro, and belly-tendon electrodes. *Muscle & Nerve*. 37, 700-712.

Arabadzhiev, T. I., Dimitrov, G. V., Chakarov, A. G., Dimitrov, A. G., and Dimitrova, N. A. (2008b). Changes in intracellular action potential profile affect parameters used in turns/amplitude analysis. *Muscle & Nerve*. 37, 713-720.

Arabadzhiev, T. I., Dimitrov, V. G., Dimitrova, N. A., and Dimitrov, G. V. (2010). Influence of motor unit synchronization on amplitude characteristics of surface and intramuscularly recorded EMG signals. *European Journal of Applied Physiology*. 108, 227-237.

Arabadzhiev, T. I., Dimitrov, V. G., and Dimitrov, G. V. (In Press). The increase in surface EMG could be a misleading measure of neural adaptation during the early gains in strength. *European Journal of Applied Physiology*.

Arendt-Nielsen, L. and Mills, K. R. (1985). The relationship between mean power frequency of the EMG spectrum and muscle fibre conduction velocity. *Electroencephalography and Clinical Neurophysiology*. 60, 130-134.

Backus, S. I., Tomlinson, D. P., Vanadurongwan, B., Lenhoff, M. W., Cordasco, F. A., Chehab, E. L., ... Hillstrom, H. J. (2011). A spectral analysis of rotator cuff musculatlure electromyographic activity: Surface and indwelling. *Hospital for Special Surgery Journal*. 7, 21-18.

Baratta, R. V., Solomonow, M., Zhou, B.-H., and Zhu, M. (1998). Methods to reduce the variability of EMG power spectrum estimates. *Journal of Electromyography and Kinesiology*. 8, 279-285.

Bartuzi, P., Tokarski, T., and Roman-Liu, D. (2010). The effect of the fatty tissue on EMG signal in young women. *Acta of Bioengineering and Biomechanics*. 12 (2), 87-92.

Basmajian, J. V. (1972). Electromyography comes of age. *Science*. 176(4035), 603-609.

Basmajian, J. V. and De Luca, C. J. (1985). *Muscles alive: their functions revealed by electromyography*. *5th Edition.* Baltimore, MD: Williams & Wilkins.

Beach, J., Gornian, G. C., and Gans, C. (1982). A method for quantifying electromyograms. *Journal of Biomechanics*. 15 (8), 611-617.

Beck, T. W., Housh, T. J., Cramer, J. T., Malek, M. H., Mielke, M., Hendrix, R., and Weir, J. P. (2007). A comparison of monopolar and bipolar recording techniques for examining the patterns of responses for electromyographic amplitude and mean power frequency versus isometric torque for the vastus lateralis muscle. *Journal of Neuroscience Methods*. 166, 159-167.

Bell, D. G. (1993). The influence of air temperature on the EMG/force relationship of the quadriceps. *European Journal of Applied Physiology*. 67, 256-260.

Biel, A. *Trail guide to the body. Third edition.* Boulder, CO: Books of Discovery, 2005.

Bigard, A., Sanchez, H., Claveyrolas, G. Martin, S., Thimonier, B. and Arnaud, M. (2001). Effects of dehydration and rehydration on EMG changes during fatiguing contractions. *Medicine and Science in Sport and Exercise*. 33(10), 1694-1700.

Bigland-Ritchie, B., Donovan, E. F., and Roussos, C. S. (1981). Conduction velocity and EMG power spectrum changes in fatigue of sustained maximal efforts. *Journal of Applied Physiology*. 51 (5), 1300-1305.

Bigland-Ritchie, B., Johansson, R., Lippold, O. C. J., Smith, S., and Woods, J. J. (1983). Changes in motorneurone firing rates during sustained maximal voluntary contractions. *Journal of Physiology*. 340, 335-346.

Bilodeau, M., Arsenault, A. B., Gravel, D., and Bourbonnais, D. (1990). The influence of an increase in the level of force on the EMG power spectrum of elbow extensors. *European Journal of Applied Physiology*. 61, 461-466.

Bilodeau, M., Arsenault, A. B., Gravel, D., and Bourbonnais, D. (1991). EMG power spectra of elbow extensors during ramp and step isometric contractions. *European Journal of Applied Physiology*. 63, 24-28.

Bilodeau, M., Arsenault, A. B., Gravel, D., and Bourbonnais, D. (1992). Influence of gender on the EMG power spectrum during an increasing force level. *Journal of Electromyography and Kinesiology*. 2 (3), 121-129.

Bilodeau, M., Goulet, C., Nadeau, S., Arsenault, A. B., and Gravel, D. (1994). Comparison of the EMG power spectrum of the human soleus and gastrocnemius muscles. *European Journal of Applied Physiology*. 68, 395-401.

Bilodeau, M., Cincera, M, Gervais, S., Arsenault, A. B., Gravel, D., Lepage, Y., and McKinley, P. (1995). Changes in the electromyographic spectrum power distribution caused by a progressive increase in the force level. *European Journal of Applied Physiology*. 71, 113-123.

Blanchi, J. P. and Vila, A. (1985). Numerical analysis of electromyographic signals: Definition of three parameters for functional muscular value analysis. *Electromyography and Clinical Neurophysiology*. 25, 245-252.

Blank, A., Gonen, B., and Magora, A. (1980). The electrophysiologic pattern of development of muscular fatigue in muscular dystrophy. *Electromyography and Clinical Neurophysiology*. 20, 3-18.

Boe, S. G., Stashuk, D. W., Doherty, T. J. (2007). Motor unit number estimates and quantitative motor unit analysis in healthy subjects and patients with amyotrophic lateral sclerosis. *Muscle & Nerve*. 36, 62-70.

Boe, S. G., Dalton, B. H., Harwood, B., Doherty, T. J., and Rice, C. L. (2009). Inter-rater reliability of motor unit number estimates and quantitative motor unit analysis in the tibialis anterior muscle. *Clinical Neurophysiology*. 120, 947-952.

Boe, S. G., Antonowicz, N. M., Leung, V. W., Shea, S. M., Zimmerman, T. C., and Doherty, T. J. (2010). High inter-rater reliability in analyzing results of decomposition-based quantitative electromyography in subjects with or without neuromuscular disorder. *Journal of Neuroscience Methods*. 192, 138-145.

Bowden, J. L. and McNulty, P. A. (2012). Mapping the motor point in the human tibialis anterior muscle. *Clinical Neurophysiology*. 123, 386-392.

Broman, H., De Luca, C. J., and Mambrito, B. (1985). Motor unit recruitment and firing rates interaction in the control of human muscles. *Brain Research*. 337, 311-319.

Bromberg, M. B. and Spiegelberg, T. (1997). The influence of active electrode placement on CMAP amplitude. *Electroencephalography and Clinical Neurophysiology*. 105, 385-389.

Brown, R. E., Bruce, S. H., and Jakobi, J. M. (2009). Is the ability to maximally activate the dorsiflexors in men and women affected by indwelling electromyography needles?. *Archives of Physical Medicine and Rehabilitation*. 90(12), 2135-2140.

Brown, A. H. M., Brookham, R. L., and Dickerson, C. R. (2010). High-pass filtering surface EMG in an attempt to better represent the signals detected at the intramuscular level. *Muscle & Nerve*. 41, 234-239.

Brownell, A. A. and Bromberg, M. B. (2007). Effects of intramuscular needle position on motor unit action potential metrics. *Muscle & Nerve*. 35, 465-470.

Brownell, A. A. and Bromberg, M. B. (2009). Effects of high-pass filtering on MUAP metrics. *Muscle & Nerve*. 40, 1008-1011.

Buchthal, F., Pinelli, P., and Rosenfalck, P. (1954). Action potential parameters in normal human muscle and their physiological determinants. *Acta Physiologica Scandinavia*. 32, 219-229.

Calder, K. M., Agnew, M. J., Stashuk, D. W., and McLean, L. (2008). Reliability of quantitative EMG analysis of the extensor carpi radialis muscle. *Journal of Neuroscience Methods*. 168, 483-493.

Calder, K. M., Gabriel, D. A., and McLean, L. (2009). Differences in EMG spike shape between individuals with and without non-specific arm pain. *Journal of Neuroscience Methods*. 178, 148-156.

Carpentier, A., Duchateau, J., and Hainaut, K. (2001). Motor unit behaviour and contractile changes during fatigue in the human first dorsal interosseus. *Journal of Physiology*. 534 (3), 903-912.

Carrasco, D. I. and English, A. W. (1999). Mechanical actions of compartments of the cat hamstring muscle, biceps femoris. *Progress in Brain Research*. 123, 397-403.

Christensen, H., Monaco, M. L., Dahl, K., and Fuglsang-Frederiksen, A. (1984). Processing of electrical activity in human muscle during a gradual increase in force. *Electroencephalography and Clinical Neurophysiology*. 58, 230-239.

Christensen, H. and Fuglsang-Frederiksen, A. (1986). Power spectrum and turns analysis of EMG at different voluntary efforts in normal subjects. *Electroencephalography and Clinical Neurophysiology*. 64, 528-535.

Christensen, H., Lo Monaco, M., and Fuglsang-Frederiksen, A. (1991). Quantitative needle electromyography during sustained maximal effort. *Journal of Electromyography and Kinesiology*. 1 (2), 130-138.

Christensen, H., Søgard, K., Jensen, B. R., Finsen, L., and Sjøgaard, G. (1995). Intramuscular and surface EMG power spectrum from dynamic and static contractions. *Journal of Electromyography and Kinesiology*. 5(1), 27-36.

Christie, A. and Kamen, G. (2009). Motor unit firing behavior during prolonged 50% MVC dorsiflexion contractions in young and older adults. *Journal of Electromyography and Kinesiology*. 19, 543-552.

Christie, A., Inglis, J. G., Kamen, G., and Gabriel, D. A. (2009). Relationships between surface EMG variables and motor unit firing rates. *European Journal of Applied Physiology*. 107, 177-185.

Cioni, R., Giannini, F., Paradiso, C., Battistini, N., Navona, C., and Starita, A. (1994). Sex differences in surface EMG interference pattern power spectrum. *Journal of Applied Physiology*. 77 (5), 2163-2168.

Clancy, E. A. and Hogan, N. (1999). Probability density of the surface electromyogram and its relation to amplitude detectors. *IEEE Transactions on Biomedical Engineering*. 46 (6), 730-739.

Close, J. R., Nickel, E. D., and Todd, F. N. (1960). Motor unit action potential count. Their significance in isometric and isotonic contraction. *Journal of Bone Joint Surgery*. 42A, 1207-1222.

Connelly, D. M., Rice, C. L., Roos, M. R., and Vandervoort, A. A. (1999). Motor unit firing rates and contractile properties in tibialis anterior of young and old men. *Journal of Applied Physiology*. 87(2), 843-853.

Daube, J. R. and Rubin, D. I. (2009). Needle electromyography. *Muscle & Nerve*. 39, 244-270.

Day, S. J. and Hulliger, M. (2001). Experimental stimulation of cat electromyogram: evidence for algebraic summation of motor-unit action-potential trains. *Journal of Neurophysiology*. 86, 2144-2158.

De la Barrera, E. J. and Milner, T. (1994). The effects of skinfold thickness on the selectivity of surface EMG. *Electroencephalography and Clinical Neurophysiology*. 93, 91-99.

De Luca, C. J. (1975). A model for a motor unit train recorded during constant force isometric contractions. *Biological Cybernetics*. 19, 159-167.

De Luca, C. J. and Vandyk, E. J. (1975). Derivation of some parameters of myoelectric signals recorded during sustained constant force isometric contractions. *Biophysical Journal*. 15, 1167-1180.

De Luca, C. J. (1979). Physiology and mathematics of myoelectric signals. *IEEE Transactions on Biomedical Engineering*. BME-26 (6), 313-325.

De Luca, C. J. (1985). Control properties of motor units. *Journal of Experimental Biology*. 115, 125-136.

De Luca, C. J. and Merletti, R. (1988). Surface myoelectric signal cross-talk among muscles of the leg. *Electroencephalography and Clinical Neurophysiology*. 69, 568-575.

De Luca, C. J. and Erim, Z. (1994). Common drive of motor units in regulation of muscle force. *Trends in Neurosciences*. 17(7), 299-305.

De Luca, C. J. (1997). The use of surface electromyography in biomechanics. *Journal of Applied Biomechanics*. 13, 135-163.

De Luca, C. J. and Hostage, E. C. (2010). Relationship between firing rate and recruitment threshold of motoneurons in voluntary isometric contractions. *Journal of Neurophysiology*. 104, 1034-1046.

De Luca, C. J. and Contessa, P. (2012). Hierarchical control of motor units in voluntary contractions. *Journal of Neurophysiology*. 107, 178-195.

De Luca, C. J., Kuznetsov, M., Donald Gilmore, L., and Roy, S. H. (2012). Inter-electrode spacing of surface EMG sensors: Reduction of crosstalk contamination during voluntary contractions. *Journal of Biomechanics*. 45, 555-561.

De Vito, G., McHugh, D., Macaluso, A., and Riches, P. E. (2003). Is the coactivation of biceps femoris during isometric knee extension affected by adiposity in healthy young humans?. *Journal of Electromyography and Kinesiology*. 13, 425-431.

Del Santo, F., Gelli, F., Mazzocchio, R., and Rossi, A. (2007). Recurrence quantification analysis of surface EMG detects changes in motor unit synchronization induced by recurrent inhibition. *Experimental Brain Research*. 178, 308-315.

Delbeke, J., Kopec, J., and McComas, A. J. (1978). Effects of age, temperature, and disease on the refractoriness of human nerve and muscle. *Journal of Neurology, Neurosurgery, and Psychiatry*. 41, 65-71.

Dimitrov, G. V. and Dimitrova, N. A. (1998). Fundamentals of power spectra of extracellular potentials produced by a skeletal muscle fibre of finite length. Part I: Effect of fibre anatomy. *Medical Engineering and Physics*. 20, 580-587.

Dimitrov, G. V., Disselhorst-Klug, C., Dimitrova, N. A., Schulte, E., and Rau, G. (2003). Simulation analysis of the ability of different types of multi-electrodes to increase selectivity of detection and to reduce cross-talk. *Journal of Electromyography and Kinesiology*. 13, 125-138.

Dimitrova, N. A., Dimitrov, G. V., and Chihman, V. N. (1999). Effect of electrode dimensions on motor unit potentials. *Medical Engineering and Physics*. 21, 479-485.

Dimitrova, N. A. and Dimitrov, G. V. (2002). Ampltidue-related characteristics of motor unit and M-wave potentials during fatigue. A simulation study using literature data on intracellular potential changes found in vitro.

Dimitrova, N. A., Dimitrov, G. V., and Nikitin, O. A. (2002). Neither high-pass filtering nor mathematical differentiation of the EMG signals can considerably reduce cross-talk. *Journal of Electromyography and Kinesiology*. 12, 235-246.

Dimitrova, N. A. and Dimitrov, G. V. (2003). Interpretation of EMG changes with fatigue: facts, pitfalls, and fallacies. *Journal of Electromyography and Kinesiology*. 13, 13-36.

Dimitrova, N. A. and Dimitrov, G. V. (2006). Electromyography (EMG) modeling. *Wiley Encyclopedia of Biomedical Engineering.*

Dimitru, D., King, J. C., and Nandedkar, S. D. (1997). Comparison of single-fiber and macro electrode recordings: Relationship to motor unit action potential duration. *Muscle & Nerve*. 20(11), 1381-1388.

Dioszeghy, P., Egerhazi, A., Molnar, M., and Mechler, F. (1996). Turn-amplitude analysis in neuromuscular diseases. *Electromyography and Clinical Neurophysiology*. 36, 463-468.

Disselhorst-Klug, C., Bahm, J., Ramaekers, V., Trachterna, A., and Rau, G. (2000). Non-invasive approach of motor unit recording during muscle contractions in humans. *European Journal of Applied Physiology*. 83, 144-150.

Disselhorst-Klug, C., Schmitz-Rode, T., and Rau, G. (2009). Surface electromyography and muscle force: Limits in sEMG-force relationship and new aproaches for applications. *Clinical Biomechanics*. 24, 225-235.

Dumitru, D. and DeLisa, J. A. (1991). AAEM minimonograph #10: Volume conduction. *Muscle and Nerve*. 14, 605-624.

Dumitru, D. and King, J. C. (1992). Far-field potentials in circular volumes: Evidence to support the leading/trailing dipole model. *Muscle and Nerve*. 15, 101-105.

Dumitru, D. (2000). Physiologic basis of potentials recorded in electromyography. *Muscle and Nerve*. 23, 1667-1685.

Dupont, L., Gamet, D., and Pérot, C. (2000). Motor unit recruitment and EMG power spectra during ramp contractions of a bifunctional muscle. *Journal of Electromyography and Kinesiology*. 10, 217-224.

English, A. W., Wolf, S. T., and Segal, R. L. (1993). Compartmentalization of muscles and their motor nuclei: The partitioning hypothesis. *Physical Therapy*. 73, 857-867.

Erim, Z., De Luca, C. J., Mineo, K., and Aoki, T. (1996). Rank-ordered regulation of motor units. *Muscle and Nerve*. 19 (5), 563-573.

Evetovich, T. K., Boyd, J. C., Drake, S. M., Eschback, L. C., Magal, M., Soukup, J. T., ... and Weir, J. P. (2002). Effect of moderate dehydration on torque, electromyography, and mechanomyography. *Muscle and Nerve*. 26, 225-231.

Farina, D. and Merletti, R. (2000). Comparison of algorithms for estimation of EMG variables during voluntary isometric contractions. *Journal of Electromyography and Kinesiology*. 10, 337-349.

Farina, D., Fosci, M., and Merletti, R. (2002). Motor unit recruitment strategies investigated by surface EMG variables. *Journal of Applied Physiology*. 92, 235-247.

Farina, D., Merletti, R., Indino, B., Nazzaro, M., and Pozzo, M. (2002). Surface EMG crosstalk between knee extensor muscles: Experimental and model results. *Muscle and Nerve*. 26, 681-695.

Farina, D., Merletti, R., and Enoka, R. M. (2004). The extraction of neural strategies from the surface EMG. *Journal of Applied Physiology*. 96, 1486-1495.

Farina, D., Zagari, D., Gazzoni, M., and Merletti, R. (2004). Reproducibility of muscle-fiber conduction velocity estimates using multichannel surface EMG techniques. *Muscle & Nerve*. 29, 282-291.

Farina, D. (2006). Interpretation of the surface electromyogram in dynamic contractions. *Exercise and Sport Sciences Reviews*. 34 (3), 121-127.

Farina, D., Negro, F., Gazzoni, M., and Enoka, R. M. (2008). Detecting the unique representation of motor-unit action potentials in the surface electromyogram. *Journal of Neurophysiology*. 100 (3), 1223-1233.

Farina, D., Holobar, A., Merletti, R., and Enoka, R. M. (2010). Decoding the neural drive to muscles from the surface electromyogram. *Clinical Neurophysiology*. 121, 1616-1623.

Fattorini, L., Felici, F., Filligoi, G. C., Trabellesi, M., and Farina, D. (2005). Influence of high motor unit synchronization levels on non-linear and spectral variables of the surface EMG. *Journal of Neuroscience Methods*. 143, 133-139.

Feiereisen, P., Duchateau, J., and Hainaut, K. (1997). Motor unit recruitment order during voluntary and electrically induced contractions in the tibialis anterior. *Experimental Brain Research*. 114, 117-123.

Field, A. and Miles, J. (2010). *Discovering statistics using SAS*. Sage: Los Angeles.

Finsterer, J., Mamoli, B., and Fuglsang-Frederiksen, A. (1997). Peak-ratio interference pattern analysis in the detection of neuromuscular disorders. *Electroencephalography and Clinical Neurophysiology*. 105, 379-384.

Finsterer, J. (2001). EMG-interference pattern analysis. *Journal of Electromyography and Kinesiology*. 11, 231-246.

Finsterer, J. (2004). Effect of needle-EMG on blood-pressure and heart-rate. *Journal of Electromyography and Kinesiology*. 14, 283-286.

Flieger, M. S. (1983). Maximum speed of forearm flexion practice effects upon surface EMG signal characteristics. (M.S. Thesis).

Fling, B. W., Christie, A., and Kamen, G. (2009). Motor unit synchronization in FDI and biceps brachii muscles of strength-trained males. *Journal of Electromyography and Kinesiology*. 19, 800-809.

Frigon, A., Carroll, T. J., Jones, K. E., Zehr, P. E., and Collins, D. F. (2007). Ankle position and voluntary contraction alter maximal M waves in soleus and tibialis anterior. *Muscle & Nerve*. 35, 756-766.

Fuglevand, A. J., Winter, D. A., Patla, A. E., and Stashuk, D. (1992). Detection of motor unit action potentials with surface electrodes: influence of electrode size and spacing. *Biological Cybernetics*. 67, 143-153.

Fuglevand, A. J., Winter, D. A., and Patla, A. E. (1993). Models of recruitment and rate coding organization in motor-unit pools. *Journal of Neurophysiology*. 70 (6), 2470-2488.

Fuglevand, A. J. and Keen, D. A. (2003). Re-evaluation of muscle wisdom in the human adductor pollicis using physiological rates of stimulation. *Journal of Physiology*. 549 (3), 865-875.

Fuglsang-Frederiksen, A. and Rønager, J. (1988). The motor unit firing rate and the power spectrum of EMG in humans. *Electroencephalography and Clinical Neurophysiology*. 70, 68-72.

Fuglsang-Frederiksen, A. (2000). The utility of interference pattern analysis. *Muscle and Nerve*. 23, 18-36.

Fujimoto, T. and Nishizono, H. (1993). Muscle contractile properties by surface electrodes compared with those by needle electrodes. *Electroencephalography and Clinical Neurophysiology*. 89, 247-251.

Fukunaga, T., Roy, R. R., Shellock, F. G., Hodgson, J. A., and Edgerton, V. R. (1996). Specific tension of human plantar flexors and dorsiflexors. *Journal of Applied Physiology*. 80(1), 158-165.

Fusfeld, R. D. (1971). Analysis of electromyographic signals by measurement of wave duration. *Electroencephalography and Clinical Neurophysiology*. 30, 337-344.

Fusfeld, R. D. (1972). A study of the differentiated electromyogram. *Electroencephalography and Clinical Neurophysiology*. 33, 511-515.

Gabriel, D. A. (2000). Reliability of SEMG spike parameters during concentric contractions. *Electromyography and Clinical Neurophysiology*. 40, 423-430.

Gabriel, D. A., Basford, J. R., and An, K.-N. (2001). Assessing fatigue with electromyographic spike parameters. *IEEE Engineering in Medicine and Biology*. 20, 90-96.

Gabriel, D. A., Matsumoto, J. Y., Davis, D. H., Currier, B. L., and An, K.-N. (2004). Multidirectional neck strength and electromyographic activity of normal controls. *Clinical Biomechanics*. 19, 653-658.

Gabriel, D. A., Lester, S. M., Lenhardt, S. A., and Cambridge, E. D. J. (2007). Analysis of surface EMG spike shape across different levels of isometric force. *Journal of Neuroscience Methods*. 159, 146-152.

Gabriel, D. A. and Kamen, G. (2008). Comments on point: Counterpoint: Spectral properties of the surface EMG can charaterize/do not provide information about motor unit recruitment strategies and muscle fiber type. *Journal of Applied Physiology*. 105, 1676-1681.

Gabriel, D. A. and Kamen, G. (2009). Experimental and modeling investigation of spectral compression of biceps brachii SEMG activity with increasing force levels. *Journal of Electromyography and Kinesiology*. 19, 437-448.

Gabriel, D. A., Christie, A., Inglis, J. G., and Kamen, G. (2011). Experimental and modeling investigation of surface EMG spike analysis.*Medical Engineering and Physics*. 33, 427-437.

Gabriel, D. A. (2011). Effects of monopolar and bipolar electrode configurations on surface EMG spike analysis. *Medical Engineering and Physics*. 33, 1079-1085.

Gamet, D. and Maton, B. (1989). The fatigability of two agonistic muscles in human isometric voluntary submaximal contraction: an EMG study. *European Journal of Applied Physiology*. 58, 361-368.

Garland, S. J. and Griffin, L. (1999). Motor unit double discharges: Statistical anomaly or functional entity?. 24, 113-130.

Garland, S. J. and Gossen, E. R. (2002). The muscular wisdom hypothesis in human muscle fatigue. *Exercise and Sport Sciences Reviews*. 30 (1), 45-49.

Gath, I. and Stålberg, E. V. (1976). Techniques for improving the selectivity of electromyographic recordings. *IEEE Transactions on Biomedical Engineering*. BME-23 (6), 467-472.

Gath, I. and Stålberg, E. (1977). On the volume conduction in human skeletal muscle: In situ measurements. *Electroencephalography and Clinical Neurophysiology*. 43, 106-110.

Gath, I. and Stålberg, E. (1978). The calculated radial decline of the extracellular action potential compared with in situ measurements in the human brachial biceps. *Electroencephalography and Clinical Neurophysiology*. 44, 547-552.

Gath, I. and Stålberg, E. V. (1979). Measurements of the uptake area of small-size electromyographic electrodes. *IEEE Transactions on Biomedical Engineering*. BME-26 (6), 374-376.

Gath, I. and Stålberg, E. V. (1981). In situ measurement of the innervation ratio of motor units in human muscles. *Experimental Brain Research*. 43, 377-382.

Gerdle, B., Wretling, M.-L., and Henriksson-Larsén, K. (1988). Do the fibre-type proportion and the angular velocity influence the mean power frequency of the electromyogram?. *Acta Physiologica Scandinavia*. 134, 341-346.

Gerdle, B., Eriksson, N.-E., and Brundin, L. (1990). The behaviour of the mean power frequency of the surface electromyogram in biceps brachii with increasing force and during fatigue. With special regard to electrode distance. *Electromyography and Clinical Neurophysiology*. 30, 483-489.

Gerdle, B., Henriksson-Larsén, K., Lorentzon, R., and Wretling, M.-L. (1991). Dependence of the mean power frequency of the electromyogram on muscle force and fibre type. *Acta Physiologica Scandinavia*. 142, 457-465.

Gerdle, B., Karlsson, S., Crenshaw, A. G., and Fridén, J. (1997). The relationships between EMG and muscle morphology throughout sustained static knee extension at two submaximal force levels. *Acta Physiologica Scandinavia*. 160, 341-351.

Glass, G. V., Peckham, P. D., and Sanders, J. R. (1972). Consequences of failure to meet assumptions underlying the fixed effects analyses of variance and covariance. *Review of Educational Research*. 42 (3), 237-288.

Goodgold, J. (1984). *Anatomical correlates of clinical electromyography*. Baltimore, MD: Williams & Wilkins.

Grabiner, M. D. and Robertson, R. N. (1985). Utilization of digital discriminators for quantification of the surface electromyogram. *Electromyography and Clinical Neurophysiology*. 25, 479-487.

Green, L. A., Parro, J. J., and Gabriel, D. A. (In Press). Beneficial effects of serial contractions on muscle performance after a brief period of rest. *European Journal of Applied Physiology*.

Griep, P. A. M., Boon, K. L., and Stegeman, D. F. (1978). A study of the motor unit action potential by means of computer simulation. *Biological Cybernetics*. 30, 221-230.

Griep, P. A. M., Gielen, F. L. H., Boom, H. B. K., Boon, K. L., Hoogstraten, L. L. W., Pool, C. W., and Wallinga-de Jonge, W. (1982). Calculation and registration of the same motor unit action potential. *Electroencephalography and Clinical Neurophysiology*. 53, 388-404.

Hagberg, M. and Ericson, B.-E. (1982). Myoelectric power spectrum dependence on muscular contraction level of elbow flexors. *European Journal of Applied Physiology*. 48, 147-156.

Hannam, A. G. and McMillan, A. S. (1994). Internal organization in the human jaw muscles. *Critical Reviews in Oral Biology and Medicine*. 5(1), 55-89.

Harris, C. M. (1998). The Fourier analysis of biological transients. *Journal of Neuroscience Methods*. 83, 15-34.

Hayes, K. C. (1978). A theory of the mechanism of muscular strength development based upon EMG evidence of motor unit synchronization. *Biomechanics of Sports and Kinanthropometry*. 69-77.

Henneman, E. and Olson, C. B. (1965). Relations between structure and function in the design of skeletal muscles. *Journal of Neurophysiology*. 28, 581-598.

Henriksson-Larsén, K. (1985). Distribution, number and size of different types of fibres in whole cross-sections of female m tibialis anterior. An enzyme histochemical study. *Acta Physiologica Scandinavia*. 123 (3), 229-235.

Hermens, H. J., Boon, K. L., and Zivold, G. (1984). The clinical use of surface EMG. *Electromyography and Clinical Neurophysiology*. 24, 243-265.

Hermens, H. J., Bruggen, T. A. M. v., Baten, C. T. M., Rutten, W. L. C., and Boom, H. B. K. (1992). The median frequency of the surface EMG power spectrum in relation to motor unit firing and action potential properties. *Journal of Electromyography and Kinesiology*. 2 (1), 15-25.

Hermens, H. J., Freriks, B., Disselhorst-Klug, C., and Rau, G. (2000). Development of recommendations for SEMG sensors and sensor placement procedures. *Journal of Electromyography and Kinesiology*. 10, 361-374.

Hewson, D. J., Hogrel, J.-Y., Langeron, Y., and Duchêne, J. (2003). Evolution in impedance at the electrode-skin interface of two types of surface EMG electrodes during long-term recordings. *Journal of Electromyography and Kinesiology*. 13, 273-279.

Hirose, K. and Uono, M. (1985). Noise in quantitative electromyography. *Electromyography and Clinical Neurophysiology*. 25, 341-352.

Hodgkin, A. L. and Katz, B. (1949). The effect of sodium ions on the electrical activity of the giant axon of the squid. *Journal of Physiology*. 108, 37-77.

Hogrel, J.-Y. (2003). Use of surface EMG for studying motor unit recruitment during isometric linear force ramp. *Journal of Electromyography and Kinesiology*. 13, 417-423.

Holmback, A. M., Porter, M. M., Downham, D., Anderson, J. L., and Lexell, J. (2003). Structure and function of the ankle dorsiflexors muscles in young and moderately active men and women. *Journal of Applied Physiology*. 95, 2416-2424.

Inglis, J. G., Howard, J., McIntosh, K., Gabriel, D. A., and Vandenboom, R. (2011). Decreased motor unit discharge rate in the potentiated human tibialis anterior muscle. *Acta Physiologica*. 201, 483-492.

Isman, R. E. and Inman, V. T. (1969). Anthropometric studies of the human foot and ankle. *Bulletin of Prosthetics Research*. 11, 97-108.

Jan, M. M. S., Schwartz, M., and Benstead, T. J. (1999). EMG related anxiety and pain: A prospective study. *Canadian Journal of Neurological Science*. 26, 294-297.

Jaworowski, Å., Porter, M. M., Holmbäck, A. M., Downham, D., and Lexell, J. (2002). Enzyme activities in the tibialis anterior muscle of young moderately active men and women: relationship with body composition, muscle cross-sectional area and fibre type composition. *Acta Physiologica Scandanavia*. 176, 215-225.

Jørgensen, S. A. and Fuglsang-Frederiksen, A. (1991). Turns-amplitude analysis at different sampling frequencies. *Electroencephalography and Clinical Neurophysiology*. 81, 1-7.

Junge, D. (1993). Turns and averaging as static and dynamic measures of masseter EMG activity. *Electromyography and Clinical Neurophysiology*. 33, 11-18.

Kamen, G. and Caldwell, G. E. (1996). Physiology and interpretation of the electromyogram. *Journal of Clinical Neurophysiology*. 13(5), 366-384.

Kandel, E. R., Schwartz, J. H., and Jessell, T. M. (2000). *Principles of neural science. Fourth Edition.* Toronto, ON: McGraw Hill.

Kaplanis, P. A., Pattichis, C. S., Hadjileontiadis, L. J., and Roberts, V. C. (2009). Surface EMG analysis on normal subjects based on isometric voluntary contraction. *Journal of Electromyography and Kinesiology*. 19, 157-171.

Kasai, T. and Komiyama, T. (1990). Effects of varying force components on EMG reaction times of isometric ankle dorsiflexion. *Human Movement Science*. 9, 133-147.

Keenan, K. G., Farina, D., Maluf, K. S., Merletti, R., and Enoka, R. M. (2005). Influence of amplitude cancellation on the simulated surface electromyogram. *Journal of Applied Physiology*. 98, 120-131.

Keenan, K. G., Farina, D., Merletti, R., and Enoka, R. M. (2006). Amplitude cancellation reduces the size of motor unit potentials averaged from the surface EMG. *Journal of Applied Physiology*. 100, 1928-1937.

Keenan, K. G. and Valero-Cuevas, F. J. (2008). Epoch length to accurately estimate the amplitude of interference EMG is likely the result of unavoidable amplitude cancellation. *Biomedical Signal Processing and Control*. 3, 154-162.

Kent-Braun, J. (1999). Central and peripheral contributions to muscle fatigue in humans during sustained maximal effort. *European Journal of Applied Physiology*. 80, 57-63.

Kent-Braun, J. A. and Ng, A. V. (1999). Specific strength and voluntary muscle activation in young and elderly women and men. *Journal of Applied Physiology*. 87(1), 22-29.

Kent-Braun, J. A., Ng, A. V., Doyle, J. W., and Towse, T. F. (2002). Human skeletal muscle responses vary with age and gender during fatigue due to incremental isometric exercise. *Journal of Applied Physiology*. 93, 1813-1823.

Kim, M.-S., Masakado, Y., Tomita, Y., Chino, N., Sook Pae, Y., and Lee, K. (2001). Synchronization of single motor units during voluntary contractions in the upper and lower extremities. *Clinical Neurophysiology*. 112, 1243-1249.

Kimura, J. (1989). *Electrodiagnosis in diseases of nerve and muscle: Principles and practice. Second Edition*. Philadelphia, PA: F. A. Davis Company.

Knight, C. A. and Kamen, G. (2005). Superficial motor units are larger than deeper motor units in human vastus lateralis muscle. *Muscle and Nerve*. 31, 475-480.

Komi, P. V. and Viitasalo, J. H. T. (1976). Signal characteristics of EMG at different levels of muscle tension. *Acta Physiologica Scandinavia*. 96, 267-276.

Komi, P. V. and Viitasalo, J. T. (1977). Changes in motor unit activity and metabolism in human skeletal muscle during and after repeated eccentric and concentric contractions. *Acta Physiologica Scandinavia*. 100, 246-254.

Krogh-Lund, C. and Jørgensen, K. (1992). Modification of myo-electric power spectrum in fatigue from 15% maximal voluntary contraction of human elbow flexor muscles, to limit of endurance: reflection of conduction velocity variation and/or centrally mediated mechanisms?. *European Journal of Applied Physiology*. 64, 359-370.

Krogh-Lund, C. and Jørgensen, K. (1993). Myo-electric fatigue manifestations revisited: power spectrum, conduction velocity, and amplitude of human elbow flexor muscles during isolated and repetitive endurance contractions at 30% maximal voluntary contraction. *European Journal of Applied Physiology*. 66, 161-173.

Kukulka, C. G. and Clamann, H. P. (1981). Comparison of the recruitment and discharge properties of motor units in human brachial biceps and adductor pollicis during isometric contractions. *Brain Research*. 219, 45-55.

Kupa, E. J., Roy, S. H., Kandarian, S. C., and De Luca, C. J. (1995). Effects of muscle fiber type and size on EMG median frequency and conduction velocity. *Journal of Applied Physiology*. 79(1), 23-32.

Kurca, E. and Drobny, M. (2000). Four quantitative EMG methods and theirs individual parameter diagnostic value. *Electromyography and Clinical Neurophysiology*. 40, 451-458.

Lago, P. and Jones, N. B. (1977). Effect of motor-unit firing time statistics on e.m.g. spectra. *Medical and Biological Engineering and Computing*. 15, 648-655.

Lago, P. and Jones, N. B. (1981). Low-frequency spectral analysis of the e.m.g. *Medical and Biological Engineering and Computing*. 19, 779-782.

Lang, F. (1971). Induced myogenic activity in the neurogenic heart of limulus polyphemus. *Biology Bulletin*. 141, 269-277.

Lange, F., Van Weerden, T. W., Van der Hoven, J. H. (2002). A new surface electromyography analysis method to determine spread of muscle fiber conduction velocities. *Journal of Applied Physiology*. 93, 759-764.

Lateva, Z. C., Dimitrov, G. V., and Dimitrova, N. A. (1990). Power spectra of single infinite fibre extracellular potentials recorded by a bipolar electrode. *Medical and Biological Engineering and Computing*. 28, 537-543.

Lawrence, J. H. and De Luca, C. J. (1983). Myoelectric signal versus force relationship in different human muscles. *Journal of Applied Physiology*. 54 (6), 1653-1659.

Lenhardt, S. A., McIntosh, K. C., and Gabriel, D. A. (2009). The surface EMG-force relationship during isometric dorsiflexion in males and females. *Electromyography and Clinical Neurophysiology*. 49 (5), 227-234.

Lexell, J., Downham, D., and Sjöström, M. (1986). Distribution of different fibre types in human skeletal muscles: fibre type arrangement in m. vastus lateralis from three groups of healthy men between 15 and 83 years. *Journal of the Neurological Sciences*. 72 (2), 211-222.

Li, W. and Sakamoto, K. (1996). The influence of location of electrode on muscle fiber conduction velocity and EMG power spectrum during voluntary isometric

contraction measured with surface array electrodes. *Journal of Physiological Anthropology*. 15 (1), 25-32.

Liguori, R., Dahl, K., and Fuglsang-Frederiksen, A. (1992). Turns-amplitude analysis of the electromyographic recruitment pattern disregarding force measurement. I. Method and reference values in healthy subjects. *Muscle & Nerve*. 15(12), 1314-1318.

Lindstrõm, L. H. and Magnusson, R. I. (1977). Interpretation of myoelectric power spectra: A model and its applications. *Proceedings of the IEEE*. 65 (5), 653-662.

Liu, Y., Kankaanpaa, M., Zbilut, J. P., Webber Jr., C. L. (2004). EMG recurrence quantifications in dynamic exercise. *Biological Cybernetics*. 90, 337-348.

Lloyd, A. J. (1971). Surface electromyography during sustained isometric contractions. *Journal of Applied Physiology*. 30 (5), 713-719.

Lowery, M., Nolan, P., and O'Malley, M. (2002). Electromyogram median frequency, spectral compression and muscle fibre conduction velocity during sustained sub-maximal contraction of the brachioradialis muscle. *Journal of Electromyography and Kinesiology*. 12, 111-118.

Lowery, M. M., Stoykov, N. S., Dewald, J. P. A., and Kuiken, T. A. (2004). Volume conduction in an anatomically based surface EMG model. *IEEE Transactions on Biomedical Engineering*. 51 (12), 2138-2147.

Luttgens, K. and Wells, K. F. (1982). *Kinesiology: Scientific basis of human motion.* New York, NY: W. B. Saunders Company.

Lynn, P. A., Bettles, N. D., Hughes, A. D., and Johnson, S. W. (1978). Influences of electrode geometry on bipolar recordings of the surface electromyogram. *Medical and Biological Engineering and Computing*. 16, 651-660.

MacIntosh, K. C. D. and Gabrial, D. A. (2012). Reliability of a simple method for determining muscle fiber conduction velocity. *Muscle & Nerve*. 45, 257-265.

Madigan, M. L. and Pidcoe, P. E. (2002). A muscle temperature compensation technique for EMG fatigue measures. *Medicine and Science in Sports and Exercise*. 34 (5), 780-784.

Maganaris, C. N., Baltzopoulos, V., and Sargeant, A. J. (1999). Changes in the tibialis anterior tendon moment arm from rest to maximum isometric dorsiflexion: in vivo observations in man. *Clinical Biomechanics*. 14, 661-666.

Maganaris, C. N. and Baltzopoulos, V. (1999). Predictability of in vivo changes in pennation angle of human tibialis anterior muscle from rest to maximum isometric dorsiflexion. *Eurpoean Journal of Applied Physiology*. 79, 294-297.

Maganaris, C. N. (2000). In vivo measurement-based estimations of the moment arm in the human tibialis anterior muscle-tendon unit. *Journal of Biomechanics*. 33, 375-379.

Maganaris, C. N., Baltzopoulos, V., Ball, D., and Sargeant, A. J. (2001). In vivo specific tension of human skeletal muscle. *Journal of Applied Physiology*. 90, 865-872.

Magora, A. and Gonen, B. (1970). Computer analysis of the shape of spikes from electromyographic interference pattern. *Electromyography*. 10 (3), 261-271.

Magora, A. and Gonen, B. (1972). Clinical evaluation of the analysis of the shape of electromyographic shape. *Electromyography*. 12 (3), 255-265.

Magora, A. and Gonen, B. (1975). The amplitude of spike in the interpretation of electromyographic recordings. *Electromyography and Clinical Neurophysiology*. 15, 377-396.

Magora, A., Blank, A., and Gonen, B. (1980). Effects of artificially induced ischemia (AII) on the electrophysiological pattern of muscular fatigue in healthy humans. *Electromyography and Clinical Neurophysiology*. 20, 125-140.

Marsh, E., Sale, D., McComas, A. J., and Quinlan, J. (1981). Influence of joint position on ankle dorsiflexion in humans. *Journal of Applied Physiology: Respiratory Environmental Exercise Physiology*. 51(1), 160-167.

Masuda, T., Miyano, H. and Sadoyama, T. (1983).The propagation of motor unit action potential and the location of neuromuscular junction investigated by surface electrode arrays. *Electroencephalography and Clinical Neurophysiology*. 55, 594-600.

McNeil, C., Doherty, T., Stashuk, D. and Rice, C. (2005). Motor unit number estimates in the tibialis anterior muscle of young, old, and very old men. *Muscle & Nerve*. 31, 461-467.

Meekins, G. D., So, Y., Quan, D. (2008). American association of neuromuscular & electrodiagnostic medicine evidenced-based review: Use of surface

electromyography in the diagnosis and study of neuromuscular disorders. *Muscle & Nerve*. 38, 1219-1224.

Mello, R. G. T., Oliveira, L. F., and Nadal, J. (2007). Digital Butterworth filter for subtracting noise from low magnitude surface electromyogram. *Computer Methods and Programs in Biomedicine*. 87, 28-35.

Merletti, R., Knaflitz, M., and De Luca, C. J. (1990). Myoelectric manifestations of fatigue in voluntary and electrically elicited contractions. *Journal of Applied Physiology*. 69(5), 1810-1820.

Merletti, R., Lo Conte, L., Avignone, E., and Guglielminotti, P. (1999a). Modeling of surface myoelectric signals—Part I: Model implementation. *IEEE Transactions on Biomedical Engineering*. 46 (7), 810-820.

Merletti, R., Roy, S. H., Kupa, E., Roatta, S., and Granata, A. (1999b). Modeling of surface myoelectric signals—Part II: Model-based signal interpretation. *IEEE Transactions on Biomedical Engineering*. 46 (7), 821-829.

Merletti, R. and Farina, D. (2012). Analysis of intramuscular electromyogram signals. *Philosophical Transactions of the Royal Society A*. 367, 357-368.

Mesin, L., Merletti, R., and Rainoldi, A. (2009). Surface EMG: The issue of electrode location. *Journal of Electromyography and Kinesiology*. 19, 719-726.

Mesin, L., Merlo, E., Merletti, R., and Orizio, C. (2010). Investigation of motor unit recruitment during simulated contractions of tibialis anterior muscle. *Journal of Electromyography and Kinesiology*. 20, 580-589.

Messick, S. (1995). Standards of validity and the validity of standards in performance assessment. *Educational Measurement: Issues and Practice*. 14 (4), 5-8.

Miller, A. E. J., MacDougall, J. D., Tarnopolsky, M. A., and Sale, D. G. (1993). Gender differences in strength and muscle fiber characteristics. *European Journal of Applied Physiology*. 66, 254-262.

Milner-Brown, H. S., Stein, R. B., and Yemm, R. (1973). The contractile properties of human motor units during voluntary isometric contractions. *Journal of Physiology*. 228, 285-306.

Mogk, J. P. M. and Keir, P. J. (2003). Crosstalk in surface electromyography of the proximal forearm during gripping tasks. *Journal of Electromyography and Kinesiology*. 13, 63-71.

Moritani, T., Muro, M., and Kijima, A. (1985). Electromechanical changes during electrically induced and maximal voluntary contractions: Electrophysiologic responses of different muscle fiber types during stimulated contractions. *Experimental Neurology*. 88, 471-483.

Moritani, T., Muro, M., and Nagata, A. (1986). Intramuscular and surface electromyogram changes during muscle fatigue. *Journal of Applied Physiology*. 60 (4), 1179-1185.

Moritani, T. and Muro, M. (1987). Motor unit activity and surface electromyogram power spectrum during increasing force of contraction. *European Journal of Applied Physiology*. 56, 260-265.

Muro, M., Nagata, A., Murakami, K., and Moritani, T. (1982). Surface emg power spectral analysis of neuro-muscular disorders during isometric and isotonic contractions. *American Journal of Physical Medicine and Rehabilitation*. 61 (5), 244-254.

Muthuswamy, J. and Thakor, N. V. (1998). Spectral analysis methods for neurological signals. *Journal of Neuroscience Methods*. 83, 1-14.

Myers, L. J., Lowery, M., O'Malley, M., Vaughan, C. L., Heneghan, C., St Clair Gibson, A., Harley, Y. X. R., and Sreenivasan, R. (2003). Rectification and non-linear pre-processing of EMG signals for cortico-muscular analysis. *Journal of Neuroscience Methods*. 124, 157-165.

Nakagawa, Y., Ratkevicius, A., Mizuno, M., and Quistorff, B. (2005). ATP economy of force maintenance in human tibialis anterior muscle. *Medicine and Science in Sports and Exercise*. 37(6), 937-943.

Nandedkar, S. D., Sigl, J. C., Kim, Y. I., and Stålberg, E. V. (1984). Radial decline of the extracellular action potential. *Medical and Biological Engineering and Computing*. 22, 564-568.

Nandedkar, S. D., Sanders, D. B., Stålberg, E. V. (1985). Selectivity of electromyographic recording techniques: a simulation study. *Medical and Biological Engineering and Computing*. 23, 536-540.

Nandedkar, S. D., Sanders, D. B., and Stålberg, E. V. (1988). EMG of reinnervated motor units: a simulation study. *Electroencephalography and clinical Neurophysiology*. 70, 177-184.

Nandedkar, S. D., Sanders, D. B., and Stålberg, E. V. (1991). On the shape of the normal turns-amplitude cloud. *Muscle & Nerve*. 14, 8-13.

Nandedkar, S. D. and Barkhaus, P. E. (2007). Contribution of reference electrode to the compound muscle action potential. *Muscle and Nerve*. 36, 87-92.

Narici, M. (1999). Human skeletal muscle architecture studied in vivo by non-invasive imaging techniques: Functional significance and applications. *Journal of Electromyography and Kinesiology*. 9, 97-103.

Nawab, S. H., Wotiz, R. P., and De Luca, C. J. (2008). Decomposition of indwelling EMG signals. *Journal of Applied Physiology*. 105, 700-710.

Nawab, S. H., Chang, S.-S., and De Luca, C. J. (2010). High-yield decomposition of surface EMG signals. *Clinical Neurophysiology*. 121, 1602-1615.

Nordander, C., Willner, J., Hansson, G.-A., Larsson, B., Unge, J., Granquist, L., and Skerfving, S. (2003). Influence of the subcutaneous fat layer, as measured by ultrasound, skinfold callipers and BMI, on the EMG amplitude. *European Journal of Applied Physiology*. 89, 514-519.

O'Leary, D. D., Hope, K., and Sale, D. G. (1997). Posttetanic potentiation of human dorsiflexors. *Journal of Applied Physiology*. 83(6), 2131-2138.

Okajima, Y., Tomita, Y., Ushijima, R., and Chino, N. (2000). Motor unit sound in needle electromyography: Assessing normal and neuropathic units. *Muscle & Nerve*. 23, 1076-1083.

Ollivier, K., Portero, P., Maïsetti, O., and Hogrel, J.-Y. (2005). Repeatability of surface EMG parameters at various isometric contraction levels and during fatigue using bipolar and Laplacian electrode configurations. *Journal of Electromyography and Kinesiology*. 15, 466-473.

Park, J. and Ty Hopkins, J. (2011). Quadriceps activation normative values and the affect of subcutaneous tissue thickness. *Journal or Electromyography and Kinesiology*. 21, 136-140.

Patten, C. and Kamen, G. (2000). Adaptations in motor unit discharge activity with force control training in young and older human adults. *European Journal of Applied Physiology*. 83, 128-143.

Pérot, C., André, L., Dupont, L., Vanhoutte, C. (1996). Relative contributions of the long and short heads of the biceps brachii during single or dual isometric tasks. *Journal of Electromyography and Kinesiology*. 6 (1), 3-11.

Peters, E. J. D. and Fuglevand, A. J. (1999). Cessation of human motor unit discharge during sustained maximal voluntary contraction. *Neuroscience Letters*. 274, 66-70.

Philipson, L. and Larsson, P. G. (1988). The electromyographic signal as a measure of muscular force: a comparison of detection and quantification techniques. *Electromyography and Clinical Neurophysiology*. 28, 141-150.

Pincivero, D. M., Green, R. C., Mark, J. D., and Campy, R. M. (2000). Gender and muscle differences in EMG amplitude and median frequency, and variability during maximal voluntary contractions of the quadriceps femoris. *Journal of Electromyography and Kinesiology*. 10, 189-196.

Pincivero, D. M., Campy, R. M., Salfetnikov, Y., Bright, A., and Coelho, A. J. (2001). Influence of contraction intensity, muscle, and gender on median frequency of the quadriceps femoris. *Journal of Applied Physiology*. 90, 804-810.

Podnar, S., Rodi, Z., Lukanovic, A., Trsinar, B., and Vodusek, D. B. (1999). Standardization of anal sphincter EMG: Technique of needle examination. *Muscle & Nerve*. 22, 400-403.

Podnar, S. and Mrkaic, M. (2003). Size of motor unit potential sample. *Muscle & Nerve*. 27, 196-201.

Podnar, S. (2004). Usefulness of an increase in size of motor unit potential sample. *Clinical Neurophysiology*. 115, 1683-1688.

Porter, M. M., Stuart, S., Boij, M., and Lexell, J. (2002). Capillary supply of the tibialis anterior muscle in young, healthy, and moderately active men and women. *Journal of Applied Physiology*. 92, 1451-1457.

Preece, A. W., Wimalaranta, H. S. K., Green, J. L., Churchill, E., and Morgan, H. M. (1994). Non-invasive quantitative EMG. *Electromyography and Clinical Neurophysiology*. 34, 81-86.

Rainoldi, A., Galardi, G., Maderna, L., Comi, G., Lo Conte, L., and Merletti, R. (1999). Repeatability of surface EMG variables during voluntary isometric contractions of the biceps brachii muscle. *Journal of Electromyography and Kinesiology*. 9, 105-119.

Rainoldi, A., Melchiorri, G., and Caruso, I. (2004). A method for positioning electrodes during surface EMG recordings in lower limb muscles. *Journal of Neuroscience Methods*. 134, 37-43.

Reebye, O. (2004). Anatomical and clinical study of the common fibular nerve. Part 1: Anatomical study. *Surgical and Radiologic Anatomy*. 26, 365-370.

Robertson, R. N. and Grabiner, M. D. (1985). Relationship of IEMG to two methods of counting surface spikes during different levels of isometric tension. *Electromyography and Clinical Neurophysiology*. 25, 489-498.

Roeleveld, K., Stegeman, D. F., Vnigerhoets, H. M., and Van Oosterom, A. (1997). The motor unit potential distribution over the skin surface and its use in estimating the motor unit location. *Acta Physiologica Scandinavia*. 161, 465-472.

Roeleveld, K. and Stegeman, D. F. (2002). What do we learn from motor unit action potentials in surface electromyography?. *Muscle and Nerve Supplement*. 11, S92-S97.

Rønager, J., Christensen, H., and Fuglsang-Frederiksen, A. (1989). Power spectrum analysis of the EMG pattern in normal and diseased muscles. *Journal of the Neurological Sciences*. 94(1), 283-294.

Roy, S. H., De Luca, G., Cheng, M. S., Johansson, A., Gilmore, L. D., and De Luca, C. J. (2007). Electro-mechanical stability of surface EMG sensors. *Medical and Biological Engineering and Computing*. 45, 447-457.

Roy, S. H., De Luca, C. J., and Schneider, J. (1986). Effect of electrode location on myoelectric conduction velocity and median frequency estimates. *Journal of Applied Physiology*. 61 (4), 1510-1517.

Rutkove, S. B. (2000). Pseudofacilitation: A temperature-sensitive phenomenon. *Muscle and Nerve*. 23, 115-118.

Rutkove, S. B. (2001). Effects of temperature on neuromuscular electrophysiology. *Muscle and Nerve*. 24, 867-882.

Sadoyama, T., Masuda, T., Miyata, H., and Katsuta, S. (1988). Fibre conduction velocity and fibre composition in human vastus lateralis. *European Journal of Applied Physiology*. 57, 767-771.

Sanchez, J. H., Solomonow, M., Baratta, R. V., and D'Ambrosia, R. (1993). Control strategies of the elbow antagonist muscle pair during two types of increasing isometric contractions. *Journal of Electromyography and Kinesiology*. 3 (1), 33-40.

Sbricolli, P., Bazzucchi, I., Rosponi, A., Bernardi, M., De Vito, G., and Felici, F. (2003). Amplitude and spectral characteristics of biceps brachii sEMG depend upon the speed of isometric force gradation. *Journal of Electromyography and Kinesiology*. 13, 139-147.

Schochina, M., Magora, A., Gonen, B., and Wolf, E. (1984). Electrophysiological study of the development of fatigue in the opponens pollicis muscle. *Electromyography and Clinical Neurophysiology*. 24, 155-160.

Schochina, M., Gonen, B., Vatine, J. J., Mahler, Y., and Magora, A. (1986). Electrophysiological study of fatigue during isometric contractions interrupted by different periods of rest. *Electromyography and Clinical Neurophysiology*. 26, 655-660.

Schochina, M., Vatine, J. J., Mahler, Y., Gonen, B., and Magora, A. (1989). Effect of filter setting on the electromyographic paramters of muscles contracting to fatigue. *Electromyography and Clinical Neurophysiology*. 29, 3-8.

Schochina, M., Vatine, J. J., Mahler, Y., Gonen, B., and Magora, A. (1992). Diagnostic value of computer analysis of multipeaked EMG spikes. *Electromyography and Clinical Neurophysiology*. 32, 113-117.

Segal, R. L., Wolf, S. L., DeCamp, M. J., Chopp, M. T., and English, A. W. (1991). Anatomical partitioning of three multiarticular human muscles. *Acta Anatomica*. 266, 142-261.

Segal, R. L. (1992). Neuromuscular compartments in the human biceps brachii muscle. *Neuroscience Letters*. 140, 98-102.

Seki, K. and Narusawa, M. (1996). Firing rate modulation of human motor units in different muscles during isometric contraction with various forces. *Brain Research*. 719, 1-7.

Sica, R. E. P., McComas, A. J., and Ferreira, J. C. D. (1978). Evaluation of an automated method for analysing the electromyogram. *Le Journal Canadien des Sciences Neurologiques*. 5(3), 275-281.

Siegler, S., Hillstrom, H. J., Freedman, W., and Moskowitz, G. (1985). Effect of myoelectric signal processing on the relationship between muscle force and processed EMG. *American Journal of Physical Medicine and Rehabilitation*. 64, 130-149.

Simoneau, E. M., Longo, S., Seynnes, O. R., and Narici, M. V. (2012). Human muscle fascicle behaviour in agonist and antagonist isometric contractions. *Muscle & Nerve*. 45, 92-99.

Sinderby, C., Lindstrõm, L., and Grassino, A. E. (1995). Automatic assessment of electromyogram quality. *Journal of Applied Physiology*. 79 (5), 1803-1815.

Sinderby, C., Friberg, S., Comtois, N., and Grassino, A. (1996). Chest wall muscle cross talk in canine costal diaphragm electromyogram. *Journal of Applied Physiology*. 81(5), 2312-2327.

Smyth, G., Arsenault, A. B., Nagata, S., Gagnon, D., and Mathieu, P. A. (1990). Slope of the EMG/moment relationship as a measure of muscular fatigue: a validation study. *Medical and Biological Engineering and Computing*. 28, 379-383.

Solomonow, M., Baten, C., Smit, J., Baratta, R., Hermens, H., D'Ambrosia, R., and Shoji, H. (1990). Electromyogram power spectra frequencies associated with motor unit recruitment strategies. *Journal of Applied Physiology*. 68 (3), 1177-1185.

Solomonow, M., Baratta, R., Bernardi, M., Zhou, B., Lu, Y., Zhu, M., and Acierno, S. (1994). Surface and wire EMG crosstalk in neighbouring muscles. *Journal of Electromyography and Kinesiology*. 4, 131-142.

Spitzer, A. R., Wang, C., Luo, J., Ward, R., and Hassoun, M. H. (1992). Quantitative computer analysis of the sounds of isolated motor unit action potentials. *Neurology*. 42, 868-874.

St. Clair Gibson, A., Lamnert, M. and Noakes, T. (2001). Neural control of force output during maximal and submaximal exercise. *Sports Medicine*. 31(9), 637-650.

Stålberg, E. (1980). Some electrophysiological methods for the study of human muscle. *Journal of Biomedical Engineering*. 2, 290-298.

Staron, R. S., Hagerman, F. C., Hikida, R. S., Murray, T. F., Hostler, D. P., Crill, M. T., Ragg, K. E., and Toma, K. (2000). Fiber type composition of the vastus lateralis muscle of young men and women. *The Journal of Histochemistry and Cytochemistry*. 48 (5), 623-629.

Stashuk, D. (2001). EMG signal decomposition: how can it be accomplished and used?. *Journal of Electromyography and Kinesiology*. 11, 151-173.

Stegeman, D. F. and Linssen, W. H. J. P. (1992). Muscle fiber action potential changes and surface EMG: A simulation study. *Journal of Electromyography and Kinesiology*. 2 (3), 130-140.

Stegeman, D. F., Blok, J. H., Hermens, H. J., and Roeleveld, K. (2000). Surface EMG models: properties and applications. *Journal of Electromyography and Kinesiology*. 10, 313-326.

Stock, M. S., Beck, T. W., DeFreitas, J. M., and Dillon, M. A. (2010). An examination of the linearity and reliability of the electromyographic amplitude versus dynamic constant external resistance relationships using monopolar and bipolar recording methods. *Journal of Neuroscience Methods*. 194, 94-101.

Strommen, J. A. and Daube, J. R. (2001). Determinants of pain in needle electromyography. *Clinical Neurophysiology*. 112, 1414-1418.

Stulen, F. B. and De Luca, C. J. (1978). The relation between the myoelectric signal and physiological properties of constant-force isometric contractions. *Electroencephalography and Clinical Neurophysiology*. 45, 681-698.

Stulen, F. B. and De Luca, C. J. (1981). Frequency parameters of the myoelectric signal as a measure of muscle conduction velocity. *IEEE Transactions on Biomedical Engineering*. BME-28 (7), 515-523.

Tabachnick, B. G. and Fidell, L. S. (2007). *Experimental designs using ANOVA*. Thomson/Brooks/Cole.

Tanzi, F. and Taglietti, V. (1981). Spectral analysis of surface motor unit action potentials and surface interference electromyogram. *IEEE Transactions on Biomedical Engineering*. BME-28 (4), 318-324.

Taylor, A. M., Steege, J. W., and Enoka, R. M. (2002). Motor-unit synchronization alters spike-triggered average force in simulated contractions. *Journal of Neurophysiology*. 88, 265-276.

Toulouse, P., Carrault, G., Le Rumeur, E., and Coatrieux, J. L. (1992). Surface electromyogram automatic analysis and Guillain-Barré Syndrome follow up. *Electromyography and Clinical Neurophysiology*. 32, 51-62.

Tracey, B. and Williams, M. (2011). Computationally efficient bioelectric field modeling and effects of frequency-dependent tissue capacitance. *Journal of Neural Engineering*. 8 (3), 1-7.

Troni, W., DeMattei, M., and Contegiacomo, V. (1991). The effect of temperature on conduction velocity in human muscle fibers. *Journal of Electromyography and Kinesiology*. 1 (4), 281-287.

Tucker, K. J. and Türker, K. S. (2005). A new method to estimate signal cancellation in the human maximal M-wave. *Journal of Neuroscience Methods*. 149, 31-41.

Tucker, K. J. and Türker, K. S. (2007). Triceps surae stretch and voluntary contraction alters maximal M-wave magnitude. *Journal of Electromyography and Kinesiology*. 203-211.

van Boxtel, A., Goudswaard, P., van der Molen, G. M., and van den Bosch, E. J. (1983). Changes in electromyogram power spectra of facial and jaw-elevator muscles during fatigue. *Journal of Applied Physiology*. 54 (1), 51-58.

van Boxtel, A. and Schomaker, L. R. B. (1984). Influence of motor unit firing statistics on the median frequency of the EMG power spectrum. *European Journal of Applied Physiology*. 52, 207-213.

van Boxtel, A. (2001). Optimal signal bandwidth for the recording of surface EMG activity of facial, jaw, oral, and neck muscles. *Psychophysiology*. 38, 22-34.

Van Cutsem, M., Duchateau, J., and Hainaut, K. (1998). Changes in single motor unit behaviour contribute to the increase in contraction speed after dynamic training in humans. *Journal of Physiology*. 513(1), 295-305.

van Vugt, J. P. P. and van Dijk, J. G. (2000). A convenient method to reduce crosstalk in surface EMG. *Clinical Neurophysiology*. 112, 583-592.

Vatine, J. J., Blank, A., Shochina, M., Swissa, A., Mahler, Y., Gonen, B., and Magora, A. (1990). Comparison of the electrophysiological pattern of fatigue between athletes required to perform explosive and endurance sports. *Electromyography and Clinical Neurophysiology*. 30, 19-25.

Vigreux, B., Cnockaert, J. C., and Pertuzon, E. (1979). Factors influencing quantified surface EMGs. *European Journal of Applied Physiology*. 41, 119-129.

Viitasalo, J. H. T. and Komi, P. V. (1975). Signal characteristics of EMG with special reference to reproducibility of measurements. *Acta Physiologica Scandinavia*. 93, 531-539.

Viitasalo, J. H. T. and Komi, P. V. (1977). Signal characteristics of EMG during fatigue. *European Journal of Applied Physiology*. 37, 111-121.

Von Tscharner, V. (2000). Intensity analysis in time-frequency space of surface myoelectric signals by wavelets of specified resolution. *Journal of Electromyography and Kinesiology*. 10, 433-445.

Wakeling, J. M., Pascual, S. A., Nigg, B. M., and Von Tscharner, V. (2001). Surface EMG shows distinct populations of muscle activity when measured during sustained sub-maximal exercise. *European Journal of Applied Physiology*. 86, 40-47.

Weytjens, J. L. F. and van Steenberghe, D. (1984). Spectral analysis of the surface electromyogram as a tool for studying rate modulation: A comparison between theory, simulation, and experiment. *Biological Cybernetics*. 50, 95-103.

Wickiewicz, T. L., Roy, R. R., Powell, P. L., Perrine, J. J., and Edgerton, V. R. (1984). Muscle architecture and force-velocity relationships in humans. *Journal of Applied Physiology and Respiratory Environmental Exercise Physiology*. 57(2), 435-443.

Winkel, J. and Jørgensen, K. (1991). Significance of skin temperature changes in surface electromyography. *European Journal of Applied Physiology*. 63, 345-348.

Winter, B. B. and Webster, J. G. (1983). Reduction of interference due to common mode voltage in biopotential amplifiers. *IEEE Transactions on Biomedical Engineering*. BME-30 (1), 58-62.

Winter, D. A., Fuglevand, A. J., and Archer, S. E. (1994). Crosstalk in surface electromyography: Theoretical and practical estimates. *Journal of Electromyography and Kinesiology*. 4 (1), 15-26.

Wolf, S. L., Segal, R. L., and English, A. W. (1993). Task-oriented EMG activity recorded from partitions in human lateral gastrocnemius muscle. *Journal of Electromyography and Kinesiology*. 3 (2), 87-94.

Yao, W., Fuglevand, A. J., and Enoka, R. M. (2000). Motor-unit synchronization increases EMG amplitude and decreases force steadiness of simulated contractions. *Journal of Neurophysiology*. 83, 441-452.

Zhou, P. and Rymer, Z. (2004). Factors governing the form of the relation between muscle force and the EMG: A simulation study. *Journal of Neurophysiology*. 92, 2878-2886.

Zipp, P. (1978). Effect of electrode parameters on the bandwidth of the surface e.m.g. power-density spectrum. *Medical and Biological Engineering and Computing*. 16, 537-541.

Zipp, P. (1982). Effect of electrode geometry on the selectivity of myoelectric recordings with surface electrodes. *European Journal of Applied Physiology*. 50, 35-40.

Zwarts, M. J., Drost, G., and Stegeman, D. F. (2000). Recent progress in the diagnostic use of surface EMG for neurological diseases. *Journal of Electromyography and Kinesiology*. 10, 287-291.

Appendix A

Information Letter

Title of Project: Sex differences in motor unit discharge rates at various force levels

Principle Investigator:

J Greig Inglis MSc.
Laboratory Coordinator / PhD Student
Faculty of Applied Health SCience
Brock University
500 Glenridge Avenue
St. Catharines, Ontario, Canada
L2S 3A1
Phone: 905-688-5550 ext. 4667
E-mail: ginglis@brocku.ca

The following letter and consent form describe a study that I wish to conduct, with you as a participant. I am a PhD student within the Faculty of Applied Health Sciences. My research interests pertain to measuring muscle electrical activity during various force level voluntary contractions. I am trying to understand what information is contained in the electrical signal generated by muscle contractions. The main purpose is measure the differences between males and females in motor unit discharge rate and recruitment in skeletal muscle with the use of surface and needle electrodes.

There will be two sessions with no less than 24 hours, but no more than one-month between each session. The first session will be no longer than one hour with the following session lasting approximately one and a half hours. You are requested not to start any new physical activity during the interval between each session. The test sessions will be scheduled at the convenience of you and the investigator. If for any reason you decide to cancel a test session, I would appreciate advance notice and the opportunity to reschedule the test session. It is important to remember that you are free to withdrawal consent at any time without loss of access to any services or programs at Brock University to which you are entitled.

If you agree to participate in the study, you will be asked to complete the PAR-Q questionnaire. Your responses will determine you if you are physically fit and can participate in a study that requires rigorous physical exertion. To participate in this study you will need to wear loose fitting track pants or shorts. Changing rooms are conveniently located on the first floor of the Physical Education Complex. During the first session, we need to take some preliminary measurements: age, height, weight, the length, circumference, and skin-fold thickness of the leg being tested.

Day 1: MVC Familiarization

Day 1 Anthropometrics, MVC Familiarization

The subject will complete questionnaires, anthropometric measurements and familiarization dorsiflexion contractions. They will perform between 10-15 isometric (same length) contractions each separated by a period of rest at different force levels with the purpose of familiarizing the subject with the protocol involved for determining dorsiflexion contractions. The contractions will be 5 seconds in duration. The subjects will practice hitting and holding the force trace at the designated target on the screen. Adjustable supports and straps on the chair will ensure stability and minimize extraneous movements. A padded foot clamp will be attached on the top of the foot. The leg not being tested will be resting beside the leg being tested. It is important not to hold your breath while strength testing.

Day 2 Testing: Motor unit recruitment and discharge rate at 20, 40, 60 80 & 100 % of MVC

The subject will perform 3 maximal effort isometric (same length) contractions each separated by 3-5 minutes of rest with the purpose of determining your maximal voluntary contraction which will then be used for the remainder of the study. The contractions will be 5 seconds in duration. Strength measurements will be taken while seated with the leg secured in a chair designed to isolate the action of the dorsiflexors. Adjustable supports and straps on the chair will ensure stability and minimize extraneous movements. A padded foot clamp will be attached on the top of the foot. The leg not being tested will be resting beside the leg being tested. It is important not to hold your breath while strength testing.

The subject will contract the TA at various force levels depending on the random selection. Regardless of intensity, each contraction will last 7-10 seconds followed be at least 3 minutes rest. Each subject will perform at least 3 contractions at each force level followed by an additional 3 contractions at 100% of MVC.

Recording Voluntary Muscle Activity

Before electrode placement, the skin surface will be shaved, lightly abraded, and cleansed with alcohol to limit the at the skin-electrode impedance. Monopolar surface electrodes will record voluntary muscle activity at the skin surface of the tibialis anterior. The positions of the electrodes will be marked with indelible ink to ensure the consistency of the placement. In addition, a four-wire electrode will be inserted into the volume of tissue just below the surface electrode. We will use a 25-guage cannula that contains four 50-µm diameter platinum-iridium wires epoxied in a side port. The same recording needle will be used for each subject but will be sterilized by ethylene oxide prior to its reuse.

Participation in this study is not risk-free. As part of the informed consent process you have to be made aware that the following side effects are possible:

1. Skin irritation. Skin irritation may result from mildly abrading the skin, cleaning the skin with alcohol, then applying surface electromyographic (SEMG) recording electrodes with electrolyte gel. Washing the electrolyte gel from skin surface and applying skin lotion immediately after the test session can minimize the irritation.

2. Muscle soreness. It is possible that you might experience slight muscle soreness within 48 hours of the test. If soreness does occur, it will be very mild and dissipate within 72 hours.

3. Infection. Placement of a needle electrode into the muscle can be somewhat uncomfortable. If pain is experienced, the needle will be moved to another area. Like any foreign body, the needle electrode poses a risk of infection. The needle electrodes to be used in this investigation will be thoroughly sterilized using the following procedure. First, the electrode cannula will be mechanically sterilized using alcohol upon removal from the participants muscle, then autoclaved prior to its reuse. Again, this is a common procedure used without incident in Biomechanics Laboratories.

4. Systemic stress due to maximal exertion. Maximal effort contractions are associated with an increase in blood pressure. You must make sure that you do NOT hold your breath during maximal exertions. If you have received medical clearance and/or are already physically active, the risks are minimal. *Understand that should any of these side effects occur, you are free to withdrawal from the study because of them. It is important to remember that you are free to withdrawal consent at any time without loss of access to any services or programs at Brock University to which you are entitled. The researchers first priority as an investigator is to maintain the emotional, psychological, and physical health of those participating in the study.*

Aside from your name, address, and a limited number of physical measurements, the majority of the data collected in this study will be in the form of electronic signals stored on computer hard disk and on CD-ROM. The data generated by this study will only be used for educational and research purposes. The results will be presented at professional meetings, and then publish in scientific journals. To ensure anonymity, personal information will be coded and stored in a locked office to which only the investigator has access. The names of the participants or material identifying participants will not be released without written permission except as such release is required by law. I will maintain the data and associated records for the duration of my academic career, or until such time they are no longer useful to me.

This study has been reviewed and received approval from the Brock University Research Ethics Board (12-027). Should you have any questions or concerns about your involvement in the study, you may contact the Office of Research Services at 905-688-5550 (extension 3035).

Your written consent is needed to participate in the study. To indicate your consent, please complete the enclosed CONSENT FORM and return to the investigator before entering the study.

Thank you for your time and consideration in this matter.

Best Wishes,

J Greig Inglis PhD(s) / Senior laboratory coordinator, Faculty of Applied Health Science

Informed Consent Document

Title of Project: Sex differences in motor unit discharge rates at various force levels

Principle Investigators:

J Greig Inglis MSc.
Laboratory Coordinator / PhD Student
Faculty of Applied Health Science
Brock University
500 Glenridge Avenue
St. Catharines, Ontario, Canada
L2S 3A1
Phone: 905-688-5550 ext. 4667
E-mail: ginglis@brocku.ca

Justin Parro
MSc candidate
Department of Kinesiology
Brock University
500 Glenridge Avenue
St. Catharines, Ontario, Canada
L2S 3A1
Phone: 905-688-5550 ext. 4362
E-mail: jp07af@badger.ac.brocku.ca

Lara Green
MSc candidate
Department of Kinesiology
Brock University
500 Glenridge Avenue
St. Catharines, Ontario, Canada
L2S 3A1
Phone: 905-688-5550 ext. 4362
E-mail: lara.green@brocku.ca

David A. Gabriel, Ph.D., FACSM
Associate Professor Biomechanics
Department of Kinesiology
Brock University
500 Glenridge Avenue
St. Catharines, Ontario, Canada
L2S 3A1
Phone: 905-688-5550 ext. 4362
E-mail: dgabriel@brocku.ca

This study has been reviewed and approved by the Brock Research Ethics Board (12-027). The Brock Research Ethics Board requires written informed consent from participants prior to participation in a research study so that they can know the nature and risks of participation and can decide to participate or not to participate in a free and informed manner. You are asked to read the following material to ensure that you are informed of the nature of this research study and how you will participate in it if you consent to do so. Signing this form will indicate that you have been so informed and that you give you consent.

Introduction

You are being asked to participate in research being conducted by J Greig Inglis and supervised by David Gabriel Ph.D. The electrical signal of skeletal muscle is measured from the skin surface, similar to electrocardiography (ECG) which measures the electrical activity of cardiac (heart) muscle. The skeletal muscle electrical signal is termed, electromyography (EMG) This electrical signal can also be measured from within the muscle by intramuscular needle EMG. The signal can then be analyzed in a number of different ways to evaluate muscle activation.

The testing will take place in the Electromyographic Kinesiology Laboratory (WH21). There will be three testing sessions, the first session will last less than an hour with subsequent sessions lasting approximately one and a half hours each and separated by at least 24 hours from the previous session.

Plan and Procedures

J Greig Inglis, Justin Parro and Lara Green will conduct all testing. The following procedures will take place. Prior to commencement you will be asked to complete the PAR-Q assessment of physical health status to ensure that you are not at health risk during the following experiment.

Next our lab technicians will take anthropometric measurements of each participant's lower leg. These will include lengths, girths and the circumference around the peak of the calf muscle.

Upon completion of the assessment, the dominant lower leg will be prepared for testing. Small areas superficial of the tibialis anterior, patellar tendon, fibular head, and gastocnemius (calf) will be shaved, lightly abraded and cleansed with alcohol. These areas correspond to the location of the electrodes that will be taped to the skin surface. The electrodes will measure the electrical activity of tibialis anterior, similar to the more familiar electrocardiogram (ECG) that measures the electrical activity of the cardiac (heart) muscles.

We will locate the motor point (neuromuscular junction) with a light repeated superficial stimulation of the tibialis anterior. The motor point will be marked with indelible ink.

Next the participant will be placed in a chair and harnessed in to minimize synergistic activity from supporting muscles. The participants foot from their dominant leg will be placed in a foot harness where it will be secured by a clamp which is foam padded. Attached to the harness is a load-cell that will measure the amount of force upon dorsiflexion.

Day 1 Anthropometrics, MVC Familiarization

The subject will complete questionnaires, anthropometric measurements and familiarization dorsiflexion contractions. They will perform between 10-15 isometric (same length) contractions each separated by a period of rest at different force levels with the purpose of familiarizing the subject with the protocol involved for determining dorsiflexion contractions. The contractions will be 5 seconds in duration. The subjects will practice hitting and holding the force trace at the designated target on the screen. Adjustable supports and straps on the chair will ensure stability and minimize extraneous movements. A padded foot

clamp will be attached on the top of the foot. The leg not being tested will be resting beside the leg being tested. It is important not to hold your breath while strength testing.

Day 2 Testing: Motor unit recruitment and discharge rate at 20, 40, 60 80 & 100 % of MVC

The subject will perform 3 maximal effort isometric (same length) contractions each separated by 3-5 minutes of rest with the purpose of determining your maximal voluntary contraction which will then be used for the remainder of the study. The contractions will be 5 seconds in duration. Strength measurements will be taken while seated with the leg secured in a chair designed to isolate the action of the dorsiflexors. Adjustable supports and straps on the chair will ensure stability and minimize extraneous movements. A padded foot clamp will be attached on the top of the foot. The leg not being tested will be resting beside the leg being tested. It is important not to hold your breath while strength testing.

The subject will contract the TA at various force levels depending on the random selection. Regardless of intensity, each contraction will last 7-10 seconds followed be at least 3 minutes rest. Each subject will perform at least 3 contractions at each force level followed by an additional 3 contractions at 100% of MVC.

Recording Voluntary Muscle Activity

Before electrode placement, the skin surface will be shaved, lightly abraded, and cleansed with alcohol to limit the at the skin-electrode impedance. Monopolar surface electrodes will record voluntary muscle activity at the skin surface of the tibialis anterior. The positions of the electrodes will be marked with indelible ink to ensure the consistency of the placement. In addition, a four-wire electrode will be inserted into the volume of tissue just below the surface electrode. We will use a 25-guage cannula that contains four 50-μm diameter platinum-iridium wires epoxied in a side port. The same recording needle will be used for each subject but will be sterilized by ethylene oxide prior to its reuse.

Risks and Discomforts

It is not possible to predict all possible risks or discomforts that volunteer participants may experience in any research study. Based upon previous experience, the present investigator anticipates no major risks or discomforts will occur in the present project.

1. Participants sometimes experience mild discomfort when the skin is gently cleaned and rubbed with a mild abrasive in preparation for electrode placement. On occasion, some subjects may experience skin irritation associated with the placement of the electrodes. This is usually very mild and goes away in a few hours, or a day.

2. There may be discomfort related to the delayed onset of muscle soreness associated with isometric contractions of the arm muscles. If muscle soreness does occur, it is usually very mild and should dissipate within 72 hours.

3. Infection. Placement of a needle electrode into the muscle can be somewhat uncomfortable. If pain is experienced, the needle will be moved to another area. Like any foreign body, the needle electrode poses a risk of infection. The needle electrodes to be used in this investigation will be thoroughly sterilized using the following procedure. First, the electrode cannula will be mechanically sterilized using alcohol upon removal from the participants muscle, then placed in an ethylene oxide sterilization cycle for 14-26 hrs prior to its reuse. Again, this is a common procedure used without incident in Biomechanics Laboratories.

4. Maximal effort isometric contractions are associated with an increase in blood pressure. You must make sure that you do NOT hold your breath during maximal exertions. If you have received medical clearance and/or are already physically active, the risks are minimal.

Voluntary Participation

Participation in this study is voluntary. Refusal to participate will not result in loss of access to any services or programs at Brock University to which you are entitled. You will inform the investigator, Greig Inglis of your intention to withdrawal prior to removing yourself from this study.

Discontinuation of Participation

Participation in this research study may be discontinued under the following circumstances. The investigator, Greig Inglis or supervising faculty David A. Gabriel, Ph.D., may discontinue your involvement in the study at any time if it is felt to be in your best interest, if you not comply with study requirements, or if the study is stopped. You will be informed of any changes in the nature of the study or in the procedures described if they occur. It is important to remember that you are free to terminate your participation at any time, for any reason.

Potential Benefits

Participants will receive no direct benefits from participating in this study. However, participants should know that their willingness to serve as a subject for this experiment will help a Brock University researcher and other scientists develop new theories of exercise that will benefit individuals in the future.

Costs and Compensation

The cost of the test and procedures are free. You will not receive any form of compensation for your participation in this study.

Confidentiality

Although data from this study will be published, confidentiality of information concerning all participants will be maintained. All data will be coded without personal reference to you. Any personal information related to you will be kept in a locked office, to which only the investigator has access. Four investigators will have access to the data, however, names of participants or material identifying participants will not be released without written permission except as such release is required by law.

Persons to Contact with Questions

The investigator will be available to answer any questions concerning this research, now or in the future. You may contact the investigator, Greig Inglis by telephone 905-688-5550 ext. 4667 or by e-mail at ginglis@brocku.ca. You may also contact the supervisor David A. Gabriel by telephone 905 688-5550 ext. 4362. Also, if questions arise about your rights as a research subject, you may contact the Office of Research Services at (905) 688-5550 ext. 3035. If you wish to speak with someone not involved in the study, please call the Chair of the Department of Kinesiology at (905) 688-5550 ext. 4787.

Consent to Participate

Certify that you have read all the above, asked questions and received answers concerning areas you did not understand, and have received satisfactory answers to these questions. Furthermore, you have completed the PAR-Q questionnaire indicating that you are physically able to participate. You willingly give consent for participation in this study. (A copy of the consent form will be given to you).

Name of Participant (Please Print): _____

_____ _____

Signature of Participant Date (day/month/year)

In this document, the investigator fully intends to conduct all procedures with the subject's best interest uppermost in mind, to insure the subject's safety and comfort.

I have fully explained the procedures of this study to the above volunteer. I believe that the person signing this form understands what is involved in this study and voluntarily agrees to participate.

_____ _____

Date (day/month/year) J Greig Inglis, M.Sc.

Faculty of Applied Health Sciences

Ethical Approval

Brock University
Research Ethics Office
Tel: 905-688-5550 ext. 3035
Email: reb@brocku.ca

Bioscience Research Ethics Board

Certificate of Ethics Clearance for Human Participant Research

DATE:	8/3/2012		
PRINCIPAL INVESTIGATOR:	GABRIEL, David - Kinesiology		
FILE:	12-027 - GABRIEL		
TYPE:	Ph. D.	STUDENT:	Greig Inglis
		SUPERVISOR:	David Gabriel

TITLE: Sex Differences in motor unit discharge rates at various force levels

ETHICS CLEARANCE GRANTED

Type of Clearance: NEW Expiry Date: 8/30/2013

The Brock University Bioscience Research Ethics Board has reviewed the above named research proposal and considers the procedures, as described by the applicant, to conform to the University's ethical standards and the Tri-Council Policy Statement. Clearance granted from 8/3/2012 to 8/30/2013.

The Tri-Council Policy Statement requires that ongoing research be monitored by, at a minimum, an annual report. Should your project extend beyond the expiry date, you are required to submit a Renewal form before 8/30/2013. Continued clearance is contingent on timely submission of reports.

To comply with the Tri-Council Policy Statement, you must also submit a final report upon completion of your project. All report forms can be found on the Research Ethics web page at http://www.brocku.ca/research/policies-and-forms/research-forms.

In addition, throughout your research, you must report promptly to the REB:

a) Changes increasing the risk to the participant(s) and/or affecting significantly the conduct of the study;
b) All adverse and/or unanticipated experiences or events that may have real or potential unfavourable implications for participants;
c) New information that may adversely affect the safety of the participants or the conduct of the study;
d) Any changes in your source of funding or new funding to a previously unfunded project.

We wish you success with your research.

Approved:

Brian Roy, Chair
Bioscience Research Ethics Board

Appendix B

Demographic Information

Age: _____

Weight: _____

Height: _____

University Major: _____

How many times a week do you weight train?_____

How many hours per week do you weight train?_____

What percentage of time weight training do you spend training:

Upper body: _____

Lower body: _____

How long have you been weight training (please circle):

0-3 months 4-6 months 7-12 months 1-5 years more than 5 years

How many times per week do you do physical activity, other than weight training? _____

Other than weight training, what other physical activity are you participating in?

_____

_____

Anthropometric Measures and EMG Data Collection Sheet

Date: _____

Subject Name: _____ Age: _____ Number: _____

Gender: M F

TYPE	Measurement (cm)
Lower Leg length	
Lower Leg circumference	
Whole Foot	
Malleolus to bottom	
Malleolus to Meta Tarsals	
Calcaneus to Meta Tarsals	

EQUIPMENT SETTINGS

Amplification: Indwelling: _____ sEMG: _____

Filter Settings: Indwelling: _____ sEMG: _____

Skin Impedance Pre: _____ Post: _____

Skin Temperature Pre: _____ Post: _____

Pre MVC: _____

20% : _____

40% : _____

60% : _____

80% : _____

POST MVC : _____

Conditions and Gains

Condition	Amplification	Trial #
MVC = 100%	X	Trial_01
MVC = 100%	X	Trial_02
MVC = 100%	X	Trial_03
MVC =	X	Trial_04
MVC =	X	Trial_05
MVC =	X	Trial_06
MVC =	X	Trial_07
MVC =	X	Trial_08
MVC =	X	Trial_09
MVC =	X	Trial_10
MVC =	X	Trial_11
MVC =	X	Trial_12
MVC =	X	Trial_13
MVC =	X	Trial_14
MVC =	X	Trial_15
MVC =	X	Trial_16
MVC =	X	Trial_17
MVC =	X	Trial_18
MVC =	X	Trial_19
MVC =	X	Trial_20
MVC =	X	Trial_21
MVC =	X	Trial_22
MVC =	X	Trial_23
MVC =	X	Trial_24
MVC =	X	Trial_25

Appendix C

Spike Shape Measures

Spike shape analysis of the sEMG signal is focused on two components of the signal: spikes and peaks. Beach, Gornian, and Gans (1982) created a computer algorithm to quantify the electromyogram using spike shape. From stored data the program divides the signal into bins and detects pairs of upward and downward deflections that cross the isoelectric baseline, called spikes. These spikes are averaged across all bins and this is the mean spike amplitude. Pairs of deflections within a spike that do not cross baseline, termed peaks, are eliminated from the signal because they are considered noise. In order to be considered a spike or a peak it must also be greater than the 95% confidence interval for baseline activity. The following calculations will be used for both the surface and indwelling EMG signals for a basis of comparison.

Mean Spike Amplitude (MSA)

The mean spike amplitude (MSA) is calculated using single spike amplitudes (SA) determined by:

The sum of the SA from each spike is then taken and divided by the total number of spikes:

Mean Spike Frequency (MSF)

Mean spike frequency (MSF) is calculated by taking the number of spikes (NS) and dividing by the total duration (TD) of the data window:

Mean Spike Slope (MSS)

To determine the mean spike slope (MSS), the difference in the y-coordinates A_y and B_y is divided by the difference in the x-coordinates A_x and B_x, representing the spike slope (SS):

Each SS is summed and divided by the number of spikes in the sample to find MSS:

Mean Number of Peaks Per Spike (MNPPS)

To calculate the MNPPS, the number of peaks (P) is divided by the number of spikes (NS):

$$\frac{}{}$$

Mean Spike Duration (MSD)

The mean spike duration (MSD) is calculated using each spike duration determined by the difference of C and A. Then the duration of each spike is summed and divided by the number of spikes (NS):

$$\frac{}{}$$

Biceps Brachii sEMG Interference Pattern

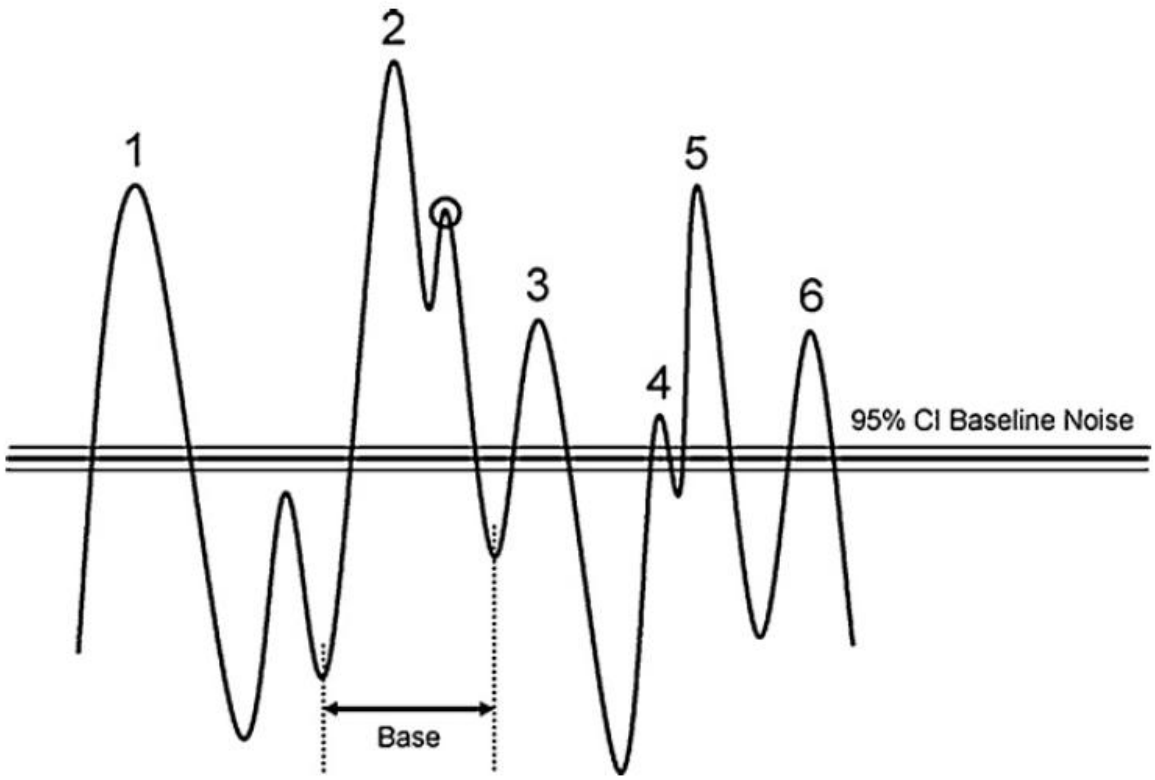

Figure 25. An example of a sEMG pattern, illustrating the difference between a spike and a peak for calculating spike shape measures. There are six spikes with upward and downward deflections crossing the isoelectric baseline with greater magnitude than the 95% confidence interval for baseline activity. The second spike has one peak denoted by a circle. Gabriel, D. A., Christie, A., Inglis, J. G., and Kamen, G. (2011). Experimental and modeling investigation of surface EMG spike analysis.*Medical Engineering and Physics*. 33, 427-437. Figure 1, page 428.

Appendix D

Traditional Measures

Frequency Domain

The power spectral density function (PSD) will be estimated using the Welch periodogram method. A 1-second segment (N = 2048 points) extracted from the most stable portion of the force (± 2.5%) will be used for frequency analysis of the surface and indwelling EMG signals. In accordance with the requirements of the Welch periodogram method, four successive and overlapping sections of N = 512 points will be used. Sections will be detrended and multiplied with an N-point Hamming window to then compute its DFT. The PSD function will be computed by squaring and averaging all DFTs:

The PSD function typically displays a positive skewness where the mean power frequency (MPF) is greater than the median power frequency (MDF). The mean and median frequencies can be determined by first calculating the total power (TP) by:

The mean frequency can then be calculated by:

where N is the number of data points in the window and *k* is the index for the frequencies (f[k] = 2048·(k/N): k = 0, 1,…N-1). The median power is the frequency that splits the spectrum in half with equal power on either side of it. It is calculated as follows:

Time Domain

The analysis of the surface and indwelling EMG signal amplitudes will be performed on a 1-second (N = 2048 points) segment of data. The window will be chosen from the most stable portion of the force recorded (± 2.5%) during the 5-second contraction. The root-mean-square (RMS) amplitude will be determined using the calculation defined by Basmajian and De Luca (1985) as follows:

where x_i is a single data point of surface or indwelling EMG activity.